

# SANDIA REPORT

SAND2020-5266

Printed 20 May 2020



Sandia  
National  
Laboratories

## Charon User Manual: v. 2.1 (revision1 )

Lawrence Musson, Gary Hennigan, Xujiao Gao, Richard Humphreys,  
Mihai Negoita, Andy Huang

Prepared by  
Sandia National Laboratories  
Albuquerque, New Mexico 87185  
Livermore, California 94550

Issued by Sandia National Laboratories, operated for the United States Department of Energy by National Technology & Engineering Solutions of Sandia, LLC.

**NOTICE:** This report was prepared as an account of work sponsored by an agency of the United States Government. Neither the United States Government, nor any agency thereof, nor any of their employees, nor any of their contractors, subcontractors, or their employees, make any warranty, express or implied, or assume any legal liability or responsibility for the accuracy, completeness, or usefulness of any information, apparatus, product, or process disclosed, or represent that its use would not infringe privately owned rights. Reference herein to any specific commercial product, process, or service by trade name, trademark, manufacturer, or otherwise, does not necessarily constitute or imply its endorsement, recommendation, or favoring by the United States Government, any agency thereof, or any of their contractors or subcontractors. The views and opinions expressed herein do not necessarily state or reflect those of the United States Government, any agency thereof, or any of their contractors.

Printed in the United States of America. This report has been reproduced directly from the best available copy.

Available to DOE and DOE contractors from

U.S. Department of Energy  
Office of Scientific and Technical Information  
P.O. Box 62  
Oak Ridge, TN 37831

Telephone: (865) 576-8401  
Facsimile: (865) 576-5728  
E-Mail: [reports@osti.gov](mailto:reports@osti.gov)  
Online ordering: <http://www.osti.gov/scitech>

Available to the public from

U.S. Department of Commerce  
National Technical Information Service  
5301 Shawnee Road  
Alexandria, VA 22312

Telephone: (800) 553-6847  
Facsimile: (703) 605-6900  
E-Mail: [orders@ntis.gov](mailto:orders@ntis.gov)  
Online order: <https://classic.ntis.gov/help/order-methods>



## **ABSTRACT**

This manual gives usage information for the Charon semiconductor device simulator. Charon was developed to meet the modeling needs of Sandia National Laboratories and to improve on the capabilities of the commercial *TCAD* simulators; in particular, the additional capabilities are running very large simulations on parallel computers and modeling displacement damage and other radiation effects in significant detail.

The parallel capabilities are based around the *MPI* interface which allows the code to be ported to a large number of parallel systems, including linux clusters and proprietary “big iron” systems found at the national laboratories and in large industrial settings.

## **ACKNOWLEDGMENT**

Thanks to everyone that contributed to the project and this document.

# CONTENTS

Nomenclature .....	10
1. Introduction .....	11
1.1. Drift Diffusion Equations .....	11
1.2. Nonlinear Poisson Equation .....	12
1.3. Solution Methods .....	12
2. Installation .....	13
2.1. Prerequisites .....	13
2.2. Building Charon .....	14
2.2.1. Using the Python Build Script .....	14
3. Running Charon .....	16
3.1. General Information .....	16
3.2. Conventions .....	16
3.3. The Charon Interpreter .....	16
3.3.1. Invoking the Interpreter .....	16
3.3.2. Configuring the Interpreter .....	17
3.3.3. Essential Parts of the Interpreter Input .....	18
3.4. Example Problem: Nonlinear Poisson Simulation for a Pseudo One Dimensional Silicon PN Diode .....	19
3.4.1. Mesh Generation Using Cubit .....	19
3.4.2. Charon Input Deck for a NLP Simulation .....	20
3.4.3. Command Line Serial Execution for a NLP simulation .....	24
3.5. Example Problem: IV Sweep for a Pseudo One Dimensional Silicon PN Diode .....	24
3.5.1. Charon Input Deck for an IV Sweep .....	24
3.5.2. Command Line Serial Execution for an IV sweep .....	27
4. Boundary Conditions .....	29
4.1. Ohmic Contacts .....	29
4.2. Schottky Contacts .....	31
4.2.1. Schottky Contacts Barrier Lowering .....	32
4.2.2. Schottky Contacts Barrier Tunneling .....	33
4.3. Gate Contacts .....	35
4.4. Constraint Boundary Conditions .....	35
4.4.1. Device Contact Dimensions .....	35
4.4.2. Constant Current .....	36
4.4.3. Resistor Contact .....	36
4.4.4. Constant Current on the Base Contact of a Pseudo 1D BJT .....	39
4.4.5. Solver Specifications for Constrained Problems .....	39
5. Band Structure .....	40
5.1. Intrinsic Density .....	40

5.2. Band gap and Electron Affinity .....	45
6. Mobility Models .....	48
6.1. Arora Model .....	48
6.2. Albrecht Mobility Model .....	49
6.3. Farahmand Mobility Model .....	51
6.4. Philips-Thomas Unified Mobility Model .....	54
7. Recombination and Generation .....	57
7.1. Mid-Gap SRH Recombination .....	57
7.2. Radiative Recombination .....	59
7.3. Auger Recombination .....	59
7.4. Generic SRH Recombination .....	60
7.4.1. Model Usage .....	61
7.5. Avalanche Generation .....	64
7.5.1. Selberherr Model .....	65
7.5.2. Crowell-Sze Model .....	68
8. Incomplete Ionization .....	70
8.1. Model Implementation .....	70
8.2. Model Usage .....	71
9. Heterojunction .....	74
9.1. Thermionic Emission .....	75
9.2. Local Tunneling .....	78
9.3. Model Implementation .....	79
9.4. Model Usage .....	81
10. Harmonic Balance .....	84
10.1. Formulation .....	84
10.2. Usage .....	85
10.2.1. Physics Block .....	86
10.2.2. Boundary Conditions .....	86
10.2.3. Initial Conditions .....	87
10.3. Example cases .....	87
10.3.1. Modifying a time-domain input deck for frequency-domain analysis .....	87
11. Radiation Models .....	90
11.1. Empirical Displacement Damage Model .....	90
11.2. Total Ionizing Dose Models .....	91
11.2.1. Fixed Oxide Charge Model .....	92
11.2.2. Interface Fixed Charge Model .....	93
11.2.3. Interface Static Trap Model .....	95
11.2.4. Kimpton Model .....	98
12. Solvers .....	103

13. Charon Input File Reference .....	105
13.1. Import State File .....	105
13.2. Output Parameters .....	106
13.3. Physics Block .....	108
13.3.1. Geometry Block .....	108
13.3.2. Material Model Specification .....	109
13.3.3. Discretization .....	109
13.4. Material Block .....	109
13.4.1. Material Name .....	110
13.4.2. Relative Permittivity .....	111
13.5. Carrier Recombination .....	111
13.5.1. Shockley-Reed-Hall Recombination .....	112
13.5.2. Radiative (Direct) Recombination .....	113
13.5.3. Auger Ionization/Recombination .....	114
13.6. Variable Voltage at a Boundary .....	114
13.7. Doping .....	116
13.7.1. Uniform Doping .....	117
13.7.2. Step Junction .....	117
13.7.3. Gaussian Doping .....	118
13.7.4. Modified Gaussian Doping .....	118
References .....	120
References .....	120
Appendix A. Historical Perspective .....	124
Appendix B. Band-to-Trap Tunneling Models .....	124
Appendix C. Derivation of Heterojunction Models .....	129
Appendix D. Charon Input File for a PN step junction diode Example .....	134
D.1. NLP input file for PN step junction diode in Section 3.4 .....	134
D.2. I-V sweep input file for PN step junction diode in Section 3.5 .....	135

## LIST OF FIGURES

Figure 2-1. Partial directory tree resulting from unpacking of Charon tarball and subsequent cloning within that tree of the Trilinos repository. ....	14
Figure 3-1. Geometry for a simple pseudo one-dimensional PN diode with a step junction. The metallurgical junction is at $0.5\mu\text{m}$ . ....	19
Figure 3-2. Cubit journal commands for the PN diode geometry illustrated in Figure 3-1. ...	20
Figure 3-3. Mesh for PN diode generated with Cubit. ....	21
Figure 3-4. Results of IV sweep .....	28
Figure 4-1. Band diagram of Schottky contacts .....	32

Figure 4-2.	Diagram for illustration of a resistor attached to a device contact. ....	38
Figure 4-3.	Pseudo one-dimensional Bipolar Junction Transistor (BJT). ....	39
Figure 7-1.	Specification of parameters values for the radiative recombination model in the input file. ....	59
Figure 7-2.	Specification of parameters values for the Auger recombination model in the input file. ....	60
Figure 9-1.	(a) Schematic of a InGaP/GaAs/GaAs NPN HBT device. (b) Band diagram in the emitter and base regions. ....	74
Figure 9-2.	Different cases of $\Delta E_C$ and $\Delta E_V$ , the corresponding band diagrams, and the corresponding net thermionic emission current densities for Boltzmann statistics. ....	78
Figure 9-3.	Examples of valence band diagrams that allow for hole tunneling. ....	80
Figure 9-4.	Schematics of two element blocks with a heterojunction, showing the basic variables in each element block and the currents across the junction. ....	80
Figure 11-1.	Scaled electric potential at equilibrium for a n-channel silicon MOSFET with a positive charge density of $10^{11} \text{ cm}^{-2}$ at the Si/SiO <sub>2</sub> interface ....	94
Figure 11-2.	Scaled potential gradient along the white line in figure 11-1. The Si/SiO <sub>2</sub> interface is located at $y = 0$ . The $y < 0$ region is the Si region, while $y > 0$ is the SiO <sub>2</sub> region. The denoted numbers are the potential gradients at the Si/SiO <sub>2</sub> interface obtained from Charon. ....	95
Figure 13-1.	Example of a non-typical IV sweep possible in Charon. ....	116
Figure B-1.	Electron field enhancement factor for traps at 300 K as a function of electric field computed using the four Schenk models. ....	126
Figure B-2.	Typical band profile in the emitter and base regions of an In <sub>0.5</sub> Ga <sub>0.5</sub> P/GaAs NP <sup>+</sup> N HBT. Here $E_C$ is the conduction band, $E_V$ is the valence band, $\Delta E_V$ is the valence band offset, and $E_T$ indicates the trap location. The circle with a plus represents a hole, and the blue arrow denotes the hole-to-trap tunneling path. The red dashed curve is a linearized potential to approximate the actual valence band. ....	127
Figure B-3.	Electron field enhancement factor for the approximated potential in figure B-2 at 300 K as a function of electric field computed using the <i>Schenk ConstFDOS</i> and <i>Schenk NewDOS</i> models. The calculations were done for four different locations that are 5, 10, 15, and 20 nm in the emitter away from the heterojunction. The trap parameters are the same as those for the E5 traps in GaAs. ....	128
Figure C-1.	Example of conduction band diagram illustrating the carrier transport across a heterojunction. ....	129
Figure C-2.	Example of conduction band diagram illustrating the case of $E_{min} > 0$ . ....	131

## LIST OF TABLES

Table 2-1.	Packages and libraries required by Charon. Installation should be performed in the order as shown in the table. ....	13
Table 2-2.	Utilities required to install and run Charon. ....	14
Table 4-1.	Syntax and parameters for the Schottky contact. ....	32



Table 4-2.	Syntax and parameters for the Schottky Contact Barrier Lowering. ....	33
Table 4-3.	Syntax and parameters for the Schottky Contact Tunneling. ....	35
Table 4-4.	Syntax for specifying constant current at a contact ....	37
Table 4-5.	Syntax for specifying resistor attached to a contact ....	38
Table 5-1.	Syntax and parameters for Old Slotboom model. ....	41
Table 5-2.	Syntax and parameters for Slotboom model. ....	42
Table 5-3.	Syntax and parameters for Harmon model. ....	44
Table 5-4.	Syntax and parameters for Persson model. ....	45
Table 5-5.	Syntax and parameters for temperature-dependent bandgap. ....	46
Table 6-1.	Syntax and parameters for the Arora mobility model. ....	49
Table 6-2.	Default Arora mobility model parameter values for supported materials. ....	49
Table 6-3.	Syntax and parameters for the Albrecht mobility model. ....	51
Table 6-4.	Syntax and parameters for the Farahmand mobility model. ....	52
Table 6-5.	Farahmand low-field mobility parameters ....	53
Table 6-6.	Farahmand high field mobility parameters ....	53
Table 6-7.	Syntax and parameters for the Philips-Thomas mobility model. ....	56
Table 6-8.	Default values for dopant-related parameters used in Philips-Thomas mobility model. ....	56
Table 6-9.	Carrier dependent parameters used in Philips-Thomas mobility model. ....	56
Table 7-1.	Default parameters values for doping and temperature dependent SRH lifetime. ....	59
Table 7-2.	Available parameters for the generic SRH trap model. ....	63
Table 7-3.	Available parameters for the generic SRH band-to-trap tunneling models. $m_0$ is the free electron mass. ....	63
Table 7-4.	Syntax and parameters for Selberherr avalanche model. ....	67
Table 7-5.	Syntax and parameters for Crowell-Sze avalanche model. ....	69
Table 8-1.	Syntax and parameters for the incomplete ionization model. ....	72
Table 9-1.	Syntax and parameters for the heterojunction boundary condition. $m_0$ is the free electron effective mass. ....	82
Table 10-1.	Syntax for HB analysis in physics block. ....	86
Table 10-2.	Syntax for HB Boundary Conditions. Note that the list of <i>frequencyValues</i> , <i>amplitudeValues</i> , and <i>phaseshiftValues</i> must have the same number of parameters. ....	87
Table 10-3.	Syntax for HB Initial Conditions. ....	88
Table 11-1.	Syntax and parameters for the empirical radiation damage model. ....	90
Table 11-2.	Analytic pulse definitions. ....	91
Table 11-3.	Available parameters for the interface trap model. ....	97
Table 11-4.	Syntax and general parameters for Kimpton model. ....	100
Table 11-5.	Syntax and parameters for Kimpton interface trap model. ....	100
Table 11-6.	Syntax and parameters for Kimpton volume trap model. ....	102
Table 13-1.	Import state file syntax ....	106
Table 13-2.	Output state file syntax ....	106
Table 13-3.	Output nodal variables syntax ....	107
Table 13-4.	Output cell averaged variables syntax ....	107
Table 13-5.	Specify filename of tabulated currents for transient simulations ....	107
Table 13-6.	Specify filename of tabulated currents for parameter sweep simulations ....	108

Table 13-7. How to request unscaled quantities in the exodus file. ....	108
Table 13-8. Specify the geometry block to which these physics apply. ....	109
Table 13-9. Specify the material block that accompanies a physics block. ....	109
Table 13-10. Output cell averaged variables syntax ....	110
Table 13-11. Specify the name of a material. ....	111
Table 13-12. Specify the relative permittivity of a material. ....	111
Table 13-13. Mid-gap SRH recombination toggle ....	112
Table 13-14. Mid-gap SRH constant carrierlifetime ....	112
Table 13-15. Concentration dependent SRH carrier lifetime ....	113
Table 13-16. Concentration dependent SRH carrier lifetime $\tau_{a0}$ value ....	113
Table 13-17. Electron lifetime temperature dependence ....	113
Table 13-18. Generic SRH recombination toggle ....	113
Table 13-19. Direct recombination toggle ....	114
Table 13-20. Radiative recombination coefficient. ....	114
Table 13-21. Parameters used to control voltage sweeping. ....	115

## NOMENCLATURE

**BJT** Bipolar Junction Transistor

**GaN** Gallium Nitride

**MPI** Message Passing Interface

**WRMS** Weighted Root Mean Square

## 1. INTRODUCTION

The Charon semiconductor device simulator is based on a multi-physics code for simulating general transport-reaction phenomena. The focus of this manual is on Charon's capabilities for modeling semiconductor devices. The semiconductor modeling capability in Charon was developed to work in a manner similar to other *TCAD* codes such as Medici™ and DaVinci™. Additionally Charon supports massively parallel execution and the explicit treatment of defect physics in order to accurately model radiation effects.

Generally the current release is restricted to junction-type devices, such as diodes and bipolar junction devices. There is some preliminary functionality for modeling MOSFET devices, but it should be viewed as alpha-level.

Another important note is that as of this writing Charon has *not* been approved for external distribution. As such users must treat the Charon code as *Export Controlled* material.

### 1.1. Drift Diffusion Equations

Charon was developed to solve the drift-diffusion equations for semiconductor devices. These equations are

$$-\nabla \cdot \epsilon \nabla \psi = q(p - n + C), \quad (1)$$

$$\nabla \cdot \mathbf{J}_n - qR = q \frac{\partial n}{\partial t}, \quad (2)$$

$$-\nabla \cdot \mathbf{J}_p - qR = q \frac{\partial p}{\partial t}, \quad (3)$$

with

$$\mathbf{J}_n = -qn\mu_n \nabla \psi + qD_n \nabla n, \quad (4)$$

$$\mathbf{J}_p = -qp\mu_p \nabla \psi - qD_p \nabla p, \quad (5)$$

$$C = N_d - N_a, \quad (6)$$

where

- $\psi$  - Electric potential,
- $n, p$  - Electron and hole concentrations, respectively,
- $N_{d,a}$  - The donor and acceptor doping concentrations, respectively,
- $q$  - The fundamental electron charge ( $1.602 \times 10^{-19}$ ),
- $R$  - Generation term,
- $\mu_{n,p}$  - Carrier mobilities,
- $D_{n,p}$  - Carrier diffusion coefficients, and
- $\epsilon$  - Electric permittivity of semiconductor.

## 1.2. Nonlinear Poisson Equation

The nonlinear Poisson equation uses an equilibrium approximation to the drift-diffusion equations to eliminate the flux equations in (2) and (3). For the Poisson equation, (1), the carrier densities,  $p$  and  $n$ , are approximated by

$$n = n_i e^{\frac{\psi}{kT}}, \quad (7)$$

$$p = n_i e^{-\frac{\psi}{kT}}. \quad (8)$$

Now (1) becomes

$$-\nabla \cdot \epsilon \nabla \psi = q \left[ n_i \left( e^{-\frac{\psi}{kT}} - e^{\frac{\psi}{kT}} \right) + C \right]. \quad (9)$$

## 1.3. Solution Methods

Charon uses two common discretizations for solving the PDEs associated with the semiconductor drift-diffusion model given above. The finite-element method, or *FEM*, and the “box” method used by many of the commercial *TCAD* simulators. In general the finite-element method offers a richer mathematical context in which to solve partial-differential equations such as the equations in the drift-diffusion model for semiconductor problems, but the *FEM* is much less mature than the box method. In terms of capabilities the box method is the preferred method for solving semiconductor problems in Charon. The box method can typically use a coarser discretization for an equivalent problem and thus runs to completion quicker. A good introduction to the box method can be found in [31].

## 2. INSTALLATION

Charon is currently in use on many unix and unix-like systems at Sandia National Laboratories, including multiple Linux distributions and custom operating systems on large parallel systems. Instructions for installing it on representative systems follow. Note that each system is often unique and this section is not meant to be exhaustive, only to give you the background knowledge necessary to successfully install the code. Contact the authors if you are having trouble installing on a specific system.

### 2.1. Prerequisites

Charon requires a modern compiler suite, including a C++ compiler that is compliant with the C++-11 standard. The GNU $\tilde{c}$ .x and Intel 18 compiler suites are two examples that have been successfully utilized to build Charon. Requirements of third party libraries are given in Table 2-1. Additionally, several utilities are required by either Charon itself or the Trilinos framework. Those are given in Table 2-2. Note that earlier or later versions of the packages and utilities listed in Tables 2-1 and 2-2 may work but there is no guarantee that there will not be problems with different versions. Also note that if at all possible the libraries and utilities in Table 2-1 and Table 2-2 should be installed via your OS. For example, on Ubuntu Linux `apt install netcdf` would install netcdf on your system alleviating the need to install it yourself from source.

**Table 2-1 Packages and libraries required by Charon. Installation should be performed in the order as shown in the table.**

Package Name	URL for Package	Minimum Version
OpenMPI	<a href="https://www.open-mpi.org">https://www.open-mpi.org</a>	1.10
HDF5	<a href="https://www.hdfgroup.org/HDF5">https://www.hdfgroup.org/HDF5</a>	1.10
boost	<a href="https://www.boost.org">https://www.boost.org</a>	1.68
netCDF	<a href="https://www.unidata.ucar.edu/software/netcdf/">https://www.unidata.ucar.edu/software/netcdf/</a>	4.6
TriBITS	<a href="https://tribits.org/">https://tribits.org/</a>	<i>latest</i>
Trilinos	<a href="https://trilinos.org">https://trilinos.org</a>	<i>development</i>

Note that after TriBITS is cloned you must set the environment variable `TRIBITS_BASE_DIR` to point to the location into which it was cloned prior to invoking the Charon build script, `build_charon.py`.

Also note that Charon is tightly dependent on the Trilinos framework. At the present time the build of Charon is tightly integrated with the build of Trilinos and the two cannot be separated. It is therefore required that you obtain a copy of the *develop* branch of the Trilinos distribution.

Once the prerequisites are available, the next step is to unpack the tarball that you obtained from the Charon team. On a Linux system a typical command to do this would be

```
tar xzvf charon-distrib.tar.gz
```

**Table 2-2 Utilities required to install and run Charon.**

Utility Name	URL for Utility	Minimum Version
cmake	<a href="http://www.cmake.org">http://www.cmake.org</a>	3.12
python	<a href="http://www.python.org">http://www.python.org</a>	3.x
git	<a href="http://www.git-scm.com">http://www.git-scm.com</a>	2.10
cubit	<a href="http://cubit.sandia.gov">http://cubit.sandia.gov</a>	15.3

Next change to the `tcad-charon` directory and clone a copy of the Trilinos repository. Instructions for cloning a *development* version of Trilinos can be found at the URL referenced in Table 2-1. On a typical Linux system the commands to accomplish this are given by

```
cd tcad-charon
git clone https://github.com/tcad-charon/Trilinos.git Trilinos
cd Trilinos
git checkout charon-release-v2.1-06.may.2020
```

Note that the *git checkout* step above requires that you use the version that corresponds to the distribution of charon you obtained. In the step above that would correspond to the 2.1 release. You can list the relevant tags using

```
git tag | grep charon
```

Once the distribution is unpacked and a clone of Trilinos has been performed the resulting directory structure should resemble the one shown in Figure 2-1.

```
tcad-charon
├── cmake
├── docs
├── scripts
│   └── build
├── src
├── test
│   ├── nightlyTests
│   └── nightlyTestsOUO
└── Trilinos
```

**Figure 2-1 Partial directory tree resulting from unpacking of Charon tarball and subsequent cloning within that tree of the Trilinos repository.**

## **2.2. Building Charon**

### **2.2.1. Using the Python Build Script**

The `scripts/build` subdirectory within `tcad-charon` contains utilities and data necessary to build Charon on various platforms. The python script `scripts/build/all/build_charon.py`

is the preferred method for starting a Charon build. The purpose of the script is to generate an appropriate *cmake* command line and execute it. The script has a built-in help facility which should serve as a starting point for performing the installation. To see the built-in documentation invoke the script like

```
build_charon.py --help
```

The `--manual-page` argument will output detailed help for the script similar to what you would see in a Unix *man* page. The build script should be invoked within a dedicated build directory for the code, preferably a previously empty directory.

At a minimum you will need to create a `*.opts` file in

```
tcad-charon/scripts/build/<username>,
```

where `<username>` is replaced with your unix login ID. That file should be the name of your system, as returned by the *hostname* command, and contain the location of Boost and NetCDF on your system. A good example of the contents of that file can be found in

```
tcad-charon/scripts/build/all/attaway.opts.
```

Once the `build_charon.py` script has been successfully executed a simple invocation of *make* should compile the code, including the necessary Trilinos packages, and build a Charon executable. The resulting executable can be tested via the *cmake* utility *ctest*. Invoking the *ctest* command within the build directory will run a set of tests used internally as nightly regression tests and should give you some assurance that the resulting executable is working correctly.

Should the MPICH2 or IntelMPI Message Passing Interface (MPI) implementation be required then include the following CXX flag in the build script.

```
-DMPICH_IGNORE_CXX_SEEK
```

The Intel Math Kernel Library is a highly optimized math library, if Intel compilers are being used and the Intel Math Kernel Library is available then it can be linked in the build script using the following:

```
TPL_ENABLE_MKL=ON
MKL_LIBRARY_DIRS:FILEPATH="${MKLROOT}/lib/intel64"
MKL_LIBRARY_NAMES:STRING="mkl_rt"
TPL_ENABLE_BLAS=ON
BLAS_LIBRARY_DIRS:FILEPATH="${MKLROOT}/lib/intel64"
BLAS_LIBRARY_NAMES:STRING="mkl_rt"
TPL_ENABLE_LAPACK=ON
LAPACK_LIBRARY_DIRS:FILEPATH="${MKLROOT}/lib/intel64"
LAPACK_LIBRARY_NAMES:STRING="mkl_rt"
```

### 3. RUNNING CHARON

Once the code is compiled, and the resulting executable has been tested, the next step is running a simulation. There are numerous examples, including regression tests, that are included with the distribution. The recommended approach for a new user would be to start with one of the example problems and modify it to suit their particular problem.

#### 3.1. General Information

One thing to note about Charon is that it follows the example of many other finite-element like codes in that the mesh generation phase and the analysis phase are separate entities. Specifically Charon relies on a mesh file generated elsewhere. At Sandia this generally means that a program called *Cubit* (<https://cubit.sandia.gov>) is used to generate the mesh and output a file in *Exodus* format for input into Charon. Otherwise, any mesh generator that can produce an exodus formatted mesh should be usable by Charon.

#### 3.2. Conventions

Electric current is referenced as positive if it's leaving a device contact and negative if it's entering.

#### 3.3. The Charon Interpreter

All simulations in Charon require an input file to configure the run. The input file that Charon natively reads is a parameter list that contains information that completely configures the simulation including names of initial and output state files, physics, material models, solver configuration, etc. These parameter lists are highly structured, but are lengthy, complex and therefore fragile even for the simplest of simulations and require an experienced, knowledgeable user to create and maintain. The format of the input files is either XML or YAML which incurs additional challenges in visual acuity.

The Charon interpreter is a tool that the user can employ to make configuration of a charon simulation much simpler. The user-supplied input files to the interpreter are composed of simpler, more straight-forward language that is easier for the user to comprehend. Ultimately, the interpreter will map the interpreter input file into a parameter list that Charon understands.

##### 3.3.1. Invoking the Interpreter

The charon interpreter is invoked with arguments from the command line. To see the list of available arguments, invoke the interpreter with the `--help` argument,

```
charonInterpreter.py --help
```



When the interpreter is invoked with the `-i` or `--input` option plus a file name, the interpreter will create the parameter list in an XML format and terminate execution. For example, if the user has created an interpreter input called `diode.inp` and invokes

```
charonInterpreter.py -i diode.inp
```

the interpreter will generate the equivalent parameter list in an XML format and store it in a file called `diode.inp.xml`. Advanced users can do this if they wish to see, for example, the fine details of how the solvers are configured for their simulation. Otherwise, if the user simply wishes to run the simulation, the interpreter may be invoked as

```
charonInterpreter.py -i diode.inp --run
```

and this will generate the parameter list and execute Charon with it. Often times, TCAD simulations can be high in computational effort and it may be desirable to run Charon in parallel. Domain decomposition must be completed prior to executing Charon with the scripts that are included with the Trilinos libraries. In that instance, the interpreter may be used to execute Charon on, say, 4 processors via

```
charonInterpreter.py -i diode.inp --np 4 --run
```

The syntax of the input file is available in this user manual. However, for a quick reference, syntax can be obtained through the interpreter itself and will always be current with the installed version of the interpreter. The `--syntax (-s)` and `--longsyntax (-S)` arguments will return all available input lines the interpreter knows about. The latter will return a slightly more verbose description of each individual line. There is presently no way to use the interpreter to search for a specific syntax. There are easy ways to search the output, however. The output of the syntax help is plain text. The output may be redirected to a text file and opened in any editor. Another convenient way is to pipe the output through `less` in any Linux system as follows

```
charonInterpreter.py -S | less -i
```

This will allow scrolling through the syntax help. The keys `/<searchTerm>` will allow case insensitive searching through the entire syntax help.

### **3.3.2.      *Configuring the Interpreter***

When Charon is installed in common locations for executable commands such as `/usr/bin` or any other location pointed to by the `PATH` variable, the interpreter will be able to find and use Charon without intervention. It is very common, however, that Charon is installed in a non-standard location. Less frequently, it is installed with something other than its default name (`charon_mp.exe`). Location and executable name may both be configured in the interpreter with environment variables. The environment variable, `CHARON_EXECUTABLE_PATH` set to the directory where the executable is installed will tell the interpreter where to find it. The variable `CHARON_EXECUTABLE` can be set if the name of the executable is different than `charon_mp.exe`.

### 3.3.3. *Essential Parts of the Interpreter Input*

Examples of interpreter input files will be given in later sections of this manual. There are several hundred possible lines of input that can go into an input file. In practice, only a very small fraction of those will ever be included. And there is a small amount of information that is required of any Charon simulation no matter how small. The following shows essential, generic boilerplate of an interpreter input file.

```
import state file <stateFile.exo>

start output parameters
  output state file <stateFileOutput.exo>
end output parameters

start Physics Block Semiconductor
  geometry block is <regionName>
  standard discretization type is <equations to solve>
  material model is <materialModelName>
end Physics Block Semiconductor

start Material Block <materialBlockName>
  material name is <material>
  <Doping Parameters>
end Material Block siliconParameter

BC is ohmic for <contact name> on <region> fixed at <voltage>

initial conditions for <Field> in <region> is <IC>

start solver block
  <Solver configuration>
  <termination criteria>
end solver block
```

Each of these items will be covered in considerably more detail later in this manual. But the essential items are an input exodus file, an output exodus file, a block which describes the physics to be simulated in the regions of the model (there may be more than one), the material properties and models for each region, boundary conditions, initial conditions and a solver configuration.

Some general notes on the input file format:

- Comments are delineated with the “#” symbol.
- The keywords that make up the input file are not case sensitive, but most values are case sensitive. A good example of this would be the name of the input file. It is case sensitive.
- Other than enhancing readability, indentation is not significant.
- Blocks are always delineated via *start* and *end* statements.
- Text immediately following an *end* statement, on the same line, is not significant but can enhance readability.

### 3.4. Example Problem: Nonlinear Poisson Simulation for a Pseudo One Dimensional Silicon PN Diode

A simple example of simulating a nonlinear-Poisson problem is given for a pseudo-1D PN diode with a step junction. This includes the mesh generation for the problem within cubit. An illustration of the geometry for this problem is given in Figure 3-1.

Charon can operate on either two- or three-dimensional geometries. It cannot be used for a true one-dimensional geometry. In this example the problem is one-dimensional because there is no variation in the geometry or the physics in the vertical direction. In a real problem with this one-dimensional nature you could minimize the problem size by keeping the vertical dimension one “element” thick. In this case however the vertical dimension has been extended to better illustrate the problem.

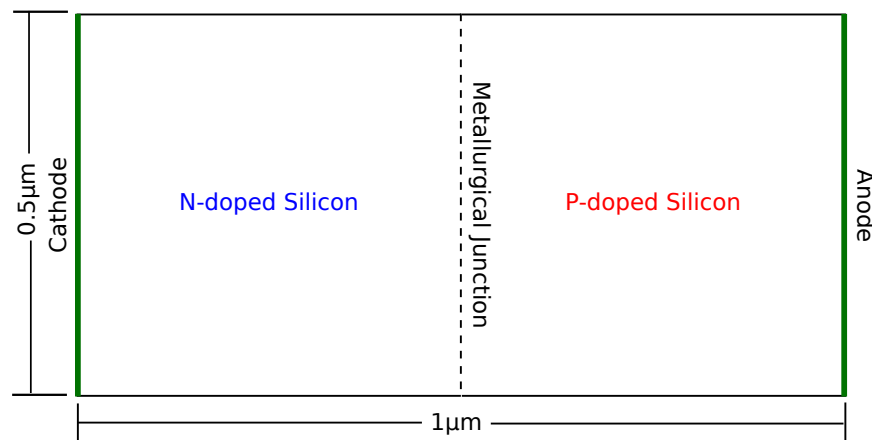


Figure 3-1 Geometry for a simple pseudo one-dimensional PN diode with a step junction. The metallurgical junction is at  $0.5\mu\text{m}$ .

#### 3.4.1. Mesh Generation Using Cubit

You can utilize Cubit using two methods: the first is via the graphical-user interface (GUI) and the second is via journal commands. The second method will be utilized here. Read the Cubit documentation for further information. Note that the journal commands can be entered from within the GUI.

The contents of a Cubit journal file used to generate a mesh are given in Figure 3-2 and the resulting mesh is shown in Figure 3-3. If you save the contents of Figure 3-2 as a file you can generate the mesh using cubit via the command line with:

```
cubit -batch -nojou <filename>
```

where <filename> is the name of the file in which the journal commands are saved.

The file is heavily commented and should be self explanatory. Further information can be found on the Cubit website (see table 2-2 for the URL) which has documentation available directly on

```

1  graphics mode wireframe
2
3  # Create a three-dimensional volume. The two-dimensional diode will be
4  # created on a surface of this three-dimensional volume. By default
5  # Charon assumes the dimensions are in microns
6  create brick x 1.0 y 0.5 z 0.1
7
8  # This makes the coordinates of the resulting mesh all positive. This
9  # isn't required but can be useful for post-processing
10 move vertex 4 location 0 0 0
11
12 # These will be the contacts, anode and cathode. The names are used in
13 # the input file to distinguish them
14 sideset 1 curve 3
15 sideset 1 name "anode"
16
17 sideset 2 curve 1
18 sideset 2 name "cathode"
19
20 # "blocks" are typically regions of different materials or distinct
21 # regions of the device. For this simple problem we only have one
22 # region
23 block 1 surface 1
24 block 1 name "si"
25
26 # Quads are currently the preferred element type for Charon
27 # simulations.
28 block 1 element type quad4
29
30
31 # The interval specifications set how dense or coarse the
32 # discretization is
33
34 ## Long side
35 curve 2 4 interval 100
36
37 ## Short side (contacts)
38 curve 3 1 interval 10
39
40 # Generate, or "mesh", the problem geometry
41 mesh surface 1
42
43 # Create the output "exodus" file, or overwrite it if it already
44 # exists.
45 export mesh "pndiode.exo" dimension 2 overwrite

```

**Figure 3-2** Cubit journal commands for the PN diode geometry illustrated in **Figure 3-1**.

the web page. The last statement in **Figure 3-2**, at line 45, instructs Cubit to output an Exodus mesh file named *pndiode.exo*. That file will be used as the input mesh file for the subsequent Charon simulation.

### **3.4.2. Charon Input Deck for a NLP Simulation**

In most Charon drift-diffusion device simulations it is necessary to first solve a simpler problem, the results of which are then used as an initial guess for the more complex simulation. The nonlinear Poisson, or NLP, simulation is used for that purpose and is mathematically described in **section 1.2**.

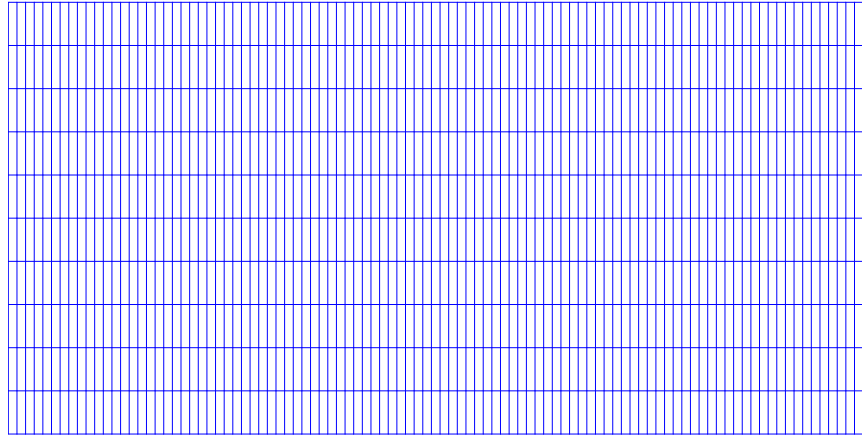


**Figure 3-3 Mesh for PN diode generated with Cubit.**

The Charon input file for the NLP simulation is shown in Listing 1 within Appendix D.1. Lines from that file will be discussed here in detail. More specifics about the syntax available via the input file can be found in Section 13.

The first block in the file is used to specify the input mesh.

```
1 # Name of the input exodus file, geometry only
2 import state file pndiode.exo
```

Line 1 contains a comment. Comments can increase the readability of the input files and should be generously utilized. Line 2 specifies that the file to be imported by Charon is named *pndiode.exo*. This file must exist and contain, at a minimum, the input mesh.

The next section specifies where and what output to perform.

```
5 start output parameters
6   output state file pndiode.nlp.exo
7 end output parameters
```

Line 5 illustrates the use of an input-file block. Such blocks encapsulate units of related specifications, in this case a block of text to specify output parameters, or how Charon will perform file output. A block begins with the `start` keyword, followed by the name of the input-file block, in this case `output parameters`, and ends with the `end` keyword. The `output parameters` text immediately following the `end` keyword is not required but can add to the readability of input-file blocks, particularly longer blocks containing a large number of lines.

Line 6 contains the name of the Exodus file to which output will be performed, *pndiode.nlp.exo*. If that file does not exist then it will be created. If the file exists then results from the simulation will be added to the existing file.

The next block is used to describe what physics is going to be solved during the simulation and how to associate material parameters with that physics.

```
9 start physics block semiconductor
10
11   # geometry block name IS case sensitive, note however that Cubit
```

```

12 # often downcases names prior to output so it is recommended
13 # that in Cubit you use all lower case for naming entities to
14 # avoid confusion.
15 geometry block is si
16
17 # The type of physics to be solved, in this case a nonlinear
18 # Poisson, or nlp, simulation will be performed
19 standard discretization type is nlp
20
21 # The name of the material model IS case sensitive. The name is

```

Line 9 is the start of the block, indicated with `start physics block`, followed by the name of the block, in this case `semiconductor`. Line 15 specifies the geometry block associated with this physics block. This name must correspond to an element block in the input Exodus file. Line 17 is the type of physics to simulate, in this case a `nlp`, or nonlinear Poisson, problem. Line 20 is the name of the material model for this physics. The name will be used to lookup the specifications for that material. Line 21 ends this input-file block. Note again that the only required keyword here is `end`, the name of the block is not required but can add to the readability of the input file.

The next block is a `material` block specification. The name of this block, `siliconParameter`, should be referenced in a physics block or it won't be utilized. In this case the reference is on line 20. Note that the material block name **is** case sensitive.

```

23 # in this input file.
24 material model is siliconParameter
25
26 end physics block semiconductor
27
28 # The material block where most material parameters for this
29 # simulation are set. It is specified in the physics block by it's
30 # name, siliconParameter.
31 start material block siliconParameter
32
33 # Material name IS case sensitive
34 material name is Silicon
35
36 # Simple, scalar, material property
37 relative permittivity = 11.9

```

The first non-comment line in this block, line 26, is the name of the material as used within Charon. This serves as a keyword by the code to look up default properties for that specific material, in this case silicon. The name **is** case sensitive and must match what is used within Charon for the specific material. Line 27 specifies the value of the `relative permittivity` material property for `Silicon`. Materials generally have default values for common material properties, such as relative permittivity, but those can be overridden via the input file, as in this case.

Lines 29–35 contain the doping specification for this problem. In this case the doping is a step junction with symmetric doping of donors and acceptors at  $1.0 \times 10^{16}/\text{cm}^3$ , the junction located at  $x = 0.5\mu\text{m}$  with the donor dopant on the left and the acceptor on the right in the  $x$  direction.

Line 37 ends the `material` block specification using the `end` keyword along with the optional `material` block `siliconParameter`.

The boundary conditions are specified on the following lines of the input file

```
39      # The doping for the diode
40      start step junction doping
```

Note that even though this example problem is a nonlinear Poisson simulation, an equilibrium problem, boundary conditions must be specified in the input file with the value of zero.

The specification of boundary conditions start with the `bc` keyword followed by the type of contact, `ohmic` in this case. Next the name of the relevant contact is given. Recall from Figure 3-1 that there were two contacts specified for the problem and they were named `anode` and `cathode`. These names were user specified during the construction of the mesh and completely arbitrary, although in this case they are physically significant.

Next, the name of `geometry` block which is adjacent to the boundary is given, in this case `si`. And finally the value of the actual boundary condition is given. In this case the specification is stated as a fixed, applied potential of zero volts. Since this is a NLP simulation and the only degree of freedom is electric potential, and there are only two contacts, no further boundary conditions are needed. Any boundary not specified, for example the top and bottom of the diode in this case, have the default zero-flux boundary condition applied to all degrees of freedom.

The initial conditions are set next via the line

```
42      donor concentration = 1e16
```

In this case the stanza simply says that `initial conditions` for the `ELECTRIC_POTENTIAL`, the only degree of freedom in this simulation, will be set using the an approximation for the equilibrium potential.

The last section in the input file deals with techniques for solving the sets of equations resulting from the simulation

```
44      dopant order is PN
45      direction is x
46      end step junction doping
```

Most settings are consolidated into a `solver` pack, in this case `solver` pack 1. A solver pack does have quantities that the user can override but it is generally best to make use of the default settings within a particular solver pack when possible. Other available solver packs, which simulation types they're relevant for, and how to override their settings will be covered in a subsequent section.

### 3.4.3. Command Line Serial Execution for a NLP simulation

The two items necessary to perform a Charon simulation are now in place, the input mesh file generated with Cubit, *pndiode.exo*, and an input file, *pndiode.nlp.inp*. The next step is to invoke the interpreter and have it perform the simulation via the Charon executable.

The basics of using *charonInterpreter.py* were covered in section 3.3.1. For the specific example here the invocation is

```
charonInterpreter.py -i pndiode.nlp.inp --run
```

If the example has never been executed before then a new Exodus output file named

```
pndiode.nlp-result.exo
```

will be created. If the file already exists then any results contained in the file will be overwritten.

This file contains a copy of the mesh as it existed in the input Exodus file as well as the results of the simulation, which in this case means the `ELECTRIC_POTENTIAL`, which was the degree of freedom in the NLP simulation. You can use a post-processing program such as Paraview (<http://www.paraview.org>) to visualize and post-process the results.

## 3.5. Example Problem: IV Sweep for a Pseudo One Dimensional Silicon PN Diode

This example problem builds on the example problem given in Section 3.4. The geometry is identical and given in Figure 3-1. The results of the NLP simulation described in that section will be used here as the initial guess for a full IV (current versus voltage) sweep of a drift diffusion simulation for the same diode. During an IV sweep the potential at one contact is incremented over a specified range while the potential at the other contact(s) is fixed at a specified value. At each bias point a simulation is performed and a scalar electric current is obtained. The voltage sweeping capability in Charon utilizes LOCA ([https://trilinos.github.io/nox\\_and\\_loca.html](https://trilinos.github.io/nox_and_loca.html)) to perform the sweep.

### 3.5.1. Charon Input Deck for an IV Sweep

The input file for the problem will be described in detail here. Note that this section will primarily cover the differences between the input file used for the IV sweep. The detail on parameters common to this IV sweep problem and the NLP simulation in the previous section were covered in Section 3.4.2.

The Charon input file for the IV simulation described here is given in Listing 2 within Appendix D.2. The first block of lines in that file to be discussed are



```

1 # Name of the input exodus file, which includes the results for
2 # ELECTRIC_POTENTIAL as obtained from a previous NLP simulation
3 import state file pndiode.nlp.exo at index 1

```

As stated in the comments on lines 1 and 2, we want to use the `ELECTRIC_POTENTIAL` as obtained from the NLP simulation as an initial guess for the IV sweep. The results from the NLP simulation were output to the file named `pndiode.nlp.exo` at the first index in that file. That file will be used for both the input geometry as well as the `ELECTRIC_POTENTIAL` at the first results index in that file.

Next, the output will go to a new file created by Charon. That is specified via input-file block

```

5 # Output exodus file for results of this simulation
6 start output parameters
7   output state file pndiode.dd.iv.exo
8 end output parameters

```

Since no special output is specified the default output, which is generally outputs all the degrees of freedom, will be output at each voltage step in the IV sweep.

The physics block for this simulation is similar to that for the NLP with the exception of lines 20 and 28.

```

10 start physics block Semiconductor
11
12   # geometry block name IS case sensitive, note however that Cubit
13   # often downcases names prior to output so it is recommended that
14   # in Cubit you use all lower case for naming entities to avoid
15   # confusion.
16   geometry block is si
17
18   # The type of physics to be solved, in this case a nonlinear
19   # Poisson, or nlp, simulation will be performed
20   standard discretization type is drift diffusion gfem
21
22   # The name of the material model IS case sensitive. The name is
23   # used as a key for the associated material block, also contained
24   # in this input file.
25   material model is siliconParameter
26
27   # Turn on Schokley-Reed-Hall recombination
28   srh recombination is on
29
30 end physics block

```

Line 20 tells the code what type of physics simulation we will be performing and what discretization we are utilizing for that simulation. In this case we are doing a full drift-diffusion simulation using the Galerkin finite-element discretization, or `gfem`. Line 28 specifies that SRH, or Shockley-Read-Hall, recombination should be enabled.

This simulation is for the same device as that in the example NLP simulation in the previous section, however, we are solving a different set of physics here, drift-diffusion in this case, NLP in

the previous case. As such, the material properties specified in the material block starting on line 32 and ending on line 49 is identical to that of the NLP problem covered in the previous section.

```
32 # The material block where most material parameters for this
33 # simulation are set. It is specified in the physics block by it's
34 # name, siliconParameter.
35 start material block siliconParameter
36
37 # Material name IS case sensitive
38 material name is Silicon
39 relative permittivity = 11.9
40
41 start step junction doping
42 acceptor concentration =1.0e16
43 donor concentration =1.0e16
44 junction location = 0.5
45 dopant order is PN
46 direction is x
47 end step junction doping
48
49 end material block siliconParameter
```

Next the initial conditions are specified in lines 51 through 61.

```
51 # This is taken from the NLP file. Note that it is read from "index 1"
52 # as specified in the input file specification. In this case there is
53 # only a single result in that file.
54 initial conditions for ELECTRIC_POTENTIAL in si is exodus file
55
56 # The NLP simulation does not include a solution for the carrier
57 # densities, therefore some other type of estimate, in this case an
58 # equilibrium calculation, is used to obtain an initial guess for
59 # the carrier densities.
60 initial conditions for ELECTRON_DENSITY in si is equilibrium density
61 initial conditions for HOLE_DENSITY in si is equilibrium density
```

The first thing to note is that as specified in line 54 the initial condition for ELECTRIC\_POTENTIAL is going to be read in from the exodus file that was specified as the input file in line 3.

Additionally line 3 specifies that the result in variable index 1 in that file is to be used. In this case, since that file is the result of a NLP simulation, there is only a single variable index contained in the file, but in more complex cases you can specify the relevant variable index. In transient simulations a variable index corresponds to a time index. In an IV sweep simulation the variable index corresponds to the index associated with a particular value of the voltage during the sweep.

For the remaining degrees of freedom in the problem, ELECTRON\_DENSITY and HOLE\_DENSITY, an approximation will be used to generate an initial guess internally since those variables were not part of the NLP simulation. In this case lines 60 and 61 specify that the equilibrium density approximation be used for the initial guess.

The boundary conditions are set for the problem in lines 64 and 65 Next the initial conditions are specified in lines 51 through 61.

```
63 # Boundary conditons at the contacts.  
64 bc is ohmic for cathode on si fixed at 0.0  
65 bc is ohmic for anode on si swept from 0.0 to 1.0
```

The boundary condition for the cathode is specified in line 64 as an `ohmic` type contact and is going to have a fixed bias of 0 volts applied to it for the entirety of the sweep.

The boundary condition for the anode is specified in line 65 as the same type, `ohmic`, but in this case also specifies that the value of the bias to be applied is going to be swept from 0 to 1 volt.

How the voltage on the anode is going to be swept is controlled by lines 68 through 72 of the input file.

```
67 # Sweep parameter controls  
68 start sweep options  
69     initial step size = 0.02  
70     minimum step size = 0.02  
71     maximum step size = 0.02  
72 end sweep options
```

The LOCA package which is used by Charon to perform parameter sweeps, like this voltage sweep, is capable of very sophisticated step control. However, in this case only a simple constant voltage step of 0.02V will be used.

As in the previous NLP example, the last section of the code deals with solver settings.

```
74 # Use a straightforward solver pack for this simulation.  
75 start solver block  
76     use solver pack 1  
77 end solver block
```

Most settings are consolidated into a `solver pack`, in this case `solver pack 1`. A solver pack does have quantities that the user can override but it is generally best to make use of the default settings within a particular solver pack when possible. Other available solver packs, which simulation types they're relevant for, and how to override their settings will be covered in a subsequent section.

### **3.5.2. Command Line Serial Execution for an IV sweep**

The items necessary to perform the IV sweep are now in place, the file containing the initial guess and input mesh, `pndiode.nlp.exo` and the input file, `pndiode.iv.inp`. In order to run the problem simply invoke the interpreter like

```
charonInterpreter.py -i pndiode.iv.inp --run
```

An initial run, without having previously executed this command, a couple of results files will be generated

```
pndiode.dd.iv.exo
currents-loca.dat
```

The first file contains the results of the simulation for each voltage step. This includes the degrees of freedom at each voltage step, `ELECTRIC_POTENTIAL`, `ELECTRON_DENSITY` and `HOLE_DENSITY`, as well as the scalar electric current at the contacts. For convenience Charon also outputs scalar electric currents to a regular text file at each of the contacts for each of the voltage steps taken during the sweep.

For post-processing a visualization program such as Paraview (<http://www.paraview.org>) can be used to examine the exodus file. If only the currents are of interest a standard plotting package, such as `gnuplot`, can be used to plot the results. For this case the results are shown in Figure 3-4.

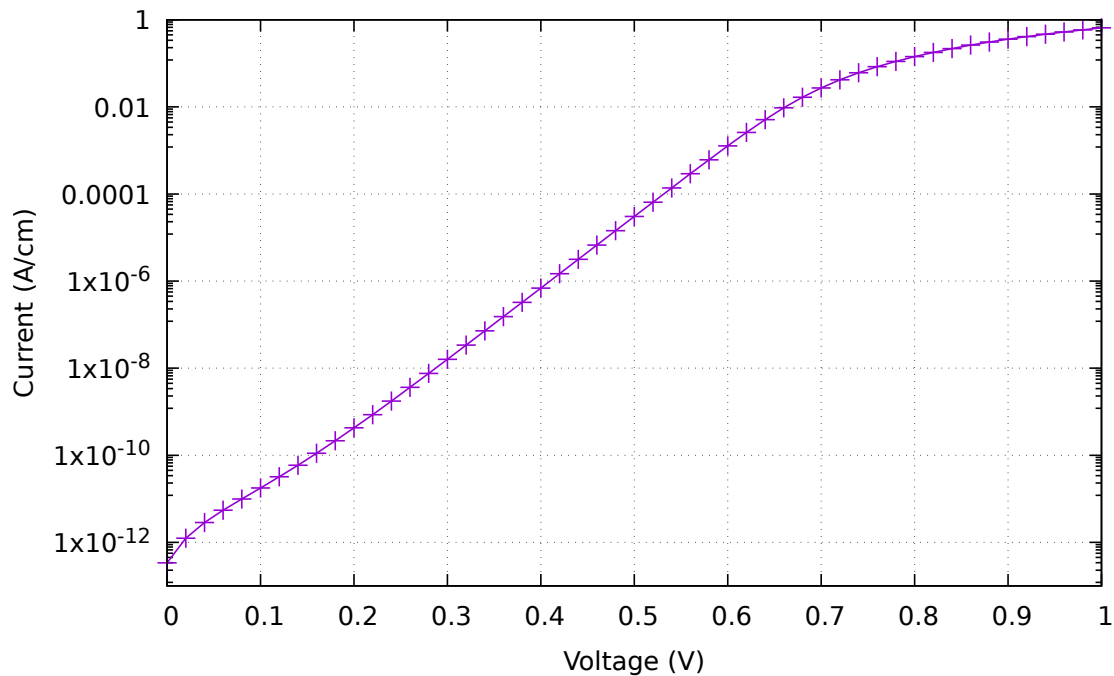


Figure 3-4 Results of IV sweep

## 4. BOUNDARY CONDITIONS

### 4.1. Ohmic Contacts

Boundary conditions for Ohmic contacts are derived assuming charge neutrality and equilibrium conditions and in relation to carrier statistics and dopant ionization. By imposing charge neutrality and equilibrium conditions:

$$\begin{aligned} n_0 - p_0 &= N_D^+ - N_A^- = C, \\ n_0 p_0 &= n_i^2 \end{aligned} \quad (10)$$

the carrier densities and contact potential assuming fully ionized dopants and Maxwell-Boltzmann statistics can be solved for at the Ohmic contacts. For a n-type semiconductor they are given by:

$$\begin{aligned} n_0 &= \frac{C}{2} + \sqrt{\left(\frac{C}{2}\right)^2 + n_i^2}, \\ p_0 &= \frac{n_i^2}{n_0}, \\ \phi &= \frac{k_B T}{q} \ln(y) + \frac{1}{q} (E_{ref} - \lambda) + V, \\ y &= \frac{C}{2N_C} + \sqrt{\left(\frac{C}{2N_C}\right)^2 + \frac{N_V}{N_C} \exp\left(-\frac{E_G}{k_B T}\right)} \end{aligned} \quad (11)$$

and for a p-type semiconductor by:

$$\begin{aligned} p_0 &= \frac{-C}{2} + \sqrt{\left(\frac{C}{2}\right)^2 + n_i^2}, \\ n_0 &= \frac{n_i^2}{p_0}, \\ \phi &= \frac{-k_B T}{q} \ln(y) + \frac{1}{q} (E_{ref} - \lambda - E_G) + V, \\ y &= -\frac{C}{2N_V} + \sqrt{\left(\frac{C}{2N_V}\right)^2 + \frac{N_C}{N_V} \exp\left(-\frac{E_G}{k_B T}\right)} \end{aligned} \quad (12)$$

where  $V$  is the voltage applied at the Ohmic contact and  $E_{ref}$  is the Fermi energy of the reference material.

For Fermi Dirac statistics the second equilibrium condition in Eq.(10) rewrites as  $n_0 p_0 = \gamma_n \gamma_p n_i^2$  where  $\gamma_n, \gamma_p$  are the electron and hole degeneracy factors. If the dopants are fully ionized, the

carrier densities and contact potential are given by

$$\begin{aligned} n_0 &= C, \\ p_0 &= N_V \exp \left( -\mathcal{F}_{1/2}^{-1} \left( \frac{n_0}{N_C} \right) - \frac{E_G}{k_B T} \right), \\ \phi &= \frac{1}{q} (E_{ref} - \lambda) + \frac{k_B T}{q} \mathcal{F}_{1/2}^{-1} \left( \frac{n_0}{N_C} \right) + V \end{aligned} \quad (13)$$

for a n-type semiconductor and by

$$\begin{aligned} p_0 &= C, \\ n_0 &= N_C \exp \left( -\mathcal{F}_{1/2}^{-1} \left( \frac{p_0}{N_V} \right) - \frac{E_G}{k_B T} \right), \\ \phi &= \frac{1}{q} (E_{ref} - \lambda - E_G) - \frac{k_B T}{q} \mathcal{F}_{1/2}^{-1} \left( \frac{p_0}{N_V} \right) + V \end{aligned} \quad (14)$$

for a p-type semiconductor.

When incomplete ionization models are used for dopants (see §8.1), implicit algebraic equations are used to solve for carrier densities instead of the explicit relations in Eq.(11), Eq.(12), Eq.(13) and Eq.(14). The carrier densities are computed using one of the system of algebraic equations, selected by the user input:

$$\begin{aligned} n_0 - p_0 &= N_D^+ - N_A^- = \frac{N_D}{1 + g_D \frac{n_0}{n_1}} - N_A, \\ n_0 p_0 &= \gamma_n \gamma_p n_i^2 \end{aligned} \quad (15)$$

$$\begin{aligned} n_0 - p_0 &= N_D^+ - N_A^- = \frac{N_D}{1 + g_D \frac{n_0}{n_1}}, \\ n_0 p_0 &= \gamma_n \gamma_p n_i^2 \end{aligned} \quad (16)$$

$$\begin{aligned} n_0 - p_0 &= N_D^+ - N_A^- = \frac{N_D}{1 + g_D \frac{n_0}{n_1}} - \frac{N_A}{1 + g_A \frac{n_i^2}{n_1 n_0}}, \\ n_0 p_0 &= \gamma_n \gamma_p n_i^2 \end{aligned} \quad (17)$$

for a n-type semiconductor and

$$\begin{aligned} n_0 - p_0 &= N_D^+ - N_A^- = N_D - \frac{N_A}{1 + g_A \frac{p_0}{p_1}}, \\ n_0 p_0 &= \gamma_n \gamma_p n_i^2 \end{aligned} \quad (18)$$

$$\begin{aligned} n_0 - p_0 &= N_D^+ - N_A^- = -\frac{N_A}{1 + g_A \frac{p_0}{p_1}}, \\ n_0 p_0 &= \gamma_n \gamma_p n_i^2 \end{aligned} \quad (19)$$

$$\begin{aligned}
n_0 - p_0 &= N_D^+ - N_A^- = \frac{N_D}{1 + g_D \frac{n_i^2}{n_1 p_0}} - \frac{N_A}{1 + g_A \frac{p_0}{p_1}}, \\
n_0 p_0 &= \gamma_n \gamma_p n_i^2
\end{aligned} \tag{20}$$

for p-type semiconductor. For Maxwell-Boltzmann statistics the electron and hole degeneracy coefficients  $\gamma_n$  and  $\gamma_p$  become both 1.

To enable/use an Ohmic contact the user must specify one of the following lines at the root level of the interpreter input file, depending on the type of biasing used

BC is Ohmic for {contactName} on {MaterialName} fixed at {voltage}

or

BC is Ohmic for {contactName} on {MaterialName} swept from {voltage1} to {voltage2}

where *contactName* is a valid sideset name to be used as an Ohmic contact, *materialName* is a valid material name the Ohmic contact is connected to, *voltage* is a fixed voltage applied at the Ohmic contact, *voltage1* and *voltage2* are the start and end voltages at the Ohmic contact in the case of a voltage sweep.

## 4.2. Schottky Contacts

Boundary conditions at Schottky contacts are based on the thermionic emission theory developed by Bethe [13]. The thermionic emission theory assumes that at the metal/semiconductor interface where the boundary conditions are derived, the barrier height is much larger than  $k_B T$ , thermal equilibrium is valid at the plane that determines emission and the net current flow through the interface does not effect the equilibrium. The energy band diagrams of the n-type and p-type Schottky interfaces between metal and semiconductor are shown in Figure 4-1, with the thick line indicating the interface where the boundary conditions are imposed. Carriers at Schottky interface are assumed to follow Maxwell-Boltzmann statistics. Under these assumptions, the boundary conditions for a n-type or p-type Schottky contact are:

$$\begin{aligned}
q\phi &= E_{ref} - W_F + qV_{app}, \\
J_{n,norm} &= \frac{A_n^* T^2}{N_C} (n - n_0^B), \\
J_{p,norm} &= -\frac{A_p^* T^2}{N_V} (p - p_0^B)
\end{aligned} \tag{21}$$

where  $E_{ref}$  is the intrinsic Fermi energy level of the reference material from vacuum,  $A_n^*$  and  $A_p^*$  are electron and hole Richardson constants,  $n_0^B = N_C \exp\left(-\frac{q\phi_B}{k_B T}\right)$  and  $p_0^B = N_V \exp\left(\frac{-E_G + q\phi_B}{k_B T}\right)$  are the electron and hole equilibrium densities,  $J_{n,norm}$  and  $J_{p,norm}$  are the electron and hole currents normal to the metal/semiconductor interface,  $W_F$  is the metal workfunction and  $V_{app}$  is the applied voltage at the Schottky contact.

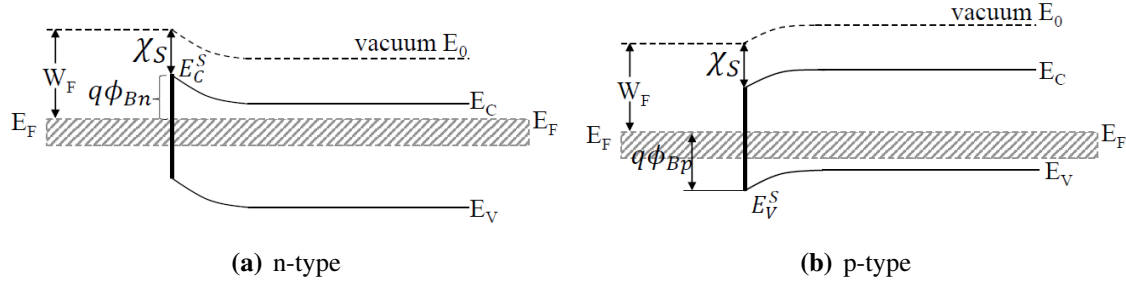


**Figure 4-1 Band diagram of Schottky contacts**

To enable/use a Schottky contact the user must specify the following blocks at the root level of the interpreter input file:

```
start Schottky BC for {contactName} on {materialName}
  voltage is fixed at {voltage}
  type is electron/hole
  (one parameter per line in the form):
  {parameter name} = {parameter value}
  (see table 4-1 for available parameters)
end
```

or

```
start Schottky BC for {contactName} on {materialName}
  voltage is swept from {voltage} to {voltage2}
  type is electron/hole
  (one parameter per line in the form):
  {parameter name} = {parameter value}
  (see table 4-1 for available parameters)
end
```

**Table 4-1 Syntax and parameters for the Schottky contact.**

Input file	Corresponding variable in (21)	Description	Units
work function	$W_F$	contact metal work function	$eV$
electron richardson constant	$A_n^*$	electron Richardson constant	$\frac{A}{K^2 cm^2}$
hole richardson constant	$A_p^*$	hole Richardson constant	$\frac{A}{K^2 cm^2}$

#### 4.2.1. Schottky Contacts Barrier Lowering

The barrier lowering model implemented by Charon accounts for two different physical mechanisms at the Schottky contacts: image force potential and dipole effect. The barrier height change is modeled as

$$\Delta\phi_B = \alpha \sqrt{\frac{qE}{4\pi\epsilon_{semic}}} + \beta E^\gamma \quad (22)$$



where the first term is due the image force potential and the second term due to dipole effect. The default values for the parameters in Eq.(22) are  $\alpha = 1.0$ ,  $\beta = 0.0$  and  $\gamma = 1.0$ . When barrier lowering model is used, the Schottky boundary conditions in Eq.(21) remains unchanged but equilibrium electron and hole densities at the contact are modified to account for the lowering of the barrier. For a n-type contact equilibrium densities change to:

$$\begin{aligned} n_0^B &= N_C \exp\left(-\frac{q(\phi_B - \Delta\phi_B(E))}{k_B T}\right), \\ p_0^B &= N_V \exp\left(\frac{-E_G + q(\phi_B - \Delta\phi_B(E))}{k_B T}\right) \end{aligned} \quad (23)$$

and for a p-type contact to

$$\begin{aligned} n_0^B &= N_C \exp\left(-\frac{q(\phi_B + \Delta\phi_B(E))}{k_B T}\right), \\ p_0^B &= N_V \exp\left(\frac{-E_G + q(\phi_B + \Delta\phi_B(E))}{k_B T}\right) \end{aligned} \quad (24)$$

Poisson equation is solved consistently with the real charge seeing a full barrier at the Schottky contact, while the electron and hole continuity equations see a combined Poisson and image-force potential.

To activate the barrier lowering model at a Schottky contact the user must specify the following block inside the Schottky contact block

```
start Schottky BC for {contactName} on {materialName}
...
start barrier lowering parameters
(one parameter per line in the form):
/*!{parameter name} = {parameter value}
(see table 4-2 for available parameters)
end
...
end
```

**Table 4-2 Syntax and parameters for the Schottky Contact Barrier Lowering.**

Input file	Corresponding variable in (22)	Description	Units	Default
alpha	$\alpha$	specifies parameter alpha	<i>none</i>	1.0
beta	$\beta$	specifies parameter beta	<i>none</i>	0.0
gamma	$\gamma$	specifies parameter gamma	<i>none</i>	1.0

#### 4.2.2. Schottky Contacts Barrier Tunneling

Effects of tunneling at the Schottky contacts can be taken into account by enabling tunneling. Charon uses a tunneling model based on Tsu-Esaki formula (see [47]) to simulate the effects of

tunneling currents through the Schottky barrier. The tunneling currents at the Schottky contact are given by:

$$\begin{aligned} J_e &= \frac{4\pi q k_B T m_{eff}^e}{h^3} \int_{E_{F,M}+qV_a}^{E_{F,M}+q\phi_{Bn}} TC_e(\xi) N_e(\xi) d\xi, \\ J_h &= \frac{4\pi q k_B T m_{eff}^h}{h^3} \int_{E_{F,M}+qV_a}^{E_{F,M}+q\phi_{Bp}} TC_h(\xi) N_h(\xi) d\xi \end{aligned} \quad (25)$$

where

$$\begin{aligned} TC_e(\xi) &= \exp\left(-\frac{8\pi\sqrt{2m_{tunnel}^e m_0}}{3qhE}(q\phi_{Bn}-\xi)^{3/2}\right), \\ TC_h(\xi) &= \exp\left(-\frac{8\pi\sqrt{2m_{tunnel}^h m_0}}{3qhE}(q\phi_{Bp}-\xi)^{3/2}\right) \end{aligned} \quad (26)$$

are the transmission coefficients of the Schottky barrier and

$$\begin{aligned} N_e(\xi) &= \ln\left(\frac{1 + \exp\left(-\frac{\xi - E_{F,M}}{k_B T}\right)}{1 + \exp\left(-\frac{\xi - (E_{F,M} + qV_a)}{k_B T}\right)}\right), \\ N_h(\xi) &= \ln\left(\frac{1 + \exp\left(-\frac{E_{F,M} - \xi}{k_B T}\right)}{1 + \exp\left(-\frac{(E_{F,M} + qV_a) - \xi}{k_B T}\right)}\right) \end{aligned} \quad (27)$$

are the carrier supply functions.

The transmission coefficients  $TC_e(\xi)$  and  $TC_h(\xi)$  are a measure of the Schottky barrier transparency and they are functions of the electric field at the contact on the semiconductor side. The supply functions  $N_e(\xi)$  and  $N_h(\xi)$  are the differences in the supply of carriers at the interface and they are derived assuming Fermi-Dirac statistics for carriers. When the tunneling model is enabled, the tunneling currents in Eq.(25) are added to the thermionic emission currents in Eq.(21) as a total current at the Schottky contact.

To activate the tunneling model at the Schottky contact the user must specify the following block inside the Schottky contact block

```
start Schottky BC for {contactName} on {materialName}
...
start barrier tunneling parameters
(one parameter per line in the form):
{parameter name} = {parameter value}
(see table 4-3 for available parameters)
end
...
end
```

**Table 4-3 Syntax and parameters for the Schottky Contact Tunneling.**

Input file	Corresponding variable in (25) and (26)	Description	Units
mass	$m_{tunnel}^e$ or $m_{tunnel}^h$	specifies carrier relative tunneling mass	<i>none</i>

### 4.3. Gate Contacts

in progress

### 4.4. Constraint Boundary Conditions

There are two types of constraints supported at device contacts:

**Constant Current** This constraint corresponds to the user attaching a current source to one terminal of the device. The user therefore specifies that current value in amps. There can be at most one of these constraints on the device.

**Resistor Contact** This constraint corresponds to the user attaching a resistor to one terminal of the device, with a voltage source on the far side of the resistor. The user therefore specifies that applied voltage in volts, along with the resistance in ohms.

All constraints have the following common attributes:

- the sideset ID denoting the terminal to which the constraint is applied;
- the initial value given to the voltage parameter corresponding to this constraint; and
- the element block ID corresponding to the sideset ID.

There can be at most one constraint on any given terminal of the device.

#### 4.4.1. Device Contact Dimensions

In addition to the common attributes listed above, all constraints can have two other common attributes that are only applicable in a two-dimensional simulation:

- the length of the contact in the simulation in  $\mu\text{m}$ ; and
- the actual device contact area in  $\mu\text{m}^2$ .

Internally Charon will deal with currents in A/cm for 2-D simulations, so these values are used to scale the currents to Amps if you would like to compare to experimental results. The first is the length of the sideset to which the constraint is applied. You should know this value from the mesh you created in Cubit. The second is the surface area of the contact on the actual device you're simulating. Note that the units here are  $\mu\text{m}$  and  $\mu\text{m}^2$ , respectively. These two quantities must be specified together; you cannot specify one without the other.

If you choose to omit these quantities for a 2-D simulation, there will be no scaling of the currents that takes place. If you accidentally specify these quantities for a 3-D simulation, they will simply be ignored.

#### **4.4.2. Constant Current**

Now let's take a look at how you would specify one of these constraints in an input deck.

```
bc is current for anode on silicon fixed at -3.9e-7 with initial voltage 0.1
```

The `bc is current` indicates to Charon that this contact has a constant-current applied to it for the simulation. The `for anode on silicon` tells Charon what contact the constant-current will be applied to, in this case the contact named `anode`, and what geometry block that contact is associated with, `silicon` in this case.

At present `fixed` is the only valid keyword when an electric current is applied to a contact and it is followed by the value of the fixed current, at  $-3.9\text{e-}7$ , or  $-0.39\mu\text{A}$ . As stated in Section 3.2, the minus sign on the value indicates the current is flowing into the specified contact.

Finally the applied bias to use as the starting point on the contact is given, `with initial voltage 0.1`. This is just a guess of the bias at the contact that would yield the given current. Generally you can get a good estimate of this by looking at IV curves associated with the device and picking off the voltage at the specified current. The better this estimate the more rapidly the simulation will complete. If the value of initial voltage is too far off the actual value then Charon may have trouble converging. You can also think of the initial voltage as the parameter that will be iteratively solved for as the simulation proceeds, thus the need for a good initial guess.

The full syntax for this boundary condition is given in Table 4-4.

#### **4.4.3. Resistor Contact**

The syntax used to perform a simulation with a resistor attached to a contact is similar to that used for a constant-current constraint.

```
bc is resistor for cathode on silicon with resistor 1e3 fixed at -4e-3 and  
initial voltage 0.1
```

**Table 4-4 Syntax for specifying constant current at a contact**

BC is current for { <i>contactName</i> } on { <i>materialName</i> } fixed at { <i>current</i> } with initial voltage { <i>voltage</i> } [ with area { <i>contact area</i> } [ and length { <i>contact length</i> } [ with base doping { <i>base doping type</i> } ] ] ]		
Option	Description	Required
fixed at	Current is fixed at this contact	Yes
with initial voltage	Voltage to start simulation with. This can be considered an initial guess for the voltage.	Yes
with area	The contact area ( $cm^2$ )	No
and length	The contact length ( $cm$ )	No
with base doping	When utilized in a pseudo-1D BJT simulation, the doping at the base contact	No
Variables	Description	Default
<i>contactName</i>	Specifies a valid sideset name to be used as an Ohmic contact	<i>none</i>
<i>materialName</i>	Specifies a valid material name the Ohmic contact is connected to.	<i>none</i>
<i>current</i>	Fixed current applied at the contact, in amps	<i>none</i>
<i>voltage</i>	Approximate starting voltage at the contact. This can be considered an initial guess for the voltage at the contact.	<i>none</i>
<i>contact area</i>	Area of the contact ( $cm^2$ )	1.0
<i>contact length</i>	Length of the contact ( $cm$ )	1.0
<i>base doping type</i>	Type of doping at the base of a pseudo-1D BJT ( <i>acceptor</i> or <i>donor</i> )	<i>none</i>

Note that the input above would be on a single line in the input file but was broken here to avoid running past the margins.

The `is resistor` indicates the boundary-condition to be used here utilizes a resistor attached to the contact that is specified via `for cathode on silicon`. The resistance of the attached resistor is specified with `with resistor 1e3`. The value is always in ohms so in this example the resistance is  $1k\Omega$ .

The `fixed at -4e3` specifies the value of the voltage on the terminal that is not attached to the device. The `initial voltage` is the same as that specified in the constant-current simulation and can be considered an initial guess for the voltage at the device terminal to which the resistor is attached. An illustration is shown in Figure 4-2.

The full syntax for this boundary condition is given in Table 4-5.

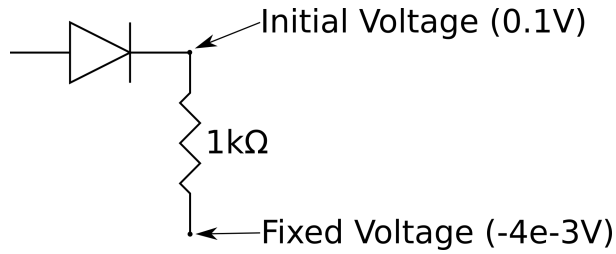


Figure 4-2 Diagram for illustration of a resistor attached to a device contact.

Table 4-5 Syntax for specifying resistor attached to a contact

BC is resistor for { <i>contactName</i> } on { <i>materialName</i> } with resistor { <i>resistance</i> } fixed at { <i>voltage1</i> } and initial voltage { <i>voltage2</i> } [ with area { <i>contact area</i> } [ and length { <i>contact length</i> } [ with base doping { <i>base doping type</i> } ] ] ]		
Option	Description	Required
with resistor	The resistance value of the attached resistor	Yes
fixed at	Voltage is fixed at the resistor contact NOT connected to the device. See Figure 4-2.	Yes
with initial voltage	Voltage to start simulation with. This can be considered an initial guess for the voltage.	Yes
with area	The contact area ( $cm^2$ )	No
and length	The contact length ( $cm$ )	No
with base doping	When utilized in a pseudo-1D BJT simulation, the doping at the base contact	No
Variables	Description	Default
<i>contactName</i>	Specifies a valid sideset name to be used as an Ohmic contact	<i>none</i>
<i>materialName</i>	Specifies a valid material name the Ohmic contact is connected to.	<i>none</i>
<i>resistance</i>	The resistance value of the attached resistor (ohms).	<i>none</i>
<i>voltage1</i>	Voltage applied at the resistor contact (volts).	<i>none</i>
<i>voltage2</i>	Approximate starting voltage at the device contact where the resistor is attached. This can be considered an initial guess for the voltage at the contact.	<i>none</i>
<i>contact area</i>	Area of the contact ( $cm^2$ )	1.0
<i>contact length</i>	Length of the contact ( $cm$ )	1.0
<i>base doping type</i>	Type of doping at the base of a pseudo-1D BJT ( <i>acceptor</i> or <i>donor</i> )	<i>none</i>

#### 4.4.4. Constant Current on the Base Contact of a Pseudo 1D BJT

In order to perform a simulation of a pseudo one-dimensional **BJT** a special boundary condition must be utilized for the base contact due to the fact that such a contact is not physical in a pseudo 1D simulation of a **BJT**. When using this boundary condition often you might want to apply a constant current to the base contact. This is possible via the input line

```
bc is current for base on silicon fixed at 1.5e-6 and initial voltage 0.0 with base
doping acceptor
```

Note that the example above was wrapped to avoid clipping. It would comprise a single line in an actual input file.

The only difference to note between this case and the one given in Section 4.4.2 is the addition of the `with base doping acceptor`. This tells Charon that the contact is a base contact in an pseudo-1D, NPN **BJT**.

An illustration of a pseudo-1D **BJT** is given in Figure 4-3. The information for this type of boundary condition can be found in Table 4-4.



Figure 4-3 Pseudo one-dimensional **BJT**.

#### 4.4.5. Solver Specifications for Constrained Problems

Constrained problems generally require slightly different solver settings than typical steady-state problems. At the present time those settings are encapsulated in Charon's `solver pack 3`. An example of a solver specification for a simulation with a constraint would be

```
start solver block
  use solver pack 3
end solver block
```

The solver settings are constantly being refined for specific problem types and so it is generally beneficial to examine the latest version of this manual, or contact the developers directly, to get recommendations on solver settings for specific problem types, particularly when convergence problems arise for your simulation.

## 5. BAND STRUCTURE

### 5.1. Intrinsic Density

Effective intrinsic density in Charon is given by

$$n_{ie}(T) = \sqrt{N_C(T)N_V(T)} \exp\left(\frac{-E_G(T)}{2k_B T}\right) \exp\left(\frac{\Delta E_G}{2k_B T}\right) \quad (28)$$

where  $N_C$ ,  $N_V$  are the conduction and valence band effective density of states,  $E_G$  is the bandgap energy and  $\Delta E_G$  is the bandgap narrowing.

By default no bandgap narrowing is taken into account ( $\Delta E_G = 0.0$ ). Four bandgap narrowing models are available in Charon on user request: Old Slotboom [42], Slotboom [30], Harmon [22] and Persson [38]. Four intrinsic models with the same names of the bandgap narrowing models are available.

Old Slotboom model computes bandgap narrowing due to the heavy doping as a function of the total doping [42]

$$\begin{aligned} \Delta E_G &= V_{0,\text{bgn}} \left( \ln\left(\frac{N_{\text{tot}}}{N_{0,\text{bgn}}}\right) + \sqrt{\left(\ln\left(\frac{N_{\text{tot}}}{N_{0,\text{bgn}}}\right)\right)^2 + C_{\text{bgn}}} \right) \quad \text{if } N_{\text{tot}} \geq 10^{10} \text{ cm}^{-3}, \\ \Delta E_G &= 0 \quad \text{if } N_{\text{tot}} < 10^{10} \text{ cm}^{-3} \end{aligned} \quad (29)$$

where  $N_{\text{tot}}$  is the total doping and parameters  $V_{0,\text{bgn}}$ ,  $N_{0,\text{bgn}}$  and  $C_{\text{bgn}}$  and their description are listed in table 5-1.

To enable Old Slotboom intrinsic density with associated bandgap narrowing model, the user must enable bandgap narrowing in the appropriate physics section

```
start Physics Block {physicsBlockName}
...
band gap narrowing is on
...
end
```

and specify the Old Slotboom intrinsic concentration model with its parameters in the material block section

```
start Material Block {materialBlockName}
start intrinsic concentration
model is old slotboom
start oldslotboom parameters
(one parameter per line in the form):
{parameter name} = {parameter value}
(see table 5-1 for available parameters)
end
end
end
```



**Table 5-1 Syntax and parameters for Old Slotboom model.**

Input file	Corresponding variable in (29)	Description	units
V0_BGN	$V_{0,bgn}$	$V_{0,bgn}$ coefficient	V
N0_BGN	$N_{0,bgn}$	$N_{0,bgn}$ coefficient	$\frac{1}{cm^3}$
CON_BGN	$C_{bgn}$	$C_{bgn}$ coefficient	none

If no parameters are specified, default parameters for the corresponding material are used.

Slotboom model [30] is similar to Old Slotboom model and it uses the same formula to compute the bandgap narrowing, but it has different default parameters for  $V_{0,bgn}$ ,  $N_{0,bgn}$  (see table 5-2) and a different  $N_{tot}$  cutoff

$$\Delta E_G = V_{0,bgn} \left( \ln \left( \frac{N_{tot}}{N_{0,bgn}} \right) + \sqrt{\left( \ln \left( \frac{N_{tot}}{N_{0,bgn}} \right) \right)^2 + C_{bgn}} \right) \quad \text{if } N_{tot} \geq 10^{15} cm^{-3},$$

$$\Delta E_G = 0 \quad \text{if } N_{tot} < 10^{15} cm^{-3} \quad (30)$$

To use Slotboom intrinsic density with associated bandgap narrowing model, the user must enable bandgap narrowing in the appropriate physics section

```
start Physics Block {physicsBlockName}
...
band gap narrowing is on
...
end
```

and specify Slotboom intrinsic concentration model with its parameters in the material block section

```
start Material Block {materialBlockName}
start intrinsic concentration
model is slotboom
start slotboom parameters
(one parameter per line in the form):
{parameter name} = {parameter value}
(see table 5-2 for available parameters)
end
end
end
```

If no parameters are specified, default parameters for the corresponding material are used.

Harmon model [22] calculates the bandgap narrowing as

$$\Delta E_G = A_n (N_D - N_A)^{1/3} + \Delta E_{G,ncor} \quad \text{if } N_D - N_A \geq 0,$$

$$\Delta E_G = A_p (N_A - N_D)^{1/3} + \Delta E_{G,pcor} \quad \text{if } N_D - N_A < 0 \quad (31)$$

**Table 5-2 Syntax and parameters for Slotboom model.**

Input file	Corresponding variable in (30)	Description	units
V0_BGN	$V_{0,bgn}$	$V_{0,bgn}$ coefficient	V
N0_BGN	$N_{0,bgn}$	$N_{0,bgn}$ coefficient	$\frac{1}{cm^3}$
CON_BGN	$C_{bgn}$	$C_{bgn}$ coefficient	none

where material parameters  $A_n$  and  $A_p$  are described in table 5-3.  $\Delta E_{G,ncor}$  and  $\Delta E_{G,pcor}$  are Fermi-Dirac correction terms which are activated when Fermi Dirac statistics for carriers is used. For Boltzmann statistics, the default statistics in Charon, the corrections terms become zero. The doping-dependent Fermi-Dirac corrections terms are given by

$$\begin{aligned}\Delta E_{G,ncor} &= k_B T \left( \ln \left( \frac{N_D - N_A}{N_C} \right) - \mathcal{F}_{1/2}^{-1} \left( \frac{N_D - N_A}{N_C} \right) \right) \quad \text{if} \quad \frac{N_D - N_A}{N_C} \geq 10^{-4}, \\ \Delta E_{G,ncor} &= 0.0 \quad \text{if} \quad \frac{N_D - N_A}{N_C} < 10^{-4}\end{aligned}\tag{32}$$

where  $N_D - N_A \geq 0$  (n-type) and

$$\begin{aligned}\Delta E_{G,ncor} &= k_B T \left( \ln \left( \frac{N_D - N_A}{N_C} \right) - \mathcal{F}_{1/2}^{-1} \left( \frac{N_D - N_A}{N_C} \right) \right) \quad \text{if} \quad \frac{N_D - N_A}{N_C} \geq 10^{-4}, \\ \Delta E_{G,pcor} &= k_B T \left( \ln \left( \frac{N_A - N_D}{N_V} \right) - \mathcal{F}_{1/2}^{-1} \left( \frac{N_A - N_D}{N_V} \right) \right) \quad \text{if} \quad \frac{N_A - N_D}{N_V} \geq 10^{-4}, \\ \Delta E_{G,pcor} &= 0.0 \quad \text{if} \quad \frac{N_A - N_D}{N_V} < 10^{-4}\end{aligned}\tag{33}$$

where  $N_A - N_D \geq 0$  (p-type).

To enable Harmon intrinsic density with associated bandgap narrowing model, the user must enable bandgap narrowing in the appropriate physics section

```
start Physics Block {physicsBlockName}
...
band gap narrowing is on
...
end
```

and specify Harmon intrinsic concentration model with its parameters in the material block section

```
start Material Block {materialBlockName}
start intrinsic concentration
model is harmon
start harmon parameters
enable fermi = {fermiCorrection}
```

```

    (one parameter per line in the form):
    {parameter name} = {parameter value}
    (see table 5-3 for available parameters)
end
end
end

```

where *fermiCorrection* flag must be true to enable Fermi-Dirac corrections in (32) and (33) or false or not specified if corrections are not used.

Harmon model has the option to calculate the bandgap narrowing directly based on a file provided by the user with lines specifying changes in conduction and valence band due to narrowing as a function of doping with the following format:

Doping <sub>1</sub>	$\Delta E_{C,1}$	$\Delta E_{V,1}$
Doping <sub>2</sub>	$\Delta E_{C,2}$	$\Delta E_{V,2}$
	.	
	.	
	.	
Doping <sub>n</sub>	$\Delta E_{C,n}$	$\Delta E_{V,n}$

In this case  $\Delta E_G = \Delta E_C + \Delta E_V$  and formulas (31), (32) and (33) are not used.

To use Harmon intrinsic density with bandgap narrowing computed from the file, the user must enable bandgap narrowing in the appropriate physics section

```

start Physics Block {physicsBlockName}
...
band gap narrowing is on
...
end

```

and specify bgn file option in the Harmon intrinsic model parameter section

```

start Material Block {materialBlockName}
start intrinsic concentration
model is harmon
start harmon parameters
bgn file = {fileName}
end
end
end

```

with *fileName* the name of the file containing the bandgap narrowing data.

Persson bandgap narrowing model [38] computes doping-induced energy shifts in the conduction and valence bands. The model takes into account the exchange energy for majority carriers, correlation energy for minority carriers, and impurity interaction between the conduction and

**Table 5-3 Syntax and parameters for Harmon model.**

Input file	Corresponding variable in (31)	Description	units
an	$A_n$	$A_n$ coefficient	$eV \cdot cm$
ap	$A_p$	$A_p$ coefficient	$eV \cdot cm$

valence bands. The band shifts of the conduction and valence band edges for n-type materials are given by

$$\begin{aligned}\Delta E_{C,n} &= A_{n,C} \left( \frac{N_D - N_A}{10^{18}} \right)^{1/3} + B_{n,C} \left( \frac{N_D - N_A}{10^{18}} \right)^{1/4} + C_{n,C} \left( \frac{N_D - N_A}{10^{18}} \right)^{1/2}, \\ \Delta E_{V,n} &= A_{n,V} \left( \frac{N_D - N_A}{10^{18}} \right)^{1/3} + B_{n,V} \left( \frac{N_D - N_A}{10^{18}} \right)^{1/4} + C_{n,V} \left( \frac{N_D - N_A}{10^{18}} \right)^{1/2}\end{aligned}\quad (34)$$

and for p-type materials by

$$\begin{aligned}\Delta E_{C,p} &= A_{p,C} \left( \frac{N_A - N_D}{10^{18}} \right)^{1/3} + B_{p,C} \left( \frac{N_A - N_D}{10^{18}} \right)^{1/4} + C_{p,C} \left( \frac{N_D - N_A}{10^{18}} \right)^{1/2}, \\ \Delta E_{V,p} &= A_{p,V} \left( \frac{N_A - N_D}{10^{18}} \right)^{1/3} + B_{p,V} \left( \frac{N_A - N_D}{10^{18}} \right)^{1/4} + C_{p,V} \left( \frac{N_A - N_D}{10^{18}} \right)^{1/2}\end{aligned}\quad (35)$$

with the parameters  $A_{n,C}$ ,  $B_{n,C}$ ,  $C_{n,C}$ ,  $A_{n,V}$ ,  $B_{n,V}$ ,  $C_{n,V}$ ,  $A_{p,C}$ ,  $B_{p,C}$ ,  $C_{p,C}$ ,  $A_{p,V}$ ,  $B_{p,V}$  and  $C_{p,V}$  described in table 5-4.

Then, the total bandgap narrowing given by the Persson model for a n-type material can be written as

$$\Delta E_G = \Delta E_{V,n} - \Delta E_{C,n} \quad (36)$$

and for a p-type material as

$$\Delta E_G = \Delta E_{V,p} - \Delta E_{C,p} \quad (37)$$

To use Persson intrinsic density with associated bandgap narrowing model, the user must enable bandgap narrowing in the appropriate physics section

```
start Physics Block {physicsBlockName}
...
band gap narrowing is on
...
end
```

and specify Persson intrinsic concentration model with its parameters in the material block section

```
start Material Block {materialBlockName}
start intrinsic concentration
model is persson
start persson parameters
```

```

    (one parameter per line in the form):
    {parameter name} = {parameter value}
    (see table 5-4 for available parameters)
end
end
end

```

If no parameters are specified, default parameters for the corresponding material are used.

**Table 5-4 Syntax and parameters for Persson model.**

Input file	Corresponding variable in (34), (35)	Description	units
ANC_BGN	$A_{n,C}$	$A_{n,C}$ coefficient	$eV$
BNC_BGN	$B_{n,C}$	$B_{n,C}$ coefficient	$eV$
CNC_BGN	$C_{n,C}$	$C_{n,C}$ coefficient	$eV$
ANV_BGN	$A_{n,V}$	$A_{n,V}$ coefficient	$eV$
BNV_BGN	$B_{n,V}$	$B_{n,V}$ coefficient	$eV$
CNV_BGN	$C_{n,V}$	$C_{n,V}$ coefficient	$eV$

## 5.2. Band gap and Electron Affinity

Charon computes a bandgap  $E_G$  and electron affinity  $\chi$  and additionally an effective bandgap  $E_{G,eff}$  and an effective electron affinity  $\chi_{eff}$ . The bandgap  $E_G$  and the electron affinity  $\chi$  can be material constants or temperature-dependent functions and they do not include any narrowing effects. The effective bandgap  $E_{G,eff}$  and effective electron affinity use the bandgap  $E_G$  and electron affinity  $\chi$  and apply bandgap narrowing effects.

To specify a constant bandgap, the user must enter in the corresponding material block section

```

start Material Block {materialBlockName}
...
constant bandgap = {value}
...
end

```

where *value* is the bandgap value for the material in  $eV$ . If no bandgap is specified, Charon automatically uses the default value for the corresponding material.

To specify a constant electron affinity, the user must enter in the corresponding material block section

```

start Material Block {materialBlockName}
...
electron affinity = {value}
...
end

```

where *value* is the electron affinity value for the material in *eV*. If no electron affinity is specified, Charon automatically uses the default value for the corresponding material.

A temperature-dependent bandgap and corresponding electron affinity are also available as

$$\begin{aligned} E_G(T) &= E_G(300) + \alpha \left( \frac{300^2}{300 + \beta} - \frac{T^2}{T + \beta} \right), \\ \chi(T) &= \chi(300) - \alpha \left( \frac{300^2}{2(300 + \beta)} - \frac{T^2}{2(T + \beta)} \right) \end{aligned} \quad (38)$$

where  $E_G(300)$ ,  $\chi(300)$ ,  $\alpha$  and  $\beta$  parameters are described in table 5-5.

To activate the temperature-dependent bandgap model described by (38), the user must specify the model in the corresponding material block section

```
start Material Block {materialBlockName}
  start band gap
    temperature dependence is on

    (one parameter per line in the form):
    {parameter name} = {parameter value}
    (see table 5-5 for available parameters)
  end
end
```

If a constant electron affinity has already been specified in the material block section as described above, then the constant electron affinity is used and the temperature-dependent affinity computation in (38) is neglected.

**Table 5-5 Syntax and parameters for temperature-dependent bandgap.**

Input file	Corresponding variable in (38)	Description	units
Eg300	$E_G(300)$	Band Gap at 300 K	<i>eV</i>
Chi300	$\chi(300)$	Electron Affinity at 300 K	<i>eV</i>
alpha	$\alpha$	$\alpha$ coefficient	$\frac{eV}{K}$
beta	$\beta$	$\beta$ coefficient	<i>K</i>

Internally, Charon uses the effective bandgap  $E_{G,eff}$  and effective electron affinity  $\chi_{eff}$  in all calculations. When bandgap narrowing is not used or turned off,  $E_{G,eff} = E_G$  and  $\chi_{eff} = \chi$ . When bandgap narrowing is turned on in physics section block

```
start Physics Block {physicsBlockName}
  ...
  band gap narrowing is on
  ...
end
```

then narrowing effects are applied depending on the narrowing model used in the intrinsic density section (see Sec. 5.1). In this case

$$\begin{aligned} E_{G,\text{eff}}(T) &= E_G - \Delta E_G, \\ \chi_{\text{eff}}(T) &= \chi + 0.5\Delta E_G \end{aligned} \tag{39}$$

for the Old Slotboom, Slotboom and Harmon bandgap narrowing models with  $\Delta E_G$  being defined in (29), (30) or (31).

For Persson model

$$\begin{aligned} E_{G,\text{eff}}(T) &= E_G - \Delta E_G, \\ \chi_{\text{eff}}(T) &= \chi - \Delta E_C \end{aligned} \tag{40}$$

where  $\Delta E_C$  is defined in (34) or (35) and  $\Delta E_G$  in (36) or (37).

## 6. MOBILITY MODELS

Various models for carrier mobility, electrons and holes, are available and described here. The mobility model is specified within the specific material contained in the *Material Block* section of the input file. A synopsis of the general usage of each mobility model, along with parameters associated with a particular mobility model, are documented in subsequent sections.

### 6.1. Arora Model

The Arora mobility is given by [10]

$$\mu = \mu_{\min} \left( \frac{T}{300} \right)^{\text{exp1}} + \frac{\mu_{\max} \left( \frac{T}{300} \right)^{\text{exp2}}}{1 + \left( \frac{N_D + N_A}{N_{\text{ref}} \left( \frac{T}{300} \right)^{\text{exp3}}} \right)^{A \left( \frac{T}{300} \right)^{\text{exp4}}}} \quad (41)$$

for each of the carriers, holes and electrons, where  $T$  is the lattice temperature and  $N_D$  and  $N_A$  are the donor and acceptor doping levels, respectively. To specify that the Arora mobility model is utilized use

```
start Material Block {materialBlockName}
  start arora mobility
    start electron parameters
      (one parameter per line in the form):
      {parameter name} = {parameter value}
      (see table 6-1 for available parameters)
    end
    start hole parameters
      (same parameters as electron above)
    end
  end
end
```

Each of the parameters in (41) has a default value for a given material which can be overridden for each carrier via the input file. The variables and the syntax to set them in the input file is given in table 6-1 and the default values for those parameters for various materials is given in table 6-2.



**Table 6-1 Syntax and parameters for the Arora mobility model. Note setting parameter values is optional, Charon provides defaults if a particular parameter is not specified. See (41) for parameter meanings.**

Input file	Corresponding variable in (41)	Description	units
mumax	$\mu_{\max}$	reference mobility parameter	$\frac{cm^2}{Vs}$
mumin	$\mu_{\min}$	reference mobility parameter	$\frac{cm^2}{Vs}$
exp1	exp1	exponent on temperature ratio 1	none
exp2	exp2	exponent on temperature ratio 2	none
exp3	exp3	exponent on temperature ratio 3	none
exp4	exp4	exponent on temperature ratio 4	none
nref	$N_{\text{ref}}$	reference impurity concentration	$cm^{-3}$
nrefexp	A	reference impurity concentration exponent	none

**Table 6-2 Default Arora mobility model parameter values for supported materials.**

Electron							
	Si	GaAs	AlGaAs	InGaAs	AlInAs	GaAsP	InGaP
$\mu_{\max}$	1252.0	8500.0	9890.0	$2.73 \times 10^4$	$2.41 \times 10^4$	200.0	200.0
$\mu_{\min}$	88.0	0.0	0.0	0.0	0.0	0.0	0.0
$N_{\text{ref}}$	$1.26 \times 10^{17}$	$1.26 \times 10^{17}$	$10^{20}$	$10^{20}$	$10^{20}$	$10^{20}$	$10^{20}$
A	0.88	1.0	1.0	1.0	1.0	1.0	1.0
exp1	-0.57	-0.57	0.0	0.0	0.0	0.0	0.0
exp2	-2.33	0.0	0.0	0.0	0.0	0.0	0.0
exp3	2.4	0.0	0.0	0.0	0.0	0.0	0.0
exp4	-0.146	0.0	0.0	0.0	0.0	0.0	0.0
Hole							
$\mu_{\max}$	407.0	400.0	400.0	480.0	480.0	150.0	150.0
$\mu_{\min}$	54.3	0.0	0.0	0.0	0.0	0.0	0.0
$N_{\text{ref}}$	$2.35 \times 10^{17}$	$2.35 \times 10^{17}$	$10^{20}$	$10^{20}$	$10^{20}$	$10^{20}$	$10^{20}$
A	0.88	1.0	1.0	1.0	1.0	1.0	1.0
exp1	-0.57	0.0	0.0	0.0	0.0	0.0	0.0
exp2	-2.23	0.0	0.0	0.0	0.0	0.0	0.0
exp3	2.4	0.0	0.0	0.0	0.0	0.0	0.0
exp4	-0.146	0.0	0.0	0.0	0.0	0.0	0.0

## 6.2. Albrecht Mobility Model

Monte Carlo simulations were performed by Albrecht *et al.* [8] of electron transport based upon an analytical representation of the lowest conduction band of bulk, wurtzite phase Gallium Nitride (GaN) to develop a set of transport parameters for devices with electron conduction in

**GaN.** The analytic form of the parameters determined from the Monte Carlo results are given by:

$$\frac{1}{\mu} = a \left( \frac{N_T}{N_0} \right) \left( \frac{T}{T_0} \right)^{-3/2} \ln(1 + \beta_{CW}^2) + b \left( \frac{T}{T_0} \right)^{3/2} + \frac{c}{e^{(T_1/T)} - 1}, \quad (42)$$

where

$$\beta_{CW}^2 = 3.0 \left( \frac{T}{T_0} \right)^2 \left( \frac{N_T}{N_0} \right)^{-2/3},$$

$$N_T = N_D + N_A.$$

For electrons, typical values of the constants in (6.2) are

$$T_1 = \frac{\hbar\omega_{LO}}{k_B} = 1065 \text{ K},$$

$$a = 2.61 \times 10^{-4} \text{ V s cm}^{-2},$$

$$b = 2.90 \times 10^{-4} \text{ V s cm}^{-2},$$

and

$$c = 1.70 \times 10^{-2} \text{ V s cm}^{-2}.$$

where  $N_D$  and  $N_A$  are the ionized donor concentration and acceptor concentrations in  $\text{cm}^{-3}$  and  $T$  is the lattice temperature in Kelvin.

The Albrecht mobility model is calibrated for electrons. The model should only be used for holes when a real set of parameters are defined.

The syntax for utilizing this model is

```
start Material Block {materialBlockName}
  start albrecht mobility
    start electron parameters
      (one parameter per line in the form):
      {parameter name} = {parameter value}
      (see table 6-3 for available parameters)
    end
    start hole parameters
      (same parameters as electron above)
    end
  end
end
```

**Table 6-3 Syntax and parameters for the Albrecht mobility model. Note setting parameter values is optional, Charon provides defaults if a particular parameter is not specified. See (6.2) for parameter meanings.**

Input file	Corresponding variable in (6.2)	Description	Units
expa	$a$	fit parameter 1	$\frac{Vs}{cm^2}$
expb	$b$	fit parameter 2	$\frac{Vs}{cm^2}$
expc	$c$	fit parameter 3	$\frac{Vs}{cm^2}$
expN0	$N_0$	reference concentration density	$cm^{-3}$
expT0	$T_0$	reference temperature	$K$
expT1	$T_1$	reference temperature in exponent	$K$

### 6.3. Farahmand Mobility Model

In [18], Farahmand *et al.* present a comprehensive study of the transport dynamics of electrons in ternary III-nitride compounds. The work includes a field dependent mobility model and extracted parameters which are included here, respectively, in equations (43 & 44) and tables 6-5 & 6-6. The model should only be used when a real set of parameters are defined.

$$\mu_0(T, N) = \mu_{min} \left( \frac{T}{300} \right)^{\beta_1} + \frac{(\mu_{max} - \mu_{min}) \left( \frac{T}{300} \right)^{\beta_2}}{1 + \left[ \frac{N}{N_{ref} \left( \frac{T}{300} \right)^{\beta_3}} \right]^{\alpha(T/300)^{\beta_4}}} \quad (43)$$

In equation (43),  $T$  is temperature in Kelvin,  $N$  is the total doping density and  $\alpha$ ,  $\beta_1$ ,  $\beta_2$ ,  $\beta_3$ ,  $\beta_4$ ,  $\mu_{min}$ ,  $\mu_{max}$ ,  $N_{ref}$  are parameters that are determined either experimentally or via Monte Carlo simulation. In this case the parameters were taken from [18] in which the parameters were determined using Monte Carlo simulation.

The field dependent mobility model is given by (44) where  $\mu_0$  is the low field mobility as expressed in (43) and  $v^{sat}$ ,  $E_c$ ,  $\alpha$ ,  $n_1$  and  $n_2$  are parameters taken from [18].

$$\mu = \frac{\mu_0(T, N) + v^{sat} \frac{E_c^{n_1-1}}{E_c^{n_1}}}{1 + a \left( \frac{E}{E_c} \right)^{n_2} + \left( \frac{E}{E_c} \right)^{n_1}} \quad (44)$$

The syntax for utilizing this model is

```
start Material Block {materialBlockName}
  start farahmand mobility
    start electron parameters
      (one parameter per line in the form):
```

```

        {parameter name} = {parameter value}
        (see table 6-4 for available parameters)
    end
    start hole parameters
        (same parameters as electron above)
    end
end
end
end

```

The table summarizing the syntax for the Farahmand mobility model is given in table 6-4 and tables with default values of the model parameters for various materials can be found in tables 6-5 and 6-6.

**Table 6-4 Syntax and parameters for the Farahmand mobility model. Note setting parameter values is optional, Charon provides defaults if a particular parameter is not specified. See (43) and (44) for parameter meanings.**

Input file	Corresponding variable in (43) and (44)	Description	Units
mu_1	$\mu_{\min}$	low-field mobility	$\frac{cm^2}{Vs}$
mu_2	$\mu_{\max}$	maximum mobility	$\frac{cm^2}{Vs}$
beta	$\beta_1$	temperature ratio exponent 1	none
delta	$\beta_2$	temperature ratio exponent 2	none
gamma	$\beta_3$	temperature ratio exponent 3	none
eps	$\beta_4$	temperature ratio exponent 4	none
alpha	$\alpha$	exponent multiplier	none
ncrit	$N_{\text{ref}}$	reference impurity concentration value	$cm^{-3}$
vsat	$v^{\text{sat}}$	saturation velocity	$\frac{cm}{s}$
ec	$E_c$	critical field	$\frac{V}{cm}$
an	$a$	fitting parameter	none
n1	$n_1$	field ratio exponent 1	none
n2	$n_2$	field ratio exponent 2	none

**Table 6-5 Extracted parameters for the low-field mobility model (43). The reference density is  $N_{\text{ref}} = 10^{17} \text{ cm}^{-3}$ .  $^{\dagger}U_{\text{alloy}} = \Delta E_c$  &  $^{\ddagger}U_{\text{alloy}} = 0$ .**

		$\mu_{\min}$ ( $\text{cm}^2/\text{Vs}$ )	$\mu_{\max}$ ( $\text{cm}^2/\text{Vs}$ )	$\alpha$	$\beta_1$	$\beta_2$	$\beta_3$	$\beta_4$
InN		774.0	3138.4	0.68	-6.39	-1.81	8.05	-0.94
In <sub>0.8</sub> Ga <sub>0.2</sub> N	$^{\dagger}$	644.3	1252.7	0.82	-1.81	-1.30	4.84	0.41
	$^{\ddagger}$	646.5	3188.7	0.66	-0.73	-3.35	2.67	0.25
In <sub>0.5</sub> Ga <sub>0.5</sub> N	$^{\dagger}$	456.4	758.1	1.04	-1.16	-1.74	2.21	-0.22
	$^{\ddagger}$	493.8	2659.9	0.66	-9.11	-2.14	7.19	-0.76
In <sub>0.2</sub> Ga <sub>0.8</sub> N	$^{\dagger}$	386.4	684.1	1.37	-1.36	-1.95	2.12	-0.99
	$^{\ddagger}$	360.9	1887.6	0.69	-0.95	-3.58	3.06	0.06
GaN		295.0	1460.7	0.66	-1.02	-3.84	3.02	0.81
Al <sub>0.2</sub> Ga <sub>0.8</sub> N	$^{\dagger}$	132.0	306.1	0.29	-1.33	-1.75	6.02	1.44
	$^{\ddagger}$	312.1	1401.3	0.74	-6.51	-2.31	7.07	-0.86
Al <sub>0.5</sub> Ga <sub>0.5</sub> N	$^{\dagger}$	41.7	208.3	0.12	-0.60	-2.08	10.45	2.00
	$^{\ddagger}$	299.4	1215.4	0.80	-5.70	-2.29	7.57	-1.08
Al <sub>0.8</sub> Ga <sub>0.2</sub> N	$^{\dagger}$	47.8	199.6	0.17	-0.74	-2.04	20.65	0.01
	$^{\ddagger}$	321.7	881.1	1.01	-1.60	-3.69	3.31	0.44
AlN		297.8	683.8	1.16	-1.82	-3.43	3.78	0.86

**Table 6-6 Parameters for high field mobility model in (44).**

$^{\dagger}U_{\text{alloy}} = \Delta E_c$  &  $^{\ddagger}U_{\text{alloy}} = 0$ .

		$v^{\text{sat}}$ ( $10^7 \text{ cm/s}$ )	$E_c$ ( $\text{kV/cm}$ )	$n_1$	$n_2$	$a$
InN		1.3959	52.4242	3.8501	0.6078	2.2623
In <sub>0.8</sub> Ga <sub>0.2</sub> N	$^{\dagger}$	0.8714	103.4550	4.2379	1.1227	3.0295
	$^{\ddagger}$	1.4812	63.4305	4.1330	0.6725	2.7321
In <sub>0.5</sub> Ga <sub>0.5</sub> N	$^{\dagger}$	0.7973	148.9098	4.0635	1.0849	3.0052
	$^{\ddagger}$	1.6652	93.8151	4.8807	0.7395	3.7387
In <sub>0.2</sub> Ga <sub>0.8</sub> N	$^{\dagger}$	1.0428	207.5922	4.7193	1.0239	3.6204
	$^{\ddagger}$	1.8169	151.8870	6.0373	0.7670	5.1791
GaN		1.9064	220.8936	7.2044	0.7857	6.1973
Al <sub>0.2</sub> Ga <sub>0.8</sub> N	$^{\dagger}$	1.1219	365.5529	5.3193	1.0396	3.2332
	$^{\ddagger}$	2.0270	245.5794	7.8138	0.7897	6.9502
Al <sub>0.5</sub> Ga <sub>0.5</sub> N	$^{\dagger}$	1.1459	455.4437	5.0264	1.0016	2.6055
	$^{\ddagger}$	2.1581	386.2440	12.5795	0.8324	8.6037
AlN		2.1670	447.0339	17.3681	0.8554	8.7253

#### 6.4. Philips-Thomas Unified Mobility Model

The Philips unified mobility model [28],[29] is utilized heavily for simulations involving silicon bipolar devices. It's usage is described in this section.

The model segregates the mobility into four parts, the lattice, donor, acceptor and electron-hole scattering contributions. The total mobility is

$$\mu_i^{-1} = \mu_{i,L}^{-1} + \mu_{i,D}^{-1} + \mu_{i,A}^{-1} + \mu_{i,j}^{-1} \quad (45)$$

where the subscripts are

$$\begin{aligned} i &\rightarrow e \text{ or } h, \\ j &\rightarrow h \text{ or } e, \\ I &\rightarrow A \text{ or } D, \\ i, j &\rightarrow \text{contribution from electron-hole,} \\ L &\rightarrow \text{contribution from lattice,} \\ D &\rightarrow \text{contribution from donor,} \\ A &\rightarrow \text{contribution from acceptor.} \end{aligned}$$

The contribution from lattice scattering is

$$\mu_{i,L} = \mu_{\max} \left( \frac{T}{300.0} \right)^{\Gamma_i} \quad (46)$$

The sum of the remaining contributions is given by

$$\mu_{i,D+A+j}(N_D, N_A, n, p) = \mu_{i,N} \frac{N_{i,sc}}{N_{i,sc,eff}} \left( \frac{N_{ref}}{N_{i,sc}} \right)^{\alpha} + \mu_{i,c} \left( \frac{n+p}{N_{i,sc,eff}} \right) \quad (47)$$

where

$$N_{e,sc} = N_D^* + N_A^* + p, \quad (48)$$

$$N_{h,sc} = N_A^* + N_D^* + n, \quad (49)$$

$$N_{e,sc,eff} = N_D^* + G(P_e)N_A^* + \frac{p}{F(P_e)}, \quad (50)$$

and

$$N_{h,sc,eff} = N_A^* + G(P_h)N_D^* + \frac{n}{F(P_h)}. \quad (51)$$

The base terms due to impurity scattering and electron-hole scattering in (47) are

$$\mu_{i,N} = \frac{\mu_{\max}^2}{\mu_{\max} - \mu_{\min}} \left( \frac{T}{300} \right)^{3\alpha-1.5}, \quad (52)$$

$$\mu_{i,c} = \frac{\mu_{\min}\mu_{\max}}{\mu_{\max} - \mu_{\min}} \left( \frac{300}{T} \right)^{0.5}. \quad (53)$$

The functions used in (50) and (51) are

$$F_{i,j}(P_i) = \frac{0.7643P_i^{0.6478} + 2.2999 + 6.5502\frac{m_i}{m_j}}{P_i^{0.6478} + 2.3670 - 0.01552\frac{m_i}{m_j}} \quad (54)$$

$$G(P_i) = 1 - \frac{0.89223}{\left[0.41372 + \left(\frac{m_0}{m_i} \frac{T}{300}\right)^{0.28227} P_i\right]^{0.19778}} + \frac{0.005978}{\left[\left(\frac{m_i}{m_0} \frac{300}{T}\right)^{0.72169} P_i\right]^{1.80618}} \quad (55)$$

where if  $P_n < P_{n,\min}$  then  $G(P_{n,\min})$  is used to avoid errors, where  $P_{n,\min}$  is the value of  $P_n$  where  $G(P_n)$  reaches it's minimum.

$$P_i = \left[ \frac{2.459}{3.97 \times 10^{13} N_{i,\text{sc}}^{-2/3}} + \frac{3.828(n+p)}{1.36 \times 10^{20} \frac{m_i}{m_0}} \right]^{-1} \left( \frac{T}{300} \right)^2 \quad (56)$$

The effective impurity levels that take into account high doping effects are given by

$$N_I^* = N_I \left[ 1 + \frac{1}{C_I + \left( \frac{NR_I}{N_I} \right)^2} \right]. \quad (57)$$

Additionally the field dependence of the mobility due to [16] can be used and is given by

$$\mu_{i,\text{hf}} = \frac{\mu_{i,\text{lf}}}{\left[ 1 + \left( \frac{E}{v_{\text{sat}}} \right)^{\beta_i} \right]^{\frac{1}{\beta_i}}} \quad (58)$$

where  $\mu_{i,\text{lf}}$  is the low-field mobility as calculated in (45).

The syntax for utilizing this model in Charon is

```
start material block {materialBlockName}
...
start philips-thomas mobility
  start electron parameters
    high field mobility is on / off
    driving force is electric field / grad quasiFermi
    (one parameter per line in the form):
    {parameter name} = {parameter value}
    (see tables 6-7, 6-8 and 6-9 for available parameters)
  end
  start hole parameters
    (same parameters as electron above)
  end
end
...
end
```

**Table 6-7 Syntax and parameters for the Philips-Thomas mobility model.**

Input file	Corresponding variable as used in section 6.4	Description	Units
exponent for mobility	$\alpha$	exponent used in model	<i>none</i>
cref_a	$C_A$	reference acceptor density used in calculate of effective density (57)	$\frac{\#}{\text{cm}^3}$
cref_d	$C_D$	reference donor density used in calculate of effective density (57)	$\frac{\#}{\text{cm}^3}$
temperature dependence exponent	$\Gamma_i$	exponent for temperature dependence of lattice scattering (46)	$K$
maximum mobility	$\mu_{\max}$	maximum mobility	$\frac{\text{cm}^2}{\text{V}\cdot\text{s}}$
minimum mobility	$\mu_{\min}$	minimum mobility	$\frac{\text{cm}^2}{\text{V}\cdot\text{s}}$
reference impurity concentration	$N_{\text{ref}}$	(47)	$\frac{\#}{\text{cm}^3}$
nref_a	$NR_A$	(57)	$\frac{\#}{\text{cm}^3}$
nref_d	$NR_D$	(57)	$\frac{\#}{\text{cm}^3}$

**Table 6-8 Default values for dopant-related parameters used in Philips-Thomas mobility model.**

Dopant Parameter	As	P	B
$\mu_{\max}$	1417.0	1414.0	470.5
$\mu_{\min}$	52.2	68.5	44.9
$N_{\text{ref}}$	$9.68 \times 10^{16}$	$9.20 \times 10^{16}$	$2.23 \times 10^{17}$
$\alpha$	0.68	0.711	0.719

**Table 6-9 Carrier dependent parameters used in Philips-Thomas mobility model.**

$i$ or $I$ Parameter	$h$ or $A$	$e$ or $D$
$\Gamma_i$	-2.247	-2.285
$C_I$	0.5	0.21
$NR_I$	$7.2 \times 10^{20}$	$4.0 \times 10^{20}$
$\beta_i$	2.0	-1.0
$v_{\text{sat}}$	$2.4 \times 10^7 / (1 + 0.8 \exp(T/600))$	(same)



## 7. RECOMBINATION AND GENERATION

There are currently four types of recombination and two types of generation models available within Charon. The recombination models include the mid-gap Shockley-Reed-Hall (SRH), Radiative, Auger, and generic Trap SRH models. The generation models include various avalanche generation (also known as impact ionization) and optical generation models. **The first step** in utilizing these models is to turn them on in the *Physics Blocks* section of the input file as illustrated below. When these options are not specified in the input file, they are set to Off by default in the code. **The second step** is to specify the models and relevant parameters in the *Closure Models* section of the input file. Each model and corresponding parameters will be described in the subsections of this chapter.

```
start Physics Block {physicsBlockName}
  srh recombination is on/off
  Auger recombination is on/off
  Radiative recombination is on/off
  avalanche is on/off
end
```

### 7.1. Mid-Gap SRH Recombination

The standard SRH recombination model within Charon is given by

$$R_{\text{SRH}} = \frac{np - n_0p_0}{\tau_p (n + \sqrt{n_0p_0}) + \tau_n (p + \sqrt{n_0p_0})}. \quad (59)$$

Here  $n_0$  and  $p_0$  are equilibrium electron and hole densities, respectively. In the case of Boltzmann statistics, the product  $n_0p_0$  is given by  $n_i^2$ , where  $n_i$  is the intrinsic carrier concentration in a material. This model represents the effect of mid-band gap traps.

The parameters  $\tau_n$  and  $\tau_p$  represent electron and hole lifetimes, respectively. They can be constant or dependent on either the dopant concentration or the temperature. For constant lifetimes you can set the values in the input file. For example

```
start material block {materialBlockName}
...
electron/hole lifetime is constant = {value}
...
end
```

The lifetimes must be in units of seconds.

As noted, carrier lifetimes can also depend on the doping concentration. In this case, the lifetime is given by

$$\tau = \frac{\tau_0}{1 + \frac{N_D + N_A}{N_{\text{srh}}}}, \quad (60)$$

where  $N_D$  and  $N_A$  are the donor and acceptor concentrations, respectively, and  $N_{\text{srh}}$  is a material dependent parameter. This doping dependent lifetime can be applied to either electrons or holes. The syntax for adding such a dependency is

```

start material block
...
electron/hole lifetime is concentration dependent (with nsrh = {value})
...
end

```

where *{value}* is the numerical value of  $N_{SRH}$  in (60). The `with nsrh` is optional and if that option is not present then a default will be used as given in table 7-1.

Another common modification to the carrier lifetime is to add a temperature dependence. In Charon, two kinds of temperature dependence are supported for the lifetime, a power law dependence where the lifetime is given by

$$\tau = \tau_0 \left( \frac{T}{300} \right)^\alpha, \quad (61)$$

and an exponential type of dependence where the lifetime is equal to

$$\tau = \tau_0 \exp \left[ \beta \left( \frac{T}{300} - 1 \right) \right]. \quad (62)$$

The syntax for adding temperature dependence of carrier lifetimes is

```

start material block {materialBlockName}
...
electron / hole lifetime is temperature dependent (with exponential variation)
...
end

```

The concentration and temperature dependencies can be combined, but only one of the two temperature dependencies can be specified for a given carrier. For example, you can achieve the following variation for carrier lifetime

$$\tau_n = \frac{\tau_0}{1 + \frac{N_D + N_A}{N_{srh}}} \left( \frac{T}{300} \right)^\alpha. \quad (63)$$

using

```

start material block {materialBlockName}
...
electron lifetime is concentration dependent
electron lifetime is temperature dependent
...
end

```

where default values will be used for  $N_{SRH}$ .

Parameter symbol	Electrons & Holes	Unit
$\tau_0$	$10^{-7}$	s
$N_{srh}$	$5.0 \times 10^{16}$	$\frac{\#}{\text{cm}^3}$
$\alpha$	-1.5	1
$\beta$	2.55	1

**Table 7-1 Default parameters values for doping and temperature dependent SRH lifetime.**

## 7.2. Radiative Recombination

The radiative (a.k.a. direct) recombination model in Charon is given by

$$R_{rad} = C(np - n_0p_0), \quad (64)$$

where  $C$  is the radiative recombination coefficient. In the case of Boltzmann statistics,  $n_0p_0 = n_i^2$ . By default, Charon uses  $C = 1 \times 10^{-10} \text{ cm}^3 \cdot \text{s}^{-1}$  for GaAs and 0 for silicon. For other materials, the default  $C$  values are often set to  $1 \times 10^{-10} \text{ cm}^3 \cdot \text{s}^{-1}$  for convenience. The user is strongly recommended specifying the proper  $C$  value when using the model. Figure 7-1 shows an example of setting the coefficient of radiative recombination in the radiative recombination model, where *Coefficient* corresponds to the  $C$  value.

```
start Material Block materialBlockName
  Radiative recombination coefficient = coefficient
end Material Block materialBlockName
```

**Figure 7-1 Specification of parameters values for the radiative recombination model in the input file.**

## 7.3. Auger Recombination

The Auger recombination model is given by

$$R_A = (C_n n + C_p p)(np - n_0p_0), \quad (65)$$

where  $C_n$  and  $C_p$  are the electron and hole Auger recombination coefficient, respectively. Only constant Auger recombination coefficients are currently supported in Charon. The default  $C_n = 2.8 \times 10^{-31}$ ,  $C_p = 9.9 \times 10^{-32} \text{ cm}^6 \cdot \text{s}^{-1}$  for Si, and  $C_n = C_p = 1 \times 10^{-30} \text{ cm}^6 \cdot \text{s}^{-1}$  for GaAs. For other materials, the default  $C_n$  and  $C_p$  are often set to  $1 \times 10^{-30} \text{ cm}^6 \cdot \text{s}^{-1}$  for convenience. The user is strongly recommended specifying the proper parameters values when using the model. Figure 7-2 shows an example of specifying parameters values for the Auger recombination model, where *Electron Auger Coefficient* corresponds to  $C_n$  and *Hole Auger Coefficient* corresponds to  $C_p$ . By default, Charon uses Eq. (65) only if  $R_A$  is positive, and replaces the value by zero if  $R_A$  is negative. To use negative  $R_A$ , i.e., to allow for Auger generation of electron-hole pairs, one can set the Boolean parameter *With Generation* to true.

```

start Material Block materialBlockName
  start Auger Recombination Parameters
    Auger Coefficient electron/hole = augerCoefficient
    Generation on/off
  end Auger Recombination Parameters
end Material Block materialBlockName

```

**Figure 7-2 Specification of parameters values for the Auger recombination model in the input file.**

#### 7.4. Generic SRH Recombination

For traps not located in the mid-band gap of a material, one can simulate their effects using a generic trap SRH recombination model available in Charon. The generic trap model is given by

$$R_{traps} = \sum_j \frac{np - n_{ie}^2}{\tau_p^j(n + n_t^j) + \tau_n^j(p + p_t^j)}, \quad (66)$$

where the summation runs over the total number of different types of traps (e.g., two traps located at two different energy levels).  $n_{ie}$  is the effective intrinsic concentration in a material. The  $n_t^j$  and  $p_t^j$  for the  $j$ th type of traps are equal to

$$n_t^j = N_C \exp\left(-\frac{E_t^j}{k_B T}\right), \quad p_t^j = N_V \exp\left(-\frac{E_g - E_t^j}{k_B T}\right), \quad (67)$$

where  $N_C$  and  $N_V$  are the effective density of states in the conduction and valence bands respectively,  $E_t^j$  is the  $j$ th trap energy measured from the conduction band edge,  $E_g$  is the effective band gap,  $k_B$  is the Boltzmann constant, and  $T$  is the lattice temperature. The lifetimes  $\tau_n^j$  and  $\tau_p^j$  depend on the lattice temperature and the electric field. They are given by

$$\tau_n^j(T, F) = \frac{\tau_{n0}^j}{1 + g_n^j(T, F)}, \quad \tau_p^j(T, F) = \frac{\tau_{p0}^j}{1 + g_p^j(T, F)}. \quad (68)$$

Here  $\tau_{n0}^j$  and  $\tau_{p0}^j$  are field-independent lifetimes, but can contain temperature dependence.  $g_n^j(T, F)$  and  $g_p^j(T, F)$  are the electron and hole field enhancement factors, which capture the recombination enhancement due to band-to-trap tunneling and will be described later in this section. Currently, Charon supports two ways of specifying  $\tau_{n0}^j$  and  $\tau_{p0}^j$ . The first one is to specify constant values in units of seconds. The second one is to compute their values using

$$\tau_{n0}^j = \frac{1}{\sigma_n^j v_n N_t^j}, \quad \tau_{p0}^j = \frac{1}{\sigma_p^j v_p N_t^j}, \quad \text{with } v_n = \sqrt{\frac{3k_B T}{m_n^*}}, \quad v_p = \sqrt{\frac{3k_B T}{m_p^*}}. \quad (69)$$

$\sigma_n^j$  and  $\sigma_p^j$  are the electron and hole cross sections in  $\text{cm}^2$ .  $v_n$  and  $v_p$  are the electron and hole average thermal velocities [43] in  $\text{cm/s}$ .  $N_t^j$  is the trap density in  $\text{cm}^{-3}$  for the  $j$ th type of traps.  $m_n^*$  and  $m_p^*$  are the electron and hole effective masses. To compute  $\tau_{n0}^j$  or  $\tau_{p0}^j$ , one has to provide the corresponding cross section value.

The traps are categorized into two types: (i) *Acceptor* traps are neutral when unoccupied, and carry the charge of one electron when fully occupied; (ii) *Donor* traps are neutral when unoccupied, and carry the charge of one hole when fully occupied. The steady-state charge due to all acceptor traps is given by

$$-q \sum_j N_t^j f_{ta}^j, \text{ where } f_{ta}^j = \frac{\tau_p^j n + \tau_n^j p_t^j}{\tau_p^j (n + n_t^j) + \tau_n^j (p + p_t^j)}, \text{ the acceptor trap occupation.} \quad (70)$$

The steady-state charge due to all donor traps is equal to

$$+q \sum_j N_t^j f_{td}^j, \text{ where } f_{td}^j = \frac{\tau_p^j n_t^j + \tau_n^j p}{\tau_p^j (n + n_t^j) + \tau_n^j (p + p_t^j)}, \text{ the donor trap occupation.} \quad (71)$$

To include the trap charge in the Poisson equation, it must be enabled in the appropriate physics as so,

```
start physics block {PhysicsBlockName}
  trap charge is on
end physics block
```

By default, trap charge is off, meaning that trap charge is not included in the Poisson equation.

The field enhancement factors,  $g_n$  and  $g_p$ , with the superscript  $j$  omitted for simpler notation, are widely used to capture the stationary effects of band-to-trap tunneling (a.k.a trap assisted tunneling). That is, band-to-trap tunneling effectively reduces carrier lifetimes and consequently increases carrier recombination. Charon supports four variation forms of the Schenk band-to-trap tunneling model [40] and also a new model [20] designed for heterojunction devices. The expressions and details for  $g_n$  are given in Appendix B for different band-to-trap tunneling models. The same expressions are also applicable to  $g_p$  as long as the proper hole parameters are used. For example, one needs to replace  $E_t$  with  $(E_g - E_t)$  and replace  $m_n^*$  with  $m_p^*$  in the expressions to compute  $g_p$ .

#### 7.4.1. Model Usage

Three steps of specification are needed to enable the generic trap SRH recombination model. First, the trap model must be toggled on by setting

```
start physics block {PhysicsBlockName}
  trap srh is on
end
```

in the appropriate physics blocks.

Second, if a band-to-trap tunneling model is turned on, a driving force needs to be specified in the appropriate physics block

```

start physics block {PhysicsBlockName}
  Driving Force is {drForce}
end

```

because the tunneling model depends on the field. The `drForce` can be one of the three options: gradient quasi fermi levell, effective field, or gradient potential. It is default to effective field when not given in a physics block.

Third, we need to specif the model parameters in a trap srh material block as below.

```

start material block {materialBlockName}
  start trap srh
    start trap {trapID}
      (one parameter per line in the form):
      {parameter name} = {parameter value}
      (see table 7-2 for available parameters)
    trap type is {type}
    spatial profile is uniform
    spatial range is {locMin} to {locMax} [ in x [ in y [ in z]]]
    start electron/hole tunneling parameters
      model is {model}
      direction [ is x [ is y [ is z ]]]
      (one parameter per line in the form):
      {parameter name} = {parameter value}
      (see table 7-3 for available parameters)
    end tunneling parameters
  end trap
end trap srh
end material block

```

`trapID` is an integer equal or greater than 0. Multiple types of traps (up to 50) can be defined by specifying multiple `start trap` blocks. `type` defines the trap type which can be either donor or acceptor. `spatial profile` and `spatial range` are used to specify a spatial distribution of traps. Currently, only a uniform spatial profile is supported which can be placed in a user-defined box. A spatial box is defined using a `spatial range` line for each axis. The `spatial profile` line is optional to specify. When `spatial range` is not given, traps are uniformly distributed in all element blocks which belong to the same physics block.

The tunneling parameters block needs to be separately defined for electrons and holes. `model` specifies a tunneling model which can be one of the six options: none, hightemp approx, lowtemp approx, asymptotic field, constant field, new. none means no band-to-trap tunneling model is enabled. hightemp approx uses the high temperature approximation of the Schenk model, corresponding to Eq. (123). lowtemp approx uses the low temperature approximation of the Schenk model, corresponding to Eq. (125). constant field uses the original Schenk model, corresponding to Eq. (126) with the constant field density of states given by Eq. (130). asymptotic field also uses the original Schenk model, Eq. (126), but uses an asymptotic form [see Eq. (131)]for the electrooptical function. new uses a new band-to-trap tunneling model that was developed for heterojunction devices and takes into account both electric field and heterojunction band offset effects. The new model uses the new density of states model, Eq. (132), in computing the field enhancement factor. When the new tunneling model is enabled, three more

parameters and their values should be given, including `heterojunction location`, `heterojunction band offset`, and `direction`. The `direction` keyword specifies the tunneling axis which can be `is x`, `is y`, or `is z`. Note that all the available band-to-trap tunneling models are one-dimensional model. A user needs to be aware of the most important tunneling direction.

If any of the five band-to-trap tunneling models is set for electrons or holes or both carriers, the `phonon energy` and `huang-rhys factor` parameters and their values must be specified. If the `band-to-trap tunneling model` is set to `none`, the `phonon energy` and `huang-rhys factor` parameters are ignored. The `energy level` parameter specifies the trap energy in a positive value measured from the conduction band edge. Note that traps are located in the band gap.

The field independent lifetimes, i.e.,  $\tau_{n0}$  and  $\tau_{p0}$  in Eq. (68), can be specified in one of the two ways. The first one is to directly specify them using the `lifetime` parameter in seconds. Alternatively, they can be computed using Eq. (69), where the cross sections in  $\text{cm}^2$ ,  $\sigma_n$  and  $\sigma_p$ , must be given through the `cross section` parameter. The `effective mass` parameter is used to provide a value in units of  $m_0$  (the free electron mass) for the carrier effective mass,  $m_n^*$  or  $m_p^*$ , in the trap model. When they are not given in an input file, they are taken from the default material database within *Charon* for a given material.

**Table 7-2 Available parameters for the generic SRH trap model.**

Input file	Corresponding variables	Description	units
energy level	$E_t$ in Eq. (67)	trap energy level measured from conduction band edge	eV
trap density	$N_t$ in Eq. (69)	trap density	$\text{cm}^{-3}$
phonon energy	$\hbar\omega$ in Eq. (123)	optical phonon energy	eV
huang-rhys factor	$S$ in Eq. (123)	Huang-Rhys factor	unitless

**Table 7-3 Available parameters for the generic SRH band-to-trap tunneling models.**  
 $m_0$  is the free electron mass.

Input file	Corresponding variables	Description	units
lifetime	$\tau_{n0}$ or $\tau_{p0}$ in Eq. (68)	field independent carrier lifetime	seconds
cross section	$\sigma_n$ or $\sigma_p$ in Eq. (69)	carrier cross section	$\text{cm}^2$
effective mass	$m_n^*$ or $m_p^*$ in Eq. (69)	effective mass	$m_0$
heterojunction location	None	heterojunction location in a simulation device	$\mu\text{m}$
heterojunction band offset	e.g., $\Delta E_V$ in figure B-2	conduction or valence band offset	eV

An example of specifying trap parameters for the InGaP emitter in an InGaP/GaAs/GaAs HBT is given below.

```
start material block InGaP-Parameter
  start trap srh
    start trap 0
```

```

trap type is donor
energy level = 0.93
trap density = 1e17
phonon energy = 0.02
huang-rhys factor = 12.2

start hole tunneling parameters
  model is new
  direction is x
  heterojunction location = 0.15
  heterojunction band offset = 0.442
  lifetime = 1e-9
end

start electron tunneling parameters
  model is none
  lifetime = 1e-9
end
end trap 0
end trap srh
end material block

```

Complete examples on the generic trap and band-to-trap tunneling models can be found at [tcad-charon/test/nightlyTests/b2ttunnel/](https://github.com/charon-test/nightlyTests/b2ttunnel/).

## 7.5. Avalanche Generation

A few models for avalanche generation (impact ionization) are available in *Charon*. The generation rate of electron-hole pairs produced by these models is described by

$$G = \alpha_n(F_n) \frac{|\mathbf{J}_n|}{q} + \alpha_p(F_p) \frac{|\mathbf{J}_p|}{q} \quad (72)$$

where  $\alpha_n(F_n)$  and  $\alpha_p(F_p)$  are the electron and hole ionization coefficients,  $F_n$ ,  $F_p$  are electron and hole driving forces and  $\mathbf{J}_e$ ,  $\mathbf{J}_h$  are the electron and hole current densities.

An avalanche generation model in Charon computes the electron and hole ionization coefficients  $\alpha_n(F_n)$  and  $\alpha_p(F_p)$  as functions of driving forces  $F_n$  and  $F_p$ .

To activate/use an avalanche model, the user must first set the *avalanche* flag to *on* and specify the *driving force* in the *Physics Block* as shown below

```

start Physics Block {physicsBlockName}
...
avalanche is on
driving force is {drForce}
...
end

```

where *drForce* can be one of three options: *effective field*, *gradient potential* or *gradient quasi fermi level*. By default *driving force* is set to *effective field* when it is not given in the input file.



Secondly, the user must specify the avalanche model used along with its relevant parameters in the *Material Block* section of the input file

```
start Material Block {materialBlockName}
...
start avalanche generation
  threshold behavior model is {avalancheModel}
  driving force is {drForceType}
  minimum field = {minField}
  start {avalancheModel} parameters
    critical field is fixed
    (one parameter per line in the form):
    {parameter name} = {parameter value}
  end
end
...
end
```

*Charon* implements two avalanche models, Selberherr and Crowell-Sze, which can be selected by *avalancheModel* above. To select Selberherr model *avalancheModel* must be set to *selberherr*. For Crowell-Sze model *avalancheModel* must be set to *crowell-sze*.

The driving force *drForceType* above must match the *drForce* in the *Physics Block* section. If *drForce* in the *Physics Block* is *effective field* then *drForceType* can be either *effective field J* or *effective field Jtot*. If *drForce* is *gradient potential* then *drForceType* can be either *gradient potential J* or *gradient potential Jtot*. Finally, if *drForce* is *gradient quasi fermi level* then *drForceType* must be *gradient quasi fermi level*.

*minField* sets the minimum value of the electric field from which the avalanche model is turn on internally.

More details about the avalanche model specification will be described in the following sections.

### 7.5.1. Selberherr Model

Selberherr avalanche generation model computes the electron and hole ionization coefficients  $\alpha_n(F_n)$  and  $\alpha_p(F_p)$  in Eq.(72) as

$$\begin{aligned}\alpha_n &= \alpha_n^\infty(T) \exp \left[ - \left( \frac{F_n^{crit}}{F_n} \right)^{\delta_n} \right], \\ \alpha_p &= \alpha_p^\infty(T) \exp \left[ - \left( \frac{F_p^{crit}}{F_p} \right)^{\delta_p} \right]\end{aligned}\tag{73}$$

The critical fields  $F_n^{crit}$  and  $F_p^{crit}$  in Eq. (73) can be set to a fixed value specified in the input file or computed using

$$\begin{aligned} F_n^{crit} &= \frac{E_g(T)}{q\lambda_n(T)}, \\ F_p^{crit} &= \frac{E_g(T)}{q\lambda_p(T)}. \end{aligned} \quad (74)$$

where  $\lambda_n$  and  $\lambda_p$  are the optical-phonon mean free paths for electrons and holes, given by

$$\begin{aligned} \lambda_n(T) &= \lambda_n^0 \tanh\left(\frac{\hbar\omega_n}{2k_B T}\right), \\ \lambda_p(T) &= \lambda_p^0 \tanh\left(\frac{\hbar\omega_p}{2k_B T}\right) \end{aligned} \quad (75)$$

The coefficients  $\alpha_n^\infty$  and  $\alpha_p^\infty$  are polynomial functions of temperature

$$\begin{aligned} \alpha_n^\infty(T) &= a_{0n} + a_{1n}T + a_{2n}T^2 \\ \alpha_p^\infty(T) &= a_{0p} + a_{1p}T + a_{2p}T^2 \end{aligned} \quad (76)$$

with the constant coefficients  $a_{0n}$ ,  $a_{1n}$ ,  $a_{2n}$ ,  $a_{0p}$ ,  $a_{1p}$  and  $a_{2p}$  specified by the user.

To improve numerical stability, the driving fields,  $F_n$  and  $F_p$  in Eq. (73) can be computed as  $\frac{nF_n}{n+n_{ref}}$  and  $\frac{pF_p}{p+p_{ref}}$  where  $n$ ,  $p$  are the electron and hole densities and  $n_{ref}$ ,  $p_{ref}$  are numerical damping density parameters. Using positive values for  $n_{ref}$  and  $p_{ref}$  may improve convergence for problems where strong generation-recombination occurs in regions with small carrier densities.

To use Selberherr avalanche model the user must first turn the avalanche on and specify the driving force in the *Physics Block*

```
start Physics Block {physicsBlockName}
...
avalanche is on
driving force is {drForce}
...
end
```

Secondly, the user must specify Selberherr avalanche model along with parameters in the *Material Block* section of the input file

```
start Material Block {materialBlockName}
...
start avalanche generation
threshold behavior model is selberherr
driving force is {drForceType}
minimum field = {minField}
electron driving force reference density = {eDfRefDens}
hole driving force reference density = {hDfRefDens}
start selberherr parameters
critical field is {critField}
```

```

(one parameter per line in the form):
{parameter name} = {parameter value}
(see table 7-4 for available parameters)
end
end
...
end

```

For a description of *drForceType* and *minField* see 7.5. Critical field can be either specified in the input file or computed. To specify critical field in the input file set *critField* to *fixed*. To force computing critical field according to Eq. (74) set *critField* to *computed*. The other Selberherr avalanche model parameters and their description are listed in table 7-4.

If *electron driving force reference density* and/or *hole driving force reference density* are specified in the list of avalanche generation parameters (see above) then the driving fields,  $F_n$  and  $F_p$  are computed as  $\frac{nF_n}{n+n_{ref}}$  and  $\frac{pF_p}{p+p_{ref}}$  where  $n$ ,  $p$  are the electron and hole densities and  $n_{ref}$ ,  $p_{ref}$  are numerical damping density parameters which can be set by the user (*eDfRefDens* and *hDfRefDens*).

**Table 7-4 Syntax and parameters for the Selberherr avalanche model.**

Input file	Corresponding variable in (73), (74), (75), (76)	Description	units
electron a0	$a_{0n}$	$\alpha_n^\infty$ coefficient	$\frac{1}{cm}$
electron a1	$a_{1n}$	$\alpha_n^\infty$ coefficient	$\frac{1}{cmK}$
electron a2	$a_{2n}$	$\alpha_n^\infty$ coefficient	$\frac{1}{cmK^2}$
hole a0	$a_{0p}$	$\alpha_p^\infty$ coefficient	$\frac{1}{cm}$
hole a1	$a_{1p}$	$\alpha_p^\infty$ coefficient	$\frac{1}{cmK}$
hole a2	$a_{2p}$	$\alpha_p^\infty$ coefficient	$\frac{1}{cmK^2}$
electron delta	$\delta_n$	electron field ratio exponent	<i>none</i>
hole delta	$\delta_p$	hole field ratio exponent	<i>none</i>
electron E0	$F_n^{crit}$	electron critical field when <i>critField</i> is <i>fixed</i>	$\frac{V}{cm}$
hole E0	$F_p^{crit}$	hole critical field when <i>critField</i> is <i>fixed</i>	$\frac{V}{cm}$
electron lambda300	$\lambda_n^0$	Phonon mean free path for electrons at 300K	<i>cm</i>
hole lambda300	$\lambda_p^0$	Phonon mean free path for hole at 300K	<i>cm</i>
electron h bar omega	$\hbar\omega_n$	Optical phonon energy for electrons	<i>eV</i>
hole h bar omega	$\hbar\omega_p$	Optical phonon energy for holes	<i>eV</i>

### 7.5.2. Crowell-Sze Model

*Crowell-Sze avalanche* generation model [17] estimates the electron and hole ionization coefficients  $\alpha_n(F_n)$  and  $\alpha_p(F_p)$  in Eq.(72) based on Baraff's theory [11] in terms of physical parameters  $E_{opt,ph}$ , the Raman optical phonon energy,  $E_{ioniz}$ , the ionization energy and  $\lambda$ , the carrier free path for optical generation. The ionization coefficients are computed as

$$\begin{aligned}\alpha_n &= \frac{1}{\lambda_n} \exp \left[ C_0(r_n) + C_1(r_n)x_n + C_2(r_n)x_n^2 \right], \\ \alpha_p &= \frac{1}{\lambda_p} \exp \left[ C_0(r_p) + C_1(r_p)x_p + C_2(r_p)x_p^2 \right]\end{aligned}\quad (77)$$

where the coefficients  $C_0$ ,  $C_1$  and  $C_2$  are given by the polynomials

$$\begin{aligned}C_0(r) &= -1.92 + 75.5r - 757r^2, \\ C_1(r) &= 1.75 \times 10^{-2} - 11.9r + 46r^2, \\ C_2(r) &= 3.9 \times 10^{-4} - 1.17r + 11.5r^2\end{aligned}\quad (78)$$

and

$$\begin{aligned}r_n &= \frac{E_{opt,ph}}{E_{ioniz}^n}, \\ r_p &= \frac{E_{opt,ph}}{E_{ioniz}^p}, \\ x_n &= \frac{E_{ioniz}^n}{q\lambda_n F_n}, \\ x_p &= \frac{E_{ioniz}^p}{q\lambda_p F_p}\end{aligned}\quad (79)$$

Similar to Selberherr model (see Eq.(76)), the carrier free paths depend on Raman optical phonon energy

$$\begin{aligned}\lambda_n(T) &= \lambda_n^0 \frac{\tanh\left(\frac{E_{opt,ph}}{2k_B T}\right)}{\tanh\left(\frac{E_{opt,ph}}{2k_B 300K}\right)}, \\ \lambda_p(T) &= \lambda_p^0 \frac{\tanh\left(\frac{E_{opt,ph}}{2k_B T}\right)}{\tanh\left(\frac{E_{opt,ph}}{2k_B 300K}\right)}\end{aligned}\quad (80)$$

To use Crowell-Sze avalanche model the user must first turn the avalanche on and specify the driving force in the *Physics Block*

```
start Physics Block {physicsBlockName}
...
avalanche is on
driving force is {drForce}
...
end
```

Secondly, the user must specify Crowell-Size avalanche model along with parameters in the *Material Block* section of the input file

```
start Material Block {materialBlockName}
...
start avalanche generation
  threshold behavior model is crowell-size
  driving force is {drForceType}
  minimum field = {minField}
  electron driving force reference density = {eDFRefDens}
  hole driving force reference density = {hDFRefDens}
  start crowell-size parameters
    (one parameter per line in the form):
    {parameter name} = {parameter value}
    (see table 7-5 for available parameters)
  end crowell-size parameters
end
...
end
```

For a description of *drForceType* and *minField* see 7.5. The other Crowell-Size avalanche model parameters and their description are listed in table 7-5.

If *electron driving force reference density* and/or *hole driving force reference density* are specified in the list of avalanche generation parameters (see above) then the driving fields,  $F_n$  and  $F_p$  are computed as  $\frac{nF_n}{n+n_{ref}}$  and  $\frac{pF_p}{p+p_{ref}}$  where  $n$ ,  $p$  are the electron and hole densities and  $n_{ref}$ ,  $p_{ref}$  are numerical damping density parameters which can be set by the user (*eDFRefDens* and *hDFRefDens*).

**Table 7-5 Syntax and parameters for the Crowell-Size avalanche model.**

Input file	Corresponding variable in (77), (78), (79), (80)	Description	units
electron lambda300	$\lambda_n^0$	Phonon mean free path for electrons at 300K	cm
hole lambda300	$\lambda_p^0$	Phonon mean free path for hole at 300K	cm
optical phonon energy	$E_{opt,ph}$	Raman optical phonon energy	eV
electron ionization energy	$E_{ioniz}^n$	ionization energy for electrons	eV
hole ionization energy	$E_{ioniz}^p$	ionization energy for holes	eV

## 8. INCOMPLETE IONIZATION

In silicon the energy levels of dopants are shallow compared to the thermal energy  $k_B T$  at room temperature. At room temperature, the dopants in silicon can be regarded for practical purposes as fully ionized. For materials where the dopant levels are deep or for silicon at low temperatures, the dopant species are only partially ionized and incomplete ionization must be accounted for in order to determine the correct effective doping concentrations.

### 8.1. Model Implementation

The densities of the ionized dopants are derived based on the Fermi-Dirac distribution of the dopant energy level:

$$\begin{aligned} N_D^+ &= \frac{N_{D,0}}{1 + g_D \exp\left(\frac{E_{Fn} - E_D}{k_B T}\right)} \quad N_{D,0} \leq N_{D,\text{crit}}, \\ N_A^- &= \frac{N_{A,0}}{1 + g_A \exp\left(\frac{E_A - E_{Fp}}{k_B T}\right)} \quad N_{A,0} \leq N_{A,\text{crit}}. \end{aligned} \quad (81)$$

where  $N_D^+$  is the ionized donor density,  $N_A^-$  is the ionized acceptor density,  $N_{D,0}$  and  $N_{A,0}$  are the substitutional dopant densities,  $g_D$ ,  $g_A$  are the dopant energy level degeneracy factors,  $E_D$ ,  $E_A$  are the donor and acceptor ionization energies and  $N_{D,\text{crit}}$  and  $N_{A,\text{crit}}$  are the dopant critical densities above which the dopants are considered fully ionized.

Using the Fermi-Dirac expressions for the carrier densities expressed as perturbations in Maxwell Boltzmann approximation:

$$\begin{aligned} n &= N_C \mathcal{F}_{1/2}(\eta_n) = \gamma_n N_C \exp(\eta_n), \\ p &= N_V \mathcal{F}_{1/2}(\eta_p) = \gamma_p N_V \exp(\eta_p), \\ \eta_n &= (E_{Fn} - E_C) / k_B T, \\ \eta_p &= (E_V - E_{Fp}) / k_B T. \end{aligned}$$

where  $\gamma_n$  and  $\gamma_p$  are the electron and hole degeneracy factors, the ionized dopant densities in (81) are expressed as a function of Charon solution variables (carrier concentrations):

$$\begin{aligned} N_D^+ &= \frac{N_{D,0}}{1 + g_D \frac{n}{\gamma_n n_1}} \quad N_{D,0} \leq N_{D,\text{crit}}, \\ N_A^- &= \frac{N_{A,0}}{1 + g_A \frac{p}{\gamma_p p_1}} \quad N_{A,0} \leq N_{A,\text{crit}}. \end{aligned} \quad (82)$$

where  $n_1 = N_C \exp\left(-\frac{\Delta E_D}{k_B T}\right)$  and  $p_1 = N_V \exp\left(-\frac{\Delta E_A}{k_B T}\right)$  are two computational energy levels depending on  $\Delta E_D$ , the energy difference between conduction band edge and donor energy level

and respectively  $\Delta E_A$ , the energy difference between the acceptor energy level and the valence band edge.

For the case where the Maxwell-Boltzmann approximation is used instead of Fermi-Dirac integral for computing the carrier densities,  $\gamma_n = 1$  and  $\gamma_p = 1$  and (82) degenerates into:

$$\begin{aligned} N_D^+ &= \frac{N_{D,0}}{1 + g_D \frac{n}{n_1}} & N_{D,0} \leq N_{D,\text{crit}}, \\ N_A^- &= \frac{N_{A,0}}{1 + g_A \frac{p}{p_1}} & N_{A,0} \leq N_{A,\text{crit}}. \end{aligned} \quad (83)$$

When incomplete ionization models are enabled (for donor, acceptor or both), Charon uses ionized dopant densities defined by (82) and (83) instead of the substitutional dopant densities ( $N_{D,0}$  and  $N_{A,0}$ ) for all closure models except mobility, intrinsic density and SRH lifetime models. For mobility, intrinsic density and SRH lifetime models the fully ionized dopant densities (substitutional densities)  $N_{D,0}$  and  $N_{A,0}$  are always used.

For contacts, ionized dopant densities are also used instead of substitutional dopant densities  $N_{D,0}$  and  $N_{A,0}$  when the corresponding ionization model is turned on. In the most general case, with the incomplete ionization, the charge neutrality and equilibrium conditions at the contact become:

$$\begin{aligned} n_0 - p_0 &= N_D^+ - N_A^- + N_{\text{ion}} = C, \\ n_0 p_0 &= \gamma_n \gamma_p n_i^2. \end{aligned} \quad (84)$$

where  $N_{\text{ion}}$  is ion charge (zero if the ionic transport is not used).

Depeding on the contact type (n-type or p-type) and the statistics used for carrier densities (Maxwell-Boltzmann or Fermi-Dirac) implicit algebraic equations of order 4, 3 or 2 have to be solved for carrier densities at the contacts. Charon allows three types of approximations for minority carrier dopant in charge neutrality condition in (84). In the first case, the minority carrier dopant is assumed to be fully ionized,  $N_D^+ = N_{D,0}$  for a p-type contact or  $N_A^- = N_{A,0}$  for a n-type contact. In the second case, the minority carrier dopant is ignored,  $N_D^+ \simeq 0$  for a p-type contact or  $N_A^- \simeq 0$  for a n-type contact. Finally, for the third case, the minority carrier dopant can be speciifed by the exact formula in (83).

## 8.2. Model Usage

The incomplete ionization model can be activated independently for donor and acceptor species. To activate the ionization model for either carrier first the appropriate `incomplete ionization` parameter has to be set to `on` in the relevant `physics` block section of the input file. For example,

```

start physics block {physics name}
.
acceptor incomplete ionization is on
donor incomplete ionization is on
.
end

```

Next the blocks setting parameters for the incomplete ionization, for each carrier that was enabled in the physics block, must be added to the relevant `material` block section of the input file. For example,

```

start material block {materialBlockName}
.
start incomplete ionization acceptor
(one parameter per line in the form):
{parameter name} = {parameter value}
(see table 8-1 for a list of parameters)
end
.
start incomplete ionization donor
(same parameter set as acceptor)
end
.
end

```

**Table 8-1 Syntax and parameters for the incomplete ionization model.**

Input file	Corresponding variables in (81) through (84)	Description	Units
critical doping	$N_{D,crit}$ or $N_{A,crit}$	doping value	$\frac{\#}{cm^2}$
degeneracy factor	$g_D$ or $g_A$	dopant energy level degeneracy factors	<i>none</i>
ionization energy	$E_D$ or $E_A$	ionization energies	<i>eV</i>
file	<i>none</i>	existing file containg doping versus ionization energy data	<i>none</i>
approximation	<i>none</i>	I - fully ionized II - no ionization III - use full model	<i>none</i>

As an option, the ionization energies  $E_D$  and  $E_A$  can be defined as doping-dependent quantities rather than constant values. The ionization energies versus doping concentration are specified in two separate files with two columns, the first column being the doping concentration in  $cm^{-3}$  and second the corresponding ionization energy for that doping in *eV*. Internally, for a certain raw doping concentration (fully ionized) the ionization energy used in incomplete ionization model is computed based on the tabulated data defined in the file. If the raw doping concentration matches a value in the file then the corresponding ionization energy is used. If the doping level is outside the doping range specified in the file then the closest doping level from file is taken and the corresponding ionization is used. For the other values of the raw doping concentration within the range defined in the file a logarithmic interpolation on doping concentration scale is used to



compute the corresponding ionization energy. If using the `file` option Charon expects the file to be a standard text file with the following format:

$$\begin{array}{ll} \text{Doping}_1 & E_{\text{ioniz},1} \\ \text{Doping}_2 & E_{\text{ioniz},2} \\ & \cdot \\ & \cdot \\ & \cdot \\ \text{Doping}_n & E_{\text{ioniz},n} \end{array}$$

## 9. HETEROJUNCTION

Carrier transport across a heterojunction (HJ) interface in a semiconductor heterostructure such as heterojunction bipolar transistor (HBT) requires special treatment. Conventional transport equations become invalid at a HJ, and the current at an abrupt HJ between two materials should be defined by interface condition at the junction.

Taking the InGaP/GaAs/GaAs NPN HBT illustrated in Fig. 9-1(a) as an example, the corresponding band diagram in the emitter and base regions is sketched in Fig. 9-1(b). Due to the wider band gap of InGaP than GaAs, the emitter-base (E-B) junction has discontinuities in both the conduction and valence bands, which cause discontinuities in electron and hole densities at the junction. Current across the E-B junction is determined by electron forward injection from the emitter to the base through the thermionic emission and tunneling processes and hole backward injection from the base to the emitter through the thermionic emission process. Given the valence band profile in Fig. 9-1(b), there is no hole tunneling across the E-B junction. Currently, Charon supports thermionic emission (TE) and local tunneling (LT) models for electrons and holes at a HJ.

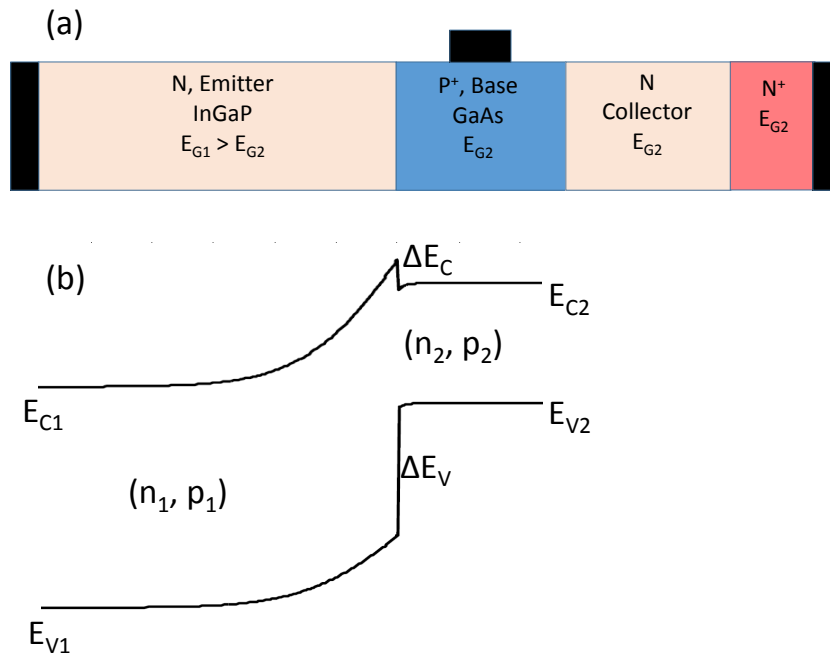


**Figure 9-1 (a) Schematic of a InGaP/GaAs/GaAs NPN HBT device. (b) Band diagram in the emitter and base regions.**

Implementation of the TE and LT models in Charon requires the support of discontinuities in carrier densities and material properties at an abrupt HJ. This is made possible by Panzer, the Trilinos package on which Charon is built. Panzer provides the heterojunction infrastructure that allows for adding different suffix to the carrier densities and material properties names for the two sides at a HJ, which enables Charon to access carrier densities and material properties of both sides. For example, given the E-B junction shown in Fig. 9-1, the emitter side is defined as side 1

and the electron (hole) density on side 1 is denoted as  $n_1$  ( $p_1$ ), while the base side is defined as side 2 and the electron (hole) density on side 2 is denoted as  $n_2$  ( $p_2$ ). It is noted that since the collector has the same material as the base, there is no carrier discontinuity at the base-collector junction, hence the electron (hole) density in collector is also denoted as  $n_2$  ( $p_2$ ). For simpler implementation, the left side of a HJ is always defined as side 1, while the right side of a HJ is always defined as side 2. The conduction band offset is defined as  $\Delta E_C = E_{C1} - E_{C2}$  where  $E_{C1}$  ( $E_{C2}$ ) is the conduction band of side 1 (side 2), whereas the valence band offset is defined as  $\Delta E_V = E_{V2} - E_{V1}$  where  $E_{V2}$  ( $E_{V1}$ ) is the valence band of side 2 (side 1). It is noted that  $\Delta E_C$  and  $\Delta E_V$  can be either positive or negative depending on the band diagram, as described in Sec. 9.1

The TE and LT models are based on the foundational work by Wu and Yang [49]. In the following, the final forms of the models are described, while derivation of the models is detailed in Appendix C.

### 9.1. Thermionic Emission

Given the conduction and valence band diagram in Fig. 9-1(b), the net electron and hole current densities due to thermionic emission across the E-B junction are given by [see the Eq. (134)]

$$\begin{aligned} J_{TE,n} &= A_n^* T^2 \left[ -\exp\left(\frac{E_{Fn1} - E_{C1}}{k_B T}\right) + \exp\left(\frac{E_{Fn2} - E_{C2} - \Delta E_C}{k_B T}\right) \right], \\ J_{TE,p} &= A_p^* T^2 \left[ \exp\left(\frac{E_{V1} - E_{Fp1}}{k_B T}\right) - \exp\left(\frac{E_{V2} - E_{Fp2} - \Delta E_V}{k_B T}\right) \right]. \end{aligned} \quad (85)$$

Where  $A_n^*$  and  $A_p^*$  are the electron and hole Richardson constants,  $E_{Fn}$  and  $E_{Fp}$  are the electron and hole quasi-Fermi levels,  $E_C$  and  $E_V$  are the conduction and valence band edges, respectively,  $k_B$  is the Boltzmann constant,  $T$  is the temperature, 1 and 2 denote side 1 and side 2. Note that  $\Delta E_C$  and  $\Delta E_V$  here are both positive. The current densities here are scalar quantities and represent the normal components perpendicular to the HJ. The Richardson constants are defined as

$$\begin{aligned} A_n^* &= \frac{4\pi q k_B^2 m_n^*}{h^3}, \\ A_p^* &= \frac{4\pi q k_B^2 m_p^*}{h^3}, \end{aligned} \quad (86)$$

where  $m_n^*$  and  $m_p^*$  are the electron and hole effective mass, respectively, and  $h$  is the Planck constant. There is an inconsistency in literature [49, 25, 50] regarding which side of effective mass should be used in computing the Richardson constant. In Charon, the effective mass used in computing the Richardson constant is not taken from either side of a HJ, but set to be a user-defined parameter. It is worthy of noting that, under the thermal equilibrium, the quasi-Fermi levels are constant, i.e.,  $E_{Fn1} = E_{Fn2}$  and  $E_{Fp1} = E_{Fp2}$ , then  $J_{TE,n} = 0$  and  $J_{TE,p} = 0$  as it should be.

Since the fundamental basic variables in Charon are electric potential, electron and hole densities, we need to rewrite Eq. (85) in terms of carrier densities and material properties. For Boltzmann

statistics, the electron and hole densities are given by  $n = N_C \exp\left(\frac{E_{Fn} - E_C}{k_B T}\right)$  and  $p = N_V \exp\left(\frac{E_V - E_{Fp}}{k_B T}\right)$ , from which Eq. (85) can be rewritten as

$$\begin{aligned} J_{TE,n} &= A_n^* T^2 \left[ -\frac{n_1}{N_{C1}} + \frac{n_2}{N_{C2}} \exp\left(-\frac{\Delta E_C}{k_B T}\right) \right], \\ J_{TE,p} &= A_p^* T^2 \left[ \frac{p_1}{N_{V1}} - \frac{p_2}{N_{V2}} \exp\left(-\frac{\Delta E_V}{k_B T}\right) \right]. \end{aligned} \quad (87)$$

If one defines  $v_n = A_n^* T^2 / q N_C$  and  $v_p = A_p^* T^2 / q N_V$ , Eq. (87) becomes

$$\begin{aligned} J_{TE,n} &= -q v_{n1} n_1 + q v_{n2} n_2 \exp\left(-\frac{\Delta E_C}{k_B T}\right), \\ J_{TE,p} &= q v_{p1} p_1 - q v_{p2} p_2 \exp\left(-\frac{\Delta E_V}{k_B T}\right) \end{aligned} \quad (88)$$

From Eq. (88), one can interpret the electron thermionic emission current density for the band diagram given in Fig. 9-1(b) as follows: electrons do not see a  $\Delta E_C$  energy barrier when thermionically emitting from side 1 to side 2, hence the electron current density from 1 to 2 is  $(-q)v_{n1}n_1$  where the minus sign is due to the negative charge of an electron; whereas, electrons going from side 2 to side 1 do see a  $\Delta E_C$  energy barrier, hence the electron current density is reduced by  $\exp\left(-\frac{\Delta E_C}{k_B T}\right)$  and becomes  $(-q)v_{n2}n_2 \exp\left(-\frac{\Delta E_C}{k_B T}\right)$ ; the difference of the two current densities determines the net electron current across the HJ. A similar interpretation is applicable to the hole thermionic emission current density except that the charge of holes is positive.

For Fermi-Dirac statistics, the electron and hole densities are given by

$$\begin{aligned} n &= N_C F_{1/2}\left(\frac{E_{Fn} - E_C}{k_B T}\right), \\ p &= N_V F_{1/2}\left(\frac{E_V - E_{Fp}}{k_B T}\right), \end{aligned} \quad (89)$$

where  $F_{1/2}(\cdot)$  is the one-half Fermi-Dirac integral [12]. From the above equations, one can inversely solve for the arguments of the Fermi-Dirac integrals, i.e.,

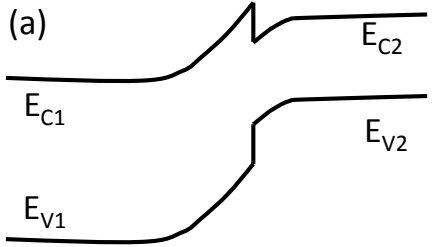
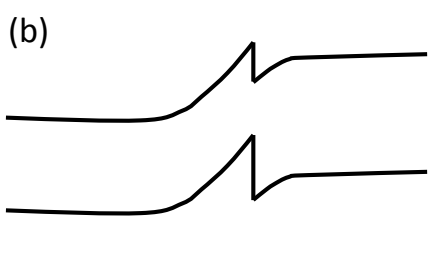
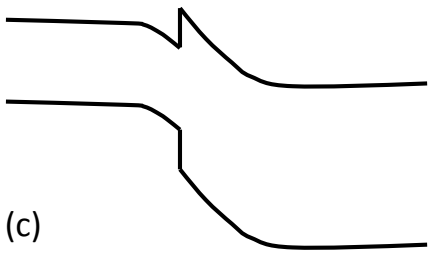
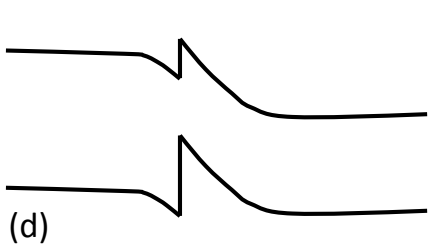
$$\begin{aligned} \eta_n &= \frac{E_{Fn} - E_C}{k_B T} = F_{1/2}^{-1}\left(\frac{n}{N_C}\right), \\ \eta_p &= \frac{E_V - E_{Fp}}{k_B T} = F_{1/2}^{-1}\left(\frac{p}{N_V}\right), \end{aligned} \quad (90)$$

where  $F_{1/2}^{-1}(\cdot)$  is the inverse of the one-half Fermi-Dirac integral [36]. Substituting  $\eta_n$  and  $\eta_p$  into Eq. (85), we obtain

$$\begin{aligned} J_{TE,n} &= A_n^* T^2 \left[ -\exp(\eta_{n1}) + \exp(\eta_{n2}) \exp\left(-\frac{\Delta E_C}{k_B T}\right) \right], \\ J_{TE,p} &= A_p^* T^2 \left[ \exp(\eta_{p1}) - \exp(\eta_{p2}) \exp\left(-\frac{\Delta E_V}{k_B T}\right) \right]. \end{aligned} \quad (91)$$

The application of either Eq. (87) or Eq. (91) is determined by a single user-defined cutoff density. When the electron or hole density is larger than this cutoff density, Eq. (87) is used; otherwise, Eq. (91) is used.

Due to some limitation in the heterojunction implementation infrastructure, it is not straightforward to automatically compute the band offset at a HJ, therefore, the band offset is provided as a user-defined parameter in the input xml. Since the left (right) side always corresponds to side 1 (side 2),  $\Delta E_C = E_{C1} - E_{C2}$ , and  $\Delta E_V = E_{V2} - E_{V1}$ , as mentioned earlier, the band offsets can be either positive or negative. The equations described above are applicable to positive  $\Delta E_C$  and  $\Delta E_V$ . For other cases of  $\Delta E_C$  and  $\Delta E_V$ , the equations require some modification. Figure 9-2 summarizes the different cases of  $\Delta E_C$  and  $\Delta E_V$ , the corresponding band structures, and the corresponding net thermionic emission current densities for Boltzmann statistics (similar modifications hold for Fermi-Dirac statistics). All the four scenarios in Fig. 9-2 are taken into account in Charon.

<p>(a)</p> 	$\Delta E_C > 0, \Delta E_V > 0$ $J_{TE,n} = A_n^* T^2 \left[ -\frac{n_1}{N_{C1}} + \frac{n_2}{N_{C2}} \exp\left(\frac{-\Delta E_C}{k_B T}\right) \right]$ $J_{TE,p} = A_p^* T^2 \left[ \frac{p_1}{N_{V1}} - \frac{p_2}{N_{V2}} \exp\left(\frac{-\Delta E_V}{k_B T}\right) \right]$
<p>(b)</p> 	$\Delta E_C > 0, \Delta E_V < 0$ $J_{TE,n} = A_n^* T^2 \left[ -\frac{n_1}{N_{C1}} + \frac{n_2}{N_{C2}} \exp\left(\frac{-\Delta E_C}{k_B T}\right) \right]$ $J_{TE,p} = A_p^* T^2 \left[ \frac{p_1}{N_{V1}} \exp\left(\frac{\Delta E_V}{k_B T}\right) - \frac{p_2}{N_{V2}} \right]$
<p>(c)</p> 	$\Delta E_C < 0, \Delta E_V < 0$ $J_{TE,n} = A_n^* T^2 \left[ -\frac{n_1}{N_{C1}} \exp\left(\frac{\Delta E_C}{k_B T}\right) + \frac{n_2}{N_{C2}} \right]$ $J_{TE,p} = A_p^* T^2 \left[ \frac{p_1}{N_{V1}} \exp\left(\frac{\Delta E_V}{k_B T}\right) - \frac{p_2}{N_{V2}} \right]$
<p>(d)</p> 	$\Delta E_C < 0, \Delta E_V > 0$ $J_{TE,n} = A_n^* T^2 \left[ -\frac{n_1}{N_{C1}} \exp\left(\frac{\Delta E_C}{k_B T}\right) + \frac{n_2}{N_{C2}} \right]$ $J_{TE,p} = A_p^* T^2 \left[ \frac{p_1}{N_{V1}} - \frac{p_2}{N_{V2}} \exp\left(\frac{-\Delta E_V}{k_B T}\right) \right]$

**Figure 9-2 Different cases of  $\Delta E_C$  and  $\Delta E_V$ , the corresponding band diagrams, and the corresponding net thermionic emission current densities for Boltzmann statistics.**

## 9.2. Local Tunneling

If the potential barrier at an abrupt HJ is sufficiently narrow, carrier tunneling will contribute significantly to the net carrier flux across the junction. This occurs when the doping in one side is high causing a large electric field in the depletion region adjacent to the junction and therefore a thin barrier. For the conduction band profile of the NPN HBT in Fig. 9-1, electrons can tunnel from the emitter (side 1) to the base (side 2) due to the high electric field in the emitter. Tunneling across a HJ can be categorized into local and non-local tunneling. The local tunneling (LT) model is basically a simplified version of the more accurate non-local tunneling model, with the local model being much easier to implement than the non-local one, especially in a distributed parallel running environment. Charon currently supports only the LT model. The LT model is derived in

detail from the original paper [49] in Appendix C, and its final form is given below.

Taking the conduction band profile in Fig. 9-2(a) as an example, the net electron current density across the HJ including both thermionic emission and local tunneling is given by

$$J_{HJ,n} = J_{TE,n}(1 + \delta_n), \quad (92)$$

where the tunneling factor  $\delta_n$  takes the form of [see Eq. (135)]

$$\delta_n = \frac{1}{k_B T} \int_0^{\Delta E_C} \exp \left[ -\frac{8\pi}{3hq\xi} \sqrt{2m_{nt}^*} (\Delta E_C - E)^{3/2} \right] \exp \left( \frac{\Delta E_C - E}{k_B T} \right) dE.$$

In this equation,  $h$  is the Planck constant,  $q$  is the elemental charge,  $\xi$  is the larger electric field of the two sides [i.e., the electric field in side 1 for Fig. 9-2(a)], and  $m_{nt}^*$  is the electron tunneling effective mass. To perform the integration over energy efficiently, one can rewrite  $\delta_n$  in the following form:

$$\delta_n = \int_0^{\frac{\Delta E_C}{k_B T}} \exp \left[ u - \left( \frac{u}{u_0} \right)^{\frac{3}{2}} \right] du, \quad (93)$$

where  $u$  and  $u_0$  are defined as

$$\begin{aligned} u &= \frac{\Delta E_C - E}{k_B T}, \\ u_0 &= \frac{1}{k_B T} \left( \frac{3hq\xi}{8\pi\sqrt{2m_{nt}^*}} \right)^{\frac{2}{3}}. \end{aligned} \quad (94)$$

The above tunneling model is also applicable to the electron tunneling over the conduction band profile in Fig. 9-2 (c), except that the absolute value of  $\Delta E_C$  and the larger electric field in side 2 should be used in computing  $\delta_n$ .

For hole tunneling through the valence band profiles in Fig. 9-3, the same equations [Eqs. (92) and (93)] are applicable, except that  $\Delta E_C$  and  $m_{nt}^*$  are replaced by  $\Delta E_V$  and  $m_{pt}^*$ , respectively. Note that the valence band profiles in Fig. 9-2(a) and (c) do not allow for hole tunneling, while hole tunneling over the valence band profiles in Fig. 9-2(b) and (d) is negligible due to the fact that the tunneling source side has a smaller electric field which is used in computing the local tunneling factor  $\delta_p$ .

### 9.3. Model Implementation

Implementation of the TE and LT models in Charon consists of two main parts: (i) compute the net current density across a HJ according to the models described above, (ii) add the HJ current density to the residual of the carrier continuity equations as an interface flux condition. The carrier continuity equations are discretized using both the finite element method with the streamline upwinding Petrov-Galerkin stabilization (FEM-SUPG) [15], and the control volume finite element method with the Scharfetter-Gummel stabilization (CVFEM-SG) [14]. Hence the

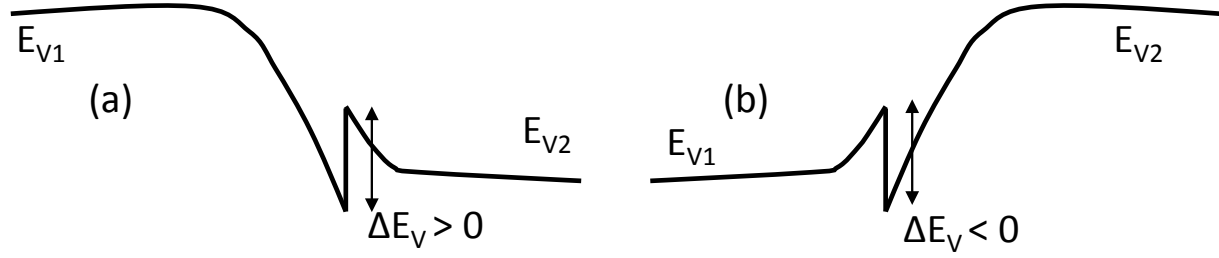


Figure 9-3 Examples of valence band diagrams that allow for hole tunneling.

HJ models are implemented for the two discretization schemes. In the following, the implementation of the HJ models is highlighted for the FEM-SUPG discretization, and a similar implementation is also done for the CVFEM-SG method.

The dimensionless carrier continuity equations take the form of

$$\begin{aligned}\frac{\partial n}{\partial t} - \nabla \cdot \mathbf{J}_n + R &= 0, \\ \frac{\partial p}{\partial t} + \nabla \cdot \mathbf{J}_p + R &= 0.\end{aligned}\tag{95}$$

For implementation purpose, the equations need to be rewritten in the FEM weak forms. Considering the two element blocks (e.g., eb1 and eb2) that share a HJ as illustrated in Fig. 9-4, the carrier densities are discontinuous at the HJ, hence the basic variables are  $(n_1, p_1, \phi)$  for eb1, and  $(n_2, p_2, \phi)$  for eb2, where  $\phi$  is the to-be-solved electric potential which is continuous across the HJ. The Galerkin finite element weak forms of the continuity equations are

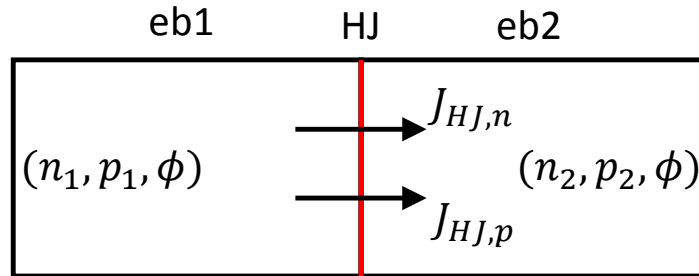


Figure 9-4 Schematics of two element blocks with a heterojunction, showing the basic variables in each element block and the currents across the junction.



$$\begin{aligned}
\int_{\Omega} \left( \frac{\partial n_1}{\partial t} + R \right) w d\Omega + \int_{\Omega} \mathbf{J}_{n1} \cdot \nabla w d\Omega - \int_{HJ} J_{HJ,n} w d\Omega &= 0, \\
\int_{\Omega} \left( \frac{\partial n_2}{\partial t} + R \right) w d\Omega + \int_{\Omega} \mathbf{J}_{n2} \cdot \nabla w d\Omega + \int_{HJ} J_{HJ,n} w d\Omega &= 0, \\
\int_{\Omega} \left( \frac{\partial p_1}{\partial t} + R \right) w d\Omega - \int_{\Omega} \mathbf{J}_{p1} \cdot \nabla w d\Omega + \int_{HJ} J_{HJ,p} w d\Omega &= 0, \\
\int_{\Omega} \left( \frac{\partial p_2}{\partial t} + R \right) w d\Omega - \int_{\Omega} \mathbf{J}_{p2} \cdot \nabla w d\Omega - \int_{HJ} J_{HJ,p} w d\Omega &= 0,
\end{aligned} \tag{96}$$

where  $w$  is the FE nodal basis function,  $J_{HJ,n}$  and  $J_{HJ,p}$  are the net heterojunction current density for electrons and holes respectively, with  $J_{HJ,n}$  given in Eq. (92). The same  $J_{HJ,n}$  is applied to the  $n_1$  and  $n_2$  equations except for the opposite sign, and the same holds true for  $J_{HJ,p}$

#### 9.4. Model Usage

To use the TE and LT models for simulating a heterodevice, besides the common settings used for simulating a homojunction device such as a silicon pn diode provided in an input file, we need two additional settings: (i) specify discontinuous suffix numbers in physics blocks; (ii) specify a heterojunction block. Taking the InGaP/GaAs/GaAs NPN HBT device in Fig. 9-1 as an example, the emitter-base junction can have electron and hole thermionic emission currents and electron tunneling current, but does not support hole tunneling.

First, the discontinuous suffix numbers are specified for the InGaP and GaAs physics blocks, as shown in the following snippet. The InGaP physics block corresponds to the emitter InGaP region which is defined as side 1, while the GaAs physics block corresponds to the base and collector regions which are defined as side 2.

```

start Physics Block InGaP
  discontinuity for hbt with suffix 1
  geometry block is emitter-ingap
  material model is InGaP-Parameter
  ...
end

start Physics Block GaAs
  discontinuity for hbt with suffix 2
  geometry block is base-gaas
  geometry block is collector-gaas
  material model is GaAs-Parameter
  ...
end Physics Block GaAs

```

Second, one needs to specify the heterojunction block as follows

```

start heterojunction on {sidesetName}
  junction is between blocks {block1var} and {block2var}
  start electron
    discretization method is fem or cvfem
    local tunneling is on or off
  end electron
end heterojunction

```

```

    (one parameter per line in the form):
    {parameter name} = {parameter value}
    (see table 9-1 for available parameters)
end electron
start hole
    discretization method is fem or cvfem
    local tunneling is on or off
    (same parameters as electron above)
end hole
end

```

The `sidesetName` keyword specifies the sideset at which the heterojunction BC is applied. The sideset needs to be defined in Cubit as a one-sided sideset. `block1var` and `block2var` are the two element blocks that touch the same sideset defined by `sidesetName`. `discretization method` specifies the discretization method for computing heterojunction current density, which can be either `fem` (finite element discretization) or `cvfem` (Scharfetter-Gummel discretization). `local tunneling` specifies if one wants to include tunneling current in heterojunction BC calculation. When it is `on`, Eq. (92) is used; otherwise, Eq. (85) is used in computing heterojunction current density.

**Table 9-1 Syntax and parameters for the heterojunction boundary condition.  $m_0$  is the free electron effective mass.**

Input file	Corresponding variables	Description	units
fermi dirac density	None	carrier density above which the Fermi-Dirac approach is used in computing current density	$cm^{-3}$
effective mass	$m_n^*$ or $m_p^*$ in Eq. (86)	carrier effective mass for computing the Richardson constants	$m_0$
band offset	$\Delta E_C$ or $\Delta E_V$ in Eq. (85)	conduction or valence band offset	eV
local tunneling mass	$m_{nt}^*$ or $m_{pt}^*$ in Eq. (94)	carrier effective mass for local tunneling calculation	$m_0$

For the InGaP/GaAs/GaAs NPN HBT example in Fig. 9-1, the heterojunction block looks like

```

start heterojunction on ebjunction
    junction is between blocks emitter-ingap and base-gaas
start hole
    effective mass = 0.58
    band offset = 0.444
    fermi dirac density = 1e11
    discretization method is fem
end hole
start electron
    effective mass = 0.088
    band offset = 0.064
    fermi dirac density = 1e11
    discretization method is fem
    local tunneling is on

```

```
    tunneling effective mass = 0.088  
  end electron  
end heterojunction
```

**Complete examples on the heterojunction BC can be found at** `tcad-charon/test`  
`/nightlyTests/b2ttunnel/`.

## 10. HARMONIC BALANCE

Frequency domain simulation of the coupled Drift-Diffusion and Poisson equations is possible in Charon via the harmonic balance (HB) method. All physical discretization schemes are supported, and either a small-signal or large-signal analysis can be chosen for the frequency-domain analysis. In this section, we will refer to the standard Charon formulation as the time-domain (TD) formulation to distinguish it from the HB formulation.

### 10.1. Formulation

For brevity in exposition, we outline Charon's harmonic balance method only for the electron drift-diffusion equation in a Galerkin finite-element spatial discretization; the same process is applied to the other equations in any discretization scheme *mutatis mutandis*. The electron drift-diffusion equation can be expressed as

$$\frac{\partial n}{\partial t} + \mathcal{F}_n(n, p, \phi) = 0, \quad (97)$$

where  $n(t)$ ,  $p(t)$ , and  $\phi(t)$  is the electron density, hole density, and electric potential, respectively. The quantity  $\mathcal{F}_n$  consists of terms which are not explicitly time-dependent. Using a spatial basis function  $\Lambda(\vec{x})$  on a spatial discretization element  $V$ , a component of the residual is

$$\int_V \frac{\partial n}{\partial t} \Lambda(\vec{x}) d\vec{x} + \mathcal{R}_n^\Lambda(n(t), p(t), \phi(t)) = 0. \quad (98)$$

Note that the  $\mathcal{R}_n^\Lambda(t)$  term denotes the spatial residual of the steady-state equation. The term  $\frac{\partial n}{\partial t}$  is approximated using a time discretization method (e.g., backward-Euler) for a TD transient simulation, or else omitted for a steady-state simulation. In the harmonic balance method, this term is transformed into the frequency domain.

The HB method (in either the small-signal and large-signal modes) has a solution ansatz whose form depends on the applied contact voltage frequencies  $\omega_1$  Hz,  $\omega_2$  Hz,  $\dots$ ,  $\omega_\ell$  Hz, called the fundamental frequencies of a simulation. Without loss of generality, we assume that  $\omega_1 < \omega_2 < \dots < \omega_\ell$ , and write  $\vec{\omega} = (\omega_1, \dots, \omega_\ell)$  for conciseness. A choice is made for the degree of intermodulation frequencies to be captured by the HB method, and the collection of those intermodulation frequencies is called a *truncation scheme*. Truncation schemes  $\mathcal{T}$  are recorded as integer lattice points  $\vec{k} = (k_1, k_2, \dots, k_\ell) \in \mathbb{Z}^\ell$  which correspond to a linear combination  $\vec{\omega} \cdot \vec{k}$  of the fundamental frequencies. Thus, the HB solution ansatz takes the form

$$n(\vec{x}, t) = N_0(\vec{x}) + \sum_{\vec{k} \in \mathcal{T}} \left[ N_k^c(\vec{x}) \cos(2\pi \vec{\omega} \cdot \vec{k} t) + N_k^s(\vec{x}) \sin(2\pi \vec{\omega} \cdot \vec{k} t) \right] \quad (99)$$

Note that the physical solution contains more frequencies than those fundamental frequencies applied, and the ansatz captures this but necessarily truncates the frequencies observed [41]. Common truncation schemes interpolate between the Box and Diamond truncation schemes [44].

To arrive at the HB equations, we first multiply (98) by a Fourier basis function, i.e.,

$$\cos(2\pi\vec{\omega} \cdot \vec{k}t) \text{ or } \sin(2\pi\vec{\omega} \cdot \vec{k}t) \text{ for } \vec{k} \in \mathcal{T},$$

and integrate over a period. This results in  $2|\mathcal{T}| + 1$  residual equations, disregarding  $\sin(2\pi 0t)$ . In the following, we explicitly describe the procedure involving  $\cos(2\pi\omega_i t)$  because all other cases are similar. We next integrate the time-derivative summand analytically, and the time-independent summand numerically using a trapezoidal rule (which converges exponentially for periodic functions [32]). Thus, we obtain the  $\cos(2\pi\omega_i t)$  HB residual equation:

$$0 = \pi\omega_i \int_V N_{\omega_i}^s(\vec{x}) \Lambda(\vec{x}) d\vec{x} + \sum_{m=0}^L w_{\omega_i}^m \mathcal{R}_{\mathbf{u}}^\Lambda(n(t_m), p(t_m), \phi(t_m)) \quad (100)$$

involving time collocation points and quadrature weights

$$t_m = \frac{m}{L} \quad \text{and} \quad w_{\omega_i}^m \equiv \frac{2 - \delta_{0m} - \delta_{mL}}{2} \cos(2\pi\omega_i t_m)$$

where  $\delta_{ab} = 1$  when  $a = b$  and  $\delta_{ab} = 0$  otherwise, and  $L = 2\omega_\ell$  by the Nyquist Sampling Theorem.

We note here that the arguments  $n(t_m)$ ,  $p(t_m)$ , and  $\phi(t_m)$  of  $\mathcal{R}_{\mathbf{u}}^\Lambda$  are evaluated via the ansatz expression (99). For this evaluation, the small-signal and large-signal formulations differ slightly: for the small-signal analysis, the summation is restricted to only  $\vec{k}$  which yields  $\vec{\omega} \cdot \vec{k} = \omega_i$ ; for the large-signal analysis, the summation ranges over all  $\vec{k} \in \mathcal{T}$ . This has the following analytic interpretation: the small-signal response at the  $\omega_i$  frequency is only influenced by the contact voltage amplitudes at 0 and  $\omega_i$  hertz; whereas the large-signal response at any frequency is influenced by the contact voltage amplitudes of all frequencies and their intermodulations.

We see that the HB residual equation (100) is assembled by constructing  $\mathcal{R}_{\mathbf{u}}^\Lambda$ , the steady-state TD model,  $L + 1$  times and substituting the HB solution ansatz equation (99) into the TD model. Clearly, any discretization methods and physical models that are implemented for the TD analysis will be carried over to the HB residual because they are incorporated into  $\mathcal{R}_{\mathbf{u}}^\Lambda$ . The parallelization we use to speed up the transform comes at two stages: we exploit the summations appearing in the ansatz (99) and the residual (100).

The Nyquist Sampling Theorem recommends a minimum of  $2\omega_\ell + 1$  time collocation points, which is too great for large frequencies. This makes the transform (100) prohibitively expensive. To address this, we have developed an efficient *minimal iso-frequency remapping* as an alternative to various frequency mapping methods in the literature [37].

## 10.2. Usage

The specification of any physics models is identical to that in the time-domain simulation, except for the specification of the frequency domain options (as a sub-block within the physics block), boundary conditions, and initial conditions. We remark that the output of the Charon simulation will be in the frequency domain. Thus, the Fourier coefficients of the current and degrees of freedom are returned. In the following, we will describe the three necessary input deck blocks in order to perform a harmonic balance analysis in Charon.

### 10.2.1. **Physics Block**

A harmonic balance analysis needs to be specified in the physics block, choosing either a small-signal or large-signal analysis. A physics sub-block specifying frequency domain parameters is also required. Within a physics block corresponding to one named *physicsBlockName*, this has form:

```
start Physics Block physicsBlockName
  apply harmonic balance
  start harmonic balance parameters
  ..
end
end
```

In Table 10-1, we provide a description of the options and parameters which can be set for a harmonic balance analysis.

**Table 10-1 Syntax for HB analysis in physics block.**

apply harmonic balance [for small signal analysis [for large signal analysis]] start harmonic balance parameters truncation order = { <i>truncationOrder</i> } truncation scheme is { <i>truncationScheme</i> } fundamental harmonics = { <i>fundamentalHarmonics</i> } end		
Option	Description	Required
for small signal analysis	Specify a small-signal frequency domain analysis.	No
for large signal analysis	Specify a large-signal frequency domain analysis. This is the default mode of harmonic balance analysis, if neither option is specified.	No
Variables	Description	Default
<i>truncationOrder</i>	Specify the order of truncation scheme.	<i>None</i>
<i>truncationScheme</i>	Specify the type of truncation scheme to use, chosen among: box, diamond.	<i>None</i>
<i>fundamentalHarmonics</i>	Space-separated sequence of fundamental harmonics.	<i>None</i>

### 10.2.2. **Boundary Conditions**

In place of the standard boundary condition option which takes the form

BC is *bcType* for *contactName* on *materialName*

we have instead, for a harmonic balance analysis, a block which takes the form

```
start hb boundary conditions for contactName on materialName
  ..
end
```

Within this block, the kind of boundary condition applied can be specified. The parameters which may be set in this block are described in Table 10-2.

**Table 10-2 Syntax for HB Boundary Conditions. Note that the list of *frequencyValues*, *amplitudeValues*, and *phaseshiftValues* must have the same number of parameters.**

start Harmonic Balance BC for <i>contactName</i> on <i>materialName</i> type is <i>bcType</i> frequencies = " <i>frequencyValues</i> " amplitudes = " <i>amplitudeValues</i> " phase shifts " <i>phaseshiftValues</i> " end		
Option	Description	Required
	<i>None</i>	
Variables	Description	Default
<i>contactName</i>	Specify a contact name on which to apply this boundary condition.	<i>None</i>
<i>materialName</i>	Specify the material name on which the contact is provided.	<i>None</i>
<i>bcType</i>	Choose among: ohmic, ...	<i>None</i>
<i>frequencyValues</i>	Space-separated values of frequencies, in quotes.	<i>None</i>
<i>amplitudeValues</i>	Space-separated values of amplitudes, in quotes.	<i>None</i>
<i>phaseshiftValues</i>	Space-separated values of phase shifts, in quotes.	<i>None</i>

### 10.2.3. Initial Conditions

In place of the standard boundary condition option which takes the form

initial conditions for *degreeOfFreedom* in *materialName* is *icType*

we have instead, for a harmonic balance analysis, an option which takes the form described in Table 10-3.

## 10.3. Example cases

### 10.3.1. Modifying a time-domain input deck for frequency-domain analysis

In this section, we describe the procedure of modifying the input deck for a (time-domain) equilibrium simulation of a p-n diode in order to apply a small-signal analysis on the same p-n diode to obtain its steady-state frequency-domain behavior.

We refer to the two nightly test inputs:

tcad-charon/test/nightlyTests/capability/pndiode.sg.equ.inp

tcad-charon/test/nightlyTests/freqdom/pndiode.hb-sgcvfem-dd.ac1-linear-SS.inp

**Table 10-3 Syntax for HB Initial Conditions.**

Harmonic Balance Initial Conditions for { <i>degreeOfFreedom</i> } in { <i>materialName</i> } is [ Exodus File [ default [ constant = { <i>constValue</i> } [ uninitialized ]]]]		
Option	Description	Required
	<i>None</i>	
Variables	Description	Default
<i>degreeOfFreedom</i>	Choose one of: ELECTRIC_POTENTIAL, ELECTRON_DENSITY, HOLE_DENSITY, LATTICE_TEMPERATURE	<i>None</i>
<i>materialName</i>	Specify the material in which this initial condition is to be specified.	<i>None</i>
<i>exodus file</i>	This will read in the degree of freedom from the input exodus file.	<i>None</i>
<i>default</i>	This uses the default initial condition for this degree of freedom.	<i>None</i>
<i>constant</i>	This specifies that a constant value will be set for this degree of freedom.	<i>None</i>
<i>constValue</i>	This will set the constant value.	<i>None</i>
<i>uninitialized</i>	This leaves the degree of freedom uninitialized.	<i>None</i>

for these p-n diode simulations. Note that the common discretization type is drift-diffusion cvfem. As described in the preceding usage section, modifications need to be made to the physics block, initial conditions, and boundary conditions to adapt the former input deck into the latter input deck to execute this change of analysis.

The equilibrium (time-domain) simulation of the p-n diode as specified in

tcad-charon/test/nightlyTests/capability/pndiode.sg.equ.inp

applies the boundary conditions

$$V_{\text{anode}} = 0.0V \text{ and } V_{\text{cathode}} = 0.0V$$

whereas the small-signal (frequency-domain) simulation of the same pn-diode as specified in

tcad-charon/test/nightlyTests/freqdom/pndiode.hb-sgcvfem-dd.ac1-linear-SS.inp

applies the boundary conditions

$$V_{\text{anode}} = (4.0 + 2.0 \cdot \sin(2\pi \cdot 1Hz \cdot t))V \text{ and } V_{\text{cathode}} = 0.0V$$

In the following excerpt from

tcad-charon/test/nightlyTests/capability/pndiode.sg.equ.inp

we highlight the commands in **violet** which were modified to support a harmonic balance analysis.



```

start Physics Block Semiconductor
  geometry block is silicon
  standard discretization type is drift diffusion cvfem
  material model is siliconParameter
  srh recombination is on
  radiative recombination is off
  auger recombination is off
end Physics Block Semiconductor
...
BC is ohmic for anode on silicon fixed at 0
BC is ohmic for cathode on silicon fixed at 0
...
initial conditions for ELECTRIC_POTENTIAL in silicon is Exodus File
Initial Conditions for ELECTRON_DENSITY in silicon is Equilibrium Density
Initial Conditions for HOLE_DENSITY in silicon is Equilibrium Density

```

In the following excerpt from

tcad-charon/test/nightlyTests/freqdom/pndiode.hb-sgcvfem-dd.ac1-linear-SS.inp

we highlight the commands in teal which were added to, or modified from, the excerpt above.

```

start Physics Block Semiconductor
  geometry block is silicon
  standard discretization type is drift diffusion cvfem
  apply harmonic balance for small signal analysis
  start harmonic balance parameters
    truncation order = 1
    truncation scheme is box
    fundamental harmonics = 1
  end harmonic balance parameters
  material model is siliconParameter
  srh recombination is off
  radiative recombination is off
  auger recombination is off
end Physics Block Semiconductor
...
start Harmonic Balance BC for anode on silicon
  type is ohmic
  frequencies "0 1"
  amplitudes "4 2"
  phase shifts "0 0"
end Harmonic Balance BC for anode on silicon
start Harmonic Balance BC for cathode on silicon
  type is ohmic
  frequencies "0"
  amplitudes "0"
  phase shifts "0"
end Harmonic Balance BC for cathode on silicon
...
Harmonic Balance initial conditions for ELECTRIC_POTENTIAL in silicon is uninitialized
Harmonic Balance Initial Conditions for ELECTRON_DENSITY in silicon is uninitialized
Harmonic Balance Initial Conditions for HOLE_DENSITY in silicon is uninitialized
Harmonic Balance Initial Conditions for LATTICE_TEMPERATURE in silicon is uninitialized

```

## 11. RADIATION MODELS

Charon includes capabilities to model what the effects of various forms of radiation are on semiconductor devices.

### 11.1. Empirical Displacement Damage Model

As the name implies the empirical radiation model utilizes data obtained from experiments to model the effects of displacement damage radiation [35]. To accomplish this a table representing this data must be input into the code.

In order to utilize the empirical model first the `physics` block sections for the portion of the problem in which it is active must be specified, for example

```
start physics block {physicsBlockName}
...
empirical damage model is on / off
...
end
```

Next a `start empirical model parameters` section is used to specify parameters for the model. That section has the following format

```
start empirical model parameters
mu table data file is {fileName}
emitter base junction bounding box is {min} to {max} in x / y / z
(one parameter per line in the form):
{parameter name} = {parameter value}
(see table 11-1 for available parameters)
end
```

**Table 11-1 Syntax and parameters for the empirical radiation damage model.**

Input file	Description	units
thermal velocity	thermal velocity of carriers	$\frac{cm}{s}$
cross section	collison cross sectional area	$cm^2$
emitter-base voltage override	voltage across the emitter-base junction	V
Parameters for Analytic Radiation Pulse		
pulse start time	set the start time of the radiation pulse	s
pulse end time	set the end time of the radiation pulse	s
pulse magnitude	magnitude of the peak of the radiation pulse	—
pulse resolution	pulse is sampled at this integer value	—
pulse waveform	analytic form of the pulse (see table 11-2)	—

**Table 11-2 Analytic pulse definitions. Unless otherwise noted the pulses are sampled over the range  $t = [\text{pulse start}, \text{pulse end}]$  at the resolution given by the user-specified *pulse resolution* parameter.**

Function name	Equation
delta	$\text{pulse}(t) = (\text{pulse magnitude}) \delta(t - \text{pulse start})$
square	$\text{pulse}(t) = \text{pulse magnitude}$
gaussian	$T_m = \frac{1}{2} (\text{pulse start} + \text{pulse end})$ $P_w = \frac{(\text{pulse start} - \text{pulse end})}{6}$ $\text{pulse}(t) = (\text{pulse magnitude}) \exp\left(-\frac{(t - T_m)^2}{2P_w^2}\right)$
gaussianlog	$T_m = \frac{1}{2} (\log(\text{pulse start}) + \log(\text{pulse end}))$ $P_w = \frac{\log(\text{pulse end}) - \log(\text{pulse start})}{6}$ $\text{pulse}(t) = (\text{pulse magnitude}) \exp\left(-\frac{(t - T_m)^2}{2P_w^2}\right)$ <p>NOTE: for this waveform <math>\log(t)</math> is incremented rather than <math>t</math> such that the data can encompass large time spans, possibly many decades, for example <math>t = [10^{-6} : 10^{-3}]</math>.</p>

## 11.2. Total Ionizing Dose Models

Charon provides several models to simulate total ionizing dose (TID) effects.

### 11.2.1. Fixed Oxide Charge Model

The simplest TID model is to assign positive or negative fixed charges in oxide regions. The effect of fixed charges is included through the Laplace equation for insulators. Currently, only a uniform spatial distribution in a specified box is supported. New analytic spatial profiles can be easily added.

To use the model, one needs to specify it in two places. The first step is to specify

```
bulk fixed charge is on/off
```

in an insulator physics block. When neither option is given, it defaults to `off`. The second step is to add the following block

```
start bulk fixed charge parameters
  distribution is uniform
  charge density = {value} or is swept from {value1} to {value2}
  spatial range is {locMin} to {locMax} in x or in y or in z
end
```

inside a material block. The `distribution` keyword specifies the spatial profile and currently only supports `uniform`. The `charge density` keyword specifies the fixed charge density in units of  $\text{cm}^{-3}$ , which can be positive for positive charges or negative for negative charges. The `charge density` can also be swept from one density to another density. This is done by using

```
charge density is swept from {value1} to {value2}
```

The `spatial range` keyword specifies a box region where bulk fixed charges are located. The `spatial range` line can be defined for each spatial axis.

An example of specifying a fixed charge density in a defined box is given below. Two complete examples are `oxide.lapl.bq-.inp` for negative charges and `oxide.sg.lapl.bq.inp` for positive charges, located under `tcad-charon/test/nightlyTests/oxidecharge/`.

```
start Material Block SiO2Parameter
  material name is SiO2
  relative permittivity = 3.9

  start bulk fixed charge parameters
    distribution is uniform
    charge density = -1e17
    spatial range is 0.2 to 0.8 in x
    spatial range is 0.1 to 0.3 in y
  end bulk fixed charge parameters
end Material Block
```

An example of sweeping charge density in a defined box is given by

```
start Material Block SiO2Parameter
  material name is SiO2
  relative permittivity = 3.9

  start bulk fixed charge parameters
```

```

distribution is uniform
charge density is swept from -1e16 to -1e17
spatial range is 0.2 to 0.8 in x
spatial range is 0.1 to 0.3 in y
end bulk fixed charge parameters
end Material Block

```

In addition to the fixed charge block, one also needs to specify a sweep options block with an example given below. Two complete examples are `oxide.lapl.bq-.loc.a.inp` for negative charge sweeping and `oxide.sg.lapl.bq.loc.a.inp` for positive charge sweeping, located under `tcad-charon/test /nightlyTests/oxidecharge/`.

```

start Sweep Options
  Initial Step Size = -1e16
  Minimum Step Size = 1e13
  Maximum Step Size = 5e16
  continuation method is Arc Length
  predictor method is tangent
  successful step increase factor = 2
  failed step reduction factor = 0.5
  Step Size Aggressiveness = 0.5
end Sweep Options

```

Here the values for initial step size, minimum step size, maximum step size are all in units of  $\text{cm}^{-3}$  for a charge sweeping option.

### 11.2.2. Interface Fixed Charge Model

TID effects in MOSFETs are often modeled by radiation induced charges at semiconductor/insulator interfaces. Charon provides the capability to place fixed positive or negative charges at outer surfaces and/or internal interfaces.

When there exist charges at an interface, the charges affect the electric field at the interface according to Gauss's Law. Given a charge density of  $\sigma$ , in units of  $\text{cm}^{-2}$ , at an interface between materials 1 and 2, Gauss's Law determines that the gradient of the electric potential needs to satisfy:

$$(\epsilon_0 \epsilon_{r2} \nabla \phi_2 - \epsilon_0 \epsilon_{r1} \nabla \phi_1) \cdot \eta_1 = q \sigma. \quad (101)$$

Here,  $q$  is the elemental charge in units of Coulombs (C),  $\epsilon_0$  is the vacuum permittivity with  $\epsilon_0 = 8.8542 \times 10^{-14} \text{ C V}^{-1} \text{ cm}^{-1}$ ,  $\epsilon_{r1}$  and  $\epsilon_{r2}$  are the relative permittivity of materials 1 and 2 respectively.  $\nabla \phi_1$  and  $\nabla \phi_2$  are the potential gradient in units of  $\text{V cm}^{-1}$  in materials 1 and 2 respectively, and  $\eta_1$  is a normal unit vector pointing from 2 to 1. If the charges are located at an outer surface of a simulation device, the potential gradient at the surface is given by:

$$\epsilon_0 \epsilon_r \nabla \phi \cdot \eta = q \sigma, \quad (102)$$

where  $\eta$  is a normal unit vector pointing outward from the device.

Two steps are required to use the Neumann charge BC. First, we need to define the charge interface as a sideset in Cubit. Care should be taken to capture the correct potential gradient when

specifying the mesh density in the vicinity of the interface. For example, if  $\sigma = 10^{11} \text{ cm}^{-2}$  is specified at an interface, the mesh interval adjacent to the interface should not be greater than 1 nanometer (nm). If a higher  $\sigma$  is specified, a mesh size finer than 1 nm at the interface would be required. The general rule of thumb is, the higher the charge density is, the finer the mesh interval required. Next, we need to specify the details of the BC in Charon's input file. The syntax for doing this is

```
start surface charge bc for {sidesetName}
  geometry block is {geometryBlockName}
  fixed charge = {chargeValue}
end
```

where {sidesetName} is the name of the sideset as given during mesh generation in Cubit, {geometryBlockName} is the name of the element block that is adjacent to the surface charge, again, as assigned during mesh generation in Cubit. If a charge sideset is located at the outer boundary of an element block, the associated element block is uniquely defined. If charges are located at an internal interface in a simulation domain then two element blocks are needed at the shared interface. When specifying the interface charge, either of the two element blocks can be used for {geometryBlockName} without affecting the simulation

To verify the accuracy of the charge BC, we first need to consider that all the quantities except energy related fields from Charon are scaled by scaling factors. The scaling factors are internally defined except the Concentration Scaling which can be specified in the Charon input file. Taking into account the scaling factors, the charge BC at an internal interface becomes:

$$(\epsilon_{r2} \nabla \phi_2^s - \epsilon_{r1} \nabla \phi_1^s) \cdot \mathbf{n}_1 = \frac{q\sigma X_0}{\epsilon_0 V_0}, \quad (103)$$

and the charge BC at an outer surface becomes:

$$\epsilon_r \nabla \phi^s \cdot \mathbf{n} = \frac{q\sigma X_0}{\epsilon_0 V_0}. \quad (104)$$

Here the superscript  $s$  denotes that the potential gradient is scaled and therefore is unitless.  $X_0$  and  $V_0$  are the length and voltage scaling factors respectively. All the scaling factors' values are output to the screen at the beginning of a Charon simulation. In Charon,  $X_0$  is hard-coded to be  $10^{-4} \text{ cm}$ , and  $V_0 = k_B T / q$  with  $k_B$  being the Boltzmann constant and  $T$  being the lattice temperature. If Lattice Temperature is set to 300 K,  $V_0$  is approximately 0.0258 V.

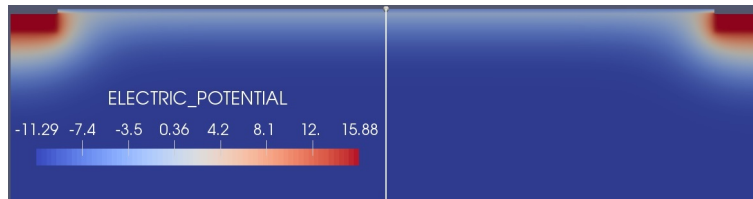


**Figure 11-1 Scaled electric potential at equilibrium for a n-channel silicon MOSFET with a positive charge density of  $10^{11} \text{ cm}^{-2}$  at the Si/SiO<sub>2</sub> interface**

Figure 11-1 shows the scaled electric potential profile for the n-channel MOSFET example given in `tcad-charon/test/nightlyTests/surfacecharge/nmosfet.ifq+.sg.equ.xml`. The example has

positive charge with a surface density of  $10^{11} \text{ cm}^{-2}$  at the Si/SiO<sub>2</sub> interface. The scaled potential gradient along the white line is shown in figure 11-2. Using the potential gradient values at the Si/SiO<sub>2</sub> interface in figure 11-2, the left hand side of Eq. (103) is equal to  $11.9 \times 31.49 - 3.9 \times (-83.27) = 699.48 \text{ V cm}^{-1}$ , while the right hand side of Eq. (103) is given by  $q\sigma X_0/(\epsilon_0 V_0) = (1.602 \times 10^{-19} \times 10^{11} \times 10^{-4})/(8.854 \times 10^{-14} \times 0.0258) = 700.75 \text{ V cm}^{-1}$ . Therefore, the potential gradient at the Si/SiO<sub>2</sub> interface obtained from Charon indeed satisfies the theoretical relation in Eq. (103).

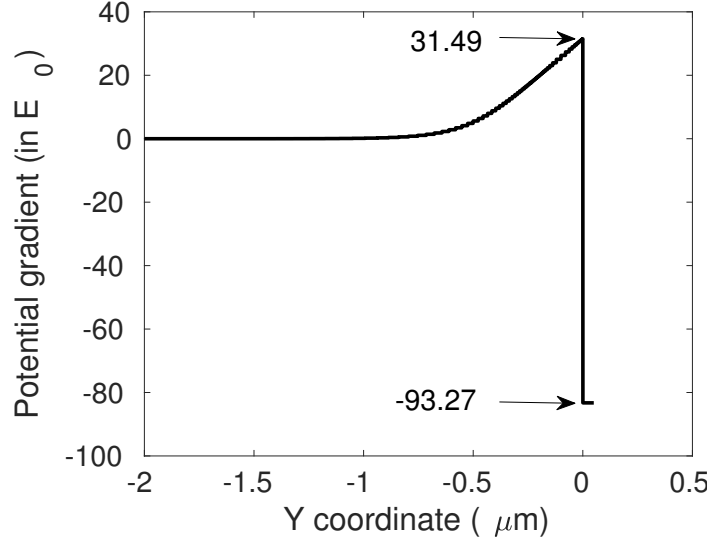


**Figure 11-2 Scaled potential gradient along the white line in figure 11-1. The Si/SiO<sub>2</sub> interface is located at  $y = 0$ . The  $y < 0$  region is the Si region, while  $y > 0$  is the SiO<sub>2</sub> region. The denoted numbers are the potential gradients at the Si/SiO<sub>2</sub> interface obtained from Charon.**

### 11.2.3. Interface Static Trap Model

Charon also provides an interface static trap model that allows to capture voltage dependent threshold voltage shift in MOSFETs due to TID effects. Interface traps act as carrier recombination centers. Traps induced surface recombination rate is given by

$$R_{surf} = \sum_j \frac{np - n_{ie}^2}{(n + n_t^j)/s_p^j + (p + p_t^j)/s_n^j}, \quad (105)$$

where the summation runs over the total number of different types of traps (e.g., two traps located at two different energy levels). For simpler notation, the superscript  $j$  is omitted in the following.  $n_{ie}$  is the effective intrinsic concentration in a material.  $s_p$  ( $s_n$ ) is the hole (electron) surface recombination velocity.  $n_t$  and  $p_t$  for the  $j$ th type of traps are equal to

$$n_t = n_{ie} \exp\left(\frac{E_t}{k_B T}\right), \quad p_t = n_{ie} \exp\left(-\frac{E_t}{k_B T}\right), \quad (106)$$

where  $E_t$  is the trap energy measured from the intrinsic Fermi level,  $E_i$ .  $E_t$  is positive for traps above  $E_i$  and negative for traps below  $E_i$ .  $k_B$  is the Boltzmann constant, and  $T$  is the lattice temperature. The carrier surface recombination velocity can be specified directly by user or computed from the following expression

$$s_v = \sigma_v v_v N_{it}, \quad v = n, p. \quad (107)$$

$\sigma$  is the carrier capture cross section in  $\text{cm}^2$ ,  $v$  is the carrier thermal velocity in  $\text{cm/s}$ ,  $N_{it}$  is the interface trap density in  $\text{cm}^{-2}$ . In Charon, the thermal velocity is computed using

$$v_v = \sqrt{\frac{3k_B T}{m_v^*}}, \quad v = n, p, \quad (108)$$

where  $m^*$  is the carrier effective mass.

Charon supports two types of interface traps, i.e., `Acceptor` and `Donor` traps. `Acceptor` traps are electron traps which are neutral when unoccupied and carry the charge of electrons when occupied. `Donor` traps are hole traps which are neutral when empty and carry the charge of holes when occupied. The occupation function of the  $j$ th electron traps is given by

$$f_{in} = \frac{s_n n + s_p p_t}{s_n(n + n_t) + s_p(p + p_t)}. \quad (109)$$

The occupation function of the  $j$ th hole traps is

$$f_{tp} = \frac{s_p p + s_n n_t}{s_n(n + n_t) + s_p(p + p_t)}. \quad (110)$$

The charge density due to occupied acceptor or donor traps contributes to the right hand side (RHS) of the Poisson equation. The charge contribution is equal to  $-q \sum_j N_{it}^j f_{in}$  for acceptor traps, and it is  $q \sum_j N_{it}^j f_{tp}$  for hole traps, with  $q$  being the elemental charge.

Specification of the interface trap model is similar to that of the interface fixed charge model except that trap related parameters must be given. The mesh size near the interface of interest should be fine as in the interface fixed charge model. The syntax for specifying the model is given below

```
start surface charge bc for {sidesetName}
  geometry block is {geometryBlockName}
  start surface trap
    effective mass for electrons = {eMass}
    effective mass for holes = {hMass}
    start trap {trapID}
      type is {trapType}
      (one parameter per line in the form):
      {parameter name} = {parameter value}
      (see table 11-3 for available parameters)
    end
  end
end
start surface recombination
```



```

    (one parameter per line in the form):
    {parameter name} = {parameter value}
    (see table 11-3 for available parameters)
end
end

```

effective mass for electrons (holes) corresponds to  $m_n^*$  ( $m_p^*$ ) in Eq. (108). Its value must be given in units of the free electron mass  $m_0$ . Multiple types of traps can be given by specifying multiple `start trap` blocks with different `trapID` numbers. `trapID` is an integer equal or greater than 0. `trapType` must be either `Acceptor` or `Donor`. `Acceptor` traps are electron traps which are neutral when empty and carry the charge of one electron when occupied. `Donor` traps are hole traps which are neutral when empty and carry the charge of one hole when occupied.

Another way of modeling surface recombination due to traps is by specifying the carrier surface recombination velocity directly. This is done by specifying the `start surface recombination` block which has three parameters, i.e., energy, surface velocity for electrons, and surface velocity for holes.

**Table 11-3 Available parameters for the interface trap model.**

Parameter name	Corresponding variables	Description	units
energy	$E_t$ in Eq. (106)	trap energy level measured from the intrinsic Fermi level $E_i$ , positive above $E_i$ and negative below $E_i$	eV
density	$N_{it}$ in Eq. (107)	trap density	$\text{cm}^{-3}$
cross section for electrons	$\sigma_n$ in Eq. (107)	electron capture cross section	$\text{cm}^{-2}$
cross section for holes	$\sigma_p$ in Eq. (107)	hole capture cross section	$\text{cm}^{-2}$
surface velocity for electrons	TBW	electron surface recombination velocity	V/cm
surface velocity for holes	TBW	hole surface recombination velocity	V/cm

An example of specifying the interface trap model with two types of traps is given below.

```

start surface charge bc for sheet
  geometry block is silicon
  start surface trap
    effective mass for electrons = 0.25
    effective mass for holes = 0.50
    start trap 0
      type is Acceptor
      density = 1e11
      energy = 0.3
      cross section for electrons = 1e-12
      cross section for holes = 1e-12
    end trap 0
  end surface trap
end surface charge bc for sheet

```

```

start trap 1
  type is Donor
  density = 1e10
  energy = -0.2
  cross section for electrons = 1e-12
  cross section for holes = 1e-14
end trap 1
end surface trap
end surface charge bc for sheet

```

Several complete examples on the model can be found at `test/nightlyTests/surfacecharge` including `nmosfet.sg.it.equ.inp`, `nmosfet.sg.it.loca.inp`, and `nmosfet.dd.it.all.equ.inp`.

#### 11.2.4. Kimpton Model

Kimpton model is a more advanced TID model for radiation tolerant insulators where radiation-induced charge and threshold voltage shift depend not only on the radiation dose but also on the electric fields. It is a trapping-detrapping model taking into account interface and volume traps distributed within the irradiated insulator.

The Kimpton model assumes that the exposure to ionizing radiation results in excess positive charge trapping in the insulator (gate oxides in MOSFETs) due to the predominance of hole traps. In radiation-tolerant insulators the hole traps behave as energy wells with no significant bonding allowing reversible trapping-detrapping processes. Detrapping process of the trapped carriers is assisted by the energy released from the recombination of some of the electron-hole pairs generated during irradiation.

For positive electric fields (holes are pushed towards the interface by the field) interface traps and hole trapping/detrapping at the interface account for the threshold voltage shifts for positive electric fields greater than  $0.1 \frac{MV}{cm}$ . The trapping, detrapping and conservation equations for interface traps are given by

$$\begin{aligned}
p_{\text{ttp}}^i &= (N_t^i - N_{\text{tf}}^i) \sigma E_{\text{ins}}^{-x} f_{(\text{ins})} n_{\text{pairs}}^{\text{gen}}, \\
p_{\text{tde}}^i &= N_{\text{tf}}^i \sigma E_{\text{ins}}^{-x} (1 - f_{(\text{ins})}) n_{\text{pairs}}^{\text{gen}}, \\
p_{\text{ttp}}^{i,\text{net}} &= N_{\text{tf}}^i + p_{\text{ttp}}^i - p_{\text{tde}}^i
\end{aligned} \tag{111}$$

where  $p_{\text{ttp}}^i$  is the interface density of new holes trapped after a small dose irradiation,  $p_{\text{tde}}^i$  is the interface density of detrapped holes assisted by the energy released from geminate recombination of electron-hole pairs after the small dose irradiation,  $p_{\text{ttp}}^{i,\text{net}}$  is the net interface density of trapped holes,  $N_t^i$  is the interface trap density,  $N_{\text{tf}}^i$  is the interface occupied trap density before irradiation,  $\sigma$  is the trap capture cross section for a positive field of  $1 \frac{MV}{cm}$ ,  $E_{\text{ins}}$  is the electric field in the insulator,  $x$  is a constant depending on technology,  $n_{\text{pairs}}^{\text{gen}}$  is the electron-hole pair density generated during irradiation and  $f_{(\text{ins})}$  is the fractional hole yield.

Electron-hole pairs density  $n_{\text{pairs}}^{\text{gen}}$  generated during irradiation is given by

$$n_{\text{pairs}}^{\text{gen}} = \rho_{\text{ins}} 10^{-5} \text{Dose} \frac{C_{\text{DEF}}}{qE_{\text{form}}} \quad (112)$$

where  $\rho_{\text{ins}}$  is the insulator mass density in  $\frac{\text{g}}{\text{cm}^3}$ ,  $\text{Dose}$  is the radiation dose in  $\text{rad}$ ,  $C_{\text{DEF}}$  is the effective dose enhancement factor and  $E_{\text{form}}$  is the effective electron-hole pair formation energy.

The fractional hole yield  $f_{(\text{ins})}$  also depends on the electrical field in the insulator  $E_{\text{ins}}$  as

$$f_{(\text{ins})} = \left[ \left( \frac{1.35}{E_{\text{ins}}} \right) - 1 \right]^{-0.9} \quad (113)$$

Charon computes the net interface density of trapped holes  $p_{\text{tip}}^{\text{i,net}}$  and add the charge to the Laplace equation solved in the irradiated insulator. The user can visualise the induced charge in the irradiated insulator and perform subsequent simulations for computing the threshold voltage shifts due to radiation induced charge.

To use the Kimpton model with interface traps in an insulator, the user must first turn on the TID model in the appropriate physics section

```
start Physics Block {physicsBlockName}
...
tid is on
...
end
```

and specify the Kimpton model with general parameters defined in table 11-4 and interface parameters defined in table 11-5 inside the tid section of the material block section

```
start Material Block {materialBlockName}
start tid
start kimpton model
(one parameter per line in the form):
{parameter name} = {parameter value}
(see table 11-4 for available parameters)

start interface traps
sideset id is {tidInterface}

(one parameter per line in the form):
{parameter name} = {parameter value}
(see table 11-5 for available parameters)
end
end
end
end
```

**Table 11-4 Syntax and general parameters for Kimpton model.**

Input file	Corresponding variable in (111), (112), (113)	Description	units
dose	$Dose$	ionizing radiation dose applied	$rad$
effective dose enhancement factor	$C_{DEF}$	effective dose enhancement factor	$none$
electron-hole pair formation energy	$E_{form}$	electron-hole pair formation energy	$eV$
electric field power dependency	$x$	electric field power dependency	$none$

**Table 11-5 Syntax and parameters for Kimpton interface trap model.**

Input file	Corresponding variable in (111), (112), (113)	Description	units
total density	$N_t^i$	interface trap total density	$cm^{-2}$
initial filling factor	$\frac{N_{tf}^i}{N_t^i}$	initial filling factor	$none$
capture cross section	$\sigma$	trap capture cross section at $1 \frac{MV}{cm}$	$cm^2$

where *tidInterface* is the sideset name of the interface between the irradiated insulator and the semiconductor where the interface traps are located.

For small positive electric fields ( $< 0.1 \frac{MV}{cm}$ ) and negative electric fields the Kimpton model with interface traps only fails to match experimental data. The difference can be accounted for by considering trapping/detrapping in oxide volume. The trapping, detrapping and conservation equations for volume traps are given by

$$\begin{aligned}
 p_{ttp}^v &= P_{capt} (N_t^v - N_{tf}^v) T_{vol}^{\frac{1MV}{cm}} E_{ins}^{-1.5x} f_{(ins)} n_{pairs}^{gen}, \\
 p_{tde}^v &= (1 - P_{capt}) N_{tf}^v T_{vol}^{\frac{1MV}{cm}} E_{ins}^{-1.5x} f_{(ins)} n_{pairs}^{gen}, \\
 p_{ttp}^{v,net} &= N_t^v + p_{ttp}^v - p_{tde}^v
 \end{aligned} \tag{114}$$

where  $T_{vol}^{\frac{1MV}{cm}}$  is the capture volume of the trap at  $1 \frac{MV}{cm}$ ,  $P_{capt}$  is the probability of hole capture from an electron-hole pair generated within a trap volume,  $p_{ttp}^v$  is the volume density of the new holes trapped after a small dose irradiation,  $p_{tde}^v$  is the volume density of the detrapped holes after the small dose irradiation,  $p_{ttp}^{v,net}$  is the net volume density of trapped holes after irradiation,  $N_t^v$  is the volume trap density and  $N_{tf}^v$  is the occupied trap volume density before irradiation.

Because the effective trap capture cross section  $\sigma_{eff} = \sigma E_{ins}^{-x}$ , then the effective capture volume of the trap becomes also field dependent  $T_{vol}^{eff} = \frac{4}{3} \pi \left( \frac{\sigma_{eff}}{\pi} \right)^{\frac{3}{2}} = T_{vol}^{\frac{1MV}{cm}} E_{ins}^{-1.5x}$ . For small electric fields

the effective trap volume saturates to the value  $\left(T_{\text{vol}}^{\text{eff}}\right)_{\text{max}} = \frac{1}{2N_t^v}$  by imposing the condition that the total maximum capture volume for the traps to be limited to half of the volume of the insulator. The probability  $P_{\text{capt}}$  is computed as

$$P_{\text{capt}} = \frac{V_{\text{crit}}}{V_{\text{crit}} + T_{\text{vol}}^{\text{eff}}},$$

$$V_{\text{crit}} = \frac{4}{3}\pi \left(\frac{\sigma_{\text{crit}}}{\pi}\right)^{\frac{3}{2}} \quad (115)$$

where  $V_{\text{crit}}$  represents the core volume around the trap within  $T_{\text{vol}}^{\text{eff}}$  where the probability of capturing the hole is greater than pair recombination and  $\sigma_{\text{crit}}$  is a user specified parameter.

In general volume traps are used in addition to interface traps in Kimpton model. To do this, the user must specify in addition to what has been specified for the interface traps a volume parameter section for the Kimpton model

```
start Material Block {materialBlockName}
  start tid
    start kimpton model
      (one parameter per line in the form):
      {parameter name} = {parameter value}
      (see table 11-4 for available parameters)

      start interface traps
        sideset id is {tidInterface}

        (one parameter per line in the form):
        {parameter name} = {parameter value}
        (see table 11-5 for available parameters)
      end

      start volume traps
        (one parameter per line in the form):
        {parameter name} = {parameter value}
        (see table 11-6 for available parameters)
      end
    end
  end
end
```

To enable threshold voltage shift evaluation or the impact of the ionizing radiation dose on the device functionality, Charon allows the positive charge trapped on the interface and volume traps in the insulator to be frozen after a radiation dose and be used as fixed charge for a bias sweep. For instance, if a radiation dose is applied to the gate oxide at zero bias and then removed, by sweeping the gate bias the  $I_d - V_g$  curve can be obtained and the threshold voltage shift can be evaluated.

To freeze the trapped charge after an irradiation dose the user must specify in the general section of the Kimpton model

**Table 11-6 Syntax and parameters for Kimpton volume trap model.**

Input file	Corresponding variable in (114), (115)	Description	units
total density	$N_t^v$	volume trap total density	$cm^{-3}$
initial filling factor	$\frac{N_{tf}^v}{N_t^v}$	initial filling factor	<i>none</i>
capture cross section	$\sigma$	volume trap capture cross section at $1 \frac{MV}{cm}$	$cm^2$
critical capture cross section	$\sigma_{crit}$	critical capture cross section	$cm^2$

```

start Material Block {materialBlockName}
  start tid
    start kimpton model
      ...
      freeze traps at voltage = {V} on {contact}
      ...
    end
  end
end

```

where  $V$  is the bias voltage on *contact* such that for voltages greater than  $V$ , trapped charge in the insulator becomes fixed charge for a voltage sweep on *contact*.

## 12. SOLVERS

The solvers in Charon are supplied by the Trilinos set of solver libraries. Because the drift-diffusion equations are nonlinear and so must be solved iteratively, the nonlinear solver NOX in the Trilinos suite is used. NOX employs Newton iterations to solve the nonlinear equation set. Within each Newton iteration, a matrix equation set must be solved for the Newton update. Charon uses a GMRES iterative solver for this with ILU preconditioning. The solver block of the interpreter input file is the place to invoke and configure the solver in a Charon simulation. At a minimum for a steady-state simulation, the solver block should look like:

```
start solver block
  use solver GMRES-ILU
end solver block
```

The GMRES solver used in Charon is called AztecOO and has three parameters that can be set. One is a tolerance that the residual of the linear solver must satisfy, one is the maximum number of iterations the solver can take and the third is the size of the Krylov subspace used in the method. They are specified in the solver block via:

```
start solver block
  aztec tolerance = tolerance
  aztec krylov subspace size = size
  aztec max iterations = maxIterations
end solver block
```

Most often, the defaults of these values should be used thus requiring no specification for them.

Most often, a simple Newton iteration is the best option for the solver. Occasionally for the initial step solving the nonlinear Poisson equation, a line search can be employed to modify a Newton update from the full step calculated by the method with a fractional step determined by a line search method. Typically, if the nonlinear iterations for the full drift-diffusion equations are not convergence, line search is usually not helpful and a return to trying a better mesh is the necessary step. By default, line search is turned off.

Most often, even when a backtrack line search isn't helpful, it also isn't harmful to have it turned on, and so by default, the line search method is turned on. Should the user wish to turn the line search method off, one can do so with

```
start solver block
  line search method is full step
end solver block
```

Likewise, the method could be specified as `backtrack`, but that just enforces the default.

The stopping criteria for Newton iterations determines when the nonlinear iterations are declared converged. The first convergence criterion is that the norm of the residual be smaller than a specified value,

$$||\mathbf{F}|| < \epsilon_{normF} \quad (116)$$

where  $||\mathbf{F}||$  is the norm of the residual, and the tolerance is specified in the solver block via:

```

start solver block
  nonlinear solver tolerance = tolerance
end solver block

```

The second criterion is that a Weighted Root Mean Square (**WRMS**) norm is satisfied,

$$||\delta x^k||_{wrms} < \epsilon_{wrms} \quad (117)$$

The **WRMS** norm is:

$$||\delta x^k||_{wrms} := \sqrt{\frac{1}{N} \sum_{i=1}^N \left( \frac{x_i^k - x_i^{k-1}}{\epsilon_{rel}|x_i^{k-1}| + \epsilon_{abs}} \right)^2} \quad (118)$$

In this equation,  $x^k$  is the vector of degrees of freedom in the system at the  $k^{th}$  nonlinear iteration.  $x_i^k$  is the  $i^{th}$  component of that vector,  $N$  is the number of degrees of freedom in the system and  $\epsilon_{rel}$  and  $\epsilon_{abs}$  are user-specified relative and absolute error tolerances. Two additional parameters can also be specified.

Even when the linear solver mentioned above doesn't satisfy its solver tolerance, Charon will still try to use that solution as a Newton update. If the linear solver isn't converging to a sufficient degree, the **WRMS** stopping criterion can cause stagnation in nonlinear iterations. This can be mitigated by specifying the  $\beta$  parameter for the **WRMS** criterion such that,

$$\eta < \beta \quad (119)$$

where  $\eta$  is the norm of the residual of the linear solver. Setting  $\beta = 1$  removes this criterion.

Sometimes when Newton iteration updates are very small, the **WRMS** norm will detect stagnation in the solver process. This can be mitigated when the line search method is used by requiring the fraction of the Newton update as determined by the line search to be greater than a specified value,  $\alpha$ .

$$\lambda > \alpha \quad (120)$$

The quantity  $\lambda$  is the fraction of the Newton step calculated by the line search method. Setting  $\alpha = 0$  eliminates this criterion.

All of these parameters for the **WRMS** norm are specified in a **WRMS** settings block inside the solver block,

```

start solver block
  start wrms parameters block
    absolute tolerance = absTol
    alpha = alphaVal
    beta = betaVal
    relative tolerance = relTol
  end wrms parameters block
end solver block

```



## 13. CHARON INPUT FILE REFERENCE

The following sections are a reference to the various models in Charon and how they're called out in the input file. All of the input file lines are case insensitive except where the input is a variable. In the tables that describe the syntax, these are bracketed in the main syntax line and *italicized* in every case. The top cell in each of the tables represents a single line—indeed, it *must occupy* a single line in the input file with no line breaks.

Occasionally, the syntax may required that at least one option be specified—On/Off for example. In the **Required** column of each table, it will indicate when an option is required. This does not mean that each option is required, only that at least one of the options is required. For example, the line

```
unscale variables is on
```

could equally be specified

```
unscale variables is off
```

This a case where “is on” and “is off” represent two different options for the interpreter line and at least one of them must be specified.

### 13.1. Import State File

File I/O is a critical part of any Charon execution. At a minimum, Charon must import a file that contains a mesh. It can also include a state, i.e. a full set of potential, carrier concentration, temperature, etc at a given parameter set. This file is called a state file even when the state is null—in other words, contains only a mesh. The mesh is a necessary part of any simulation employing finite element or finite volume methods as Charon does. The state will be used as an initial guess of the solution being sought in the present simulation.

Often times, a state file can contain multiple states. For example, the state file may have been produced by a previous simulation that swept over a range of contact voltage. If states were calculated at ten different values of the voltage in the previous simulation, then there will be ten states in the file that it produced numbered 0-9. By default, Charon will import the final state in the file.

The input file line to import the state file into the present simulation exists at the root level of the interpreter input file.

**Table 13-1 Import state file syntax**

Import State File { <i>filename</i> } [ at Index { <i>index</i> }]		
Option	Description	Required
at Index	Specifies that a specific state will be used as an initial guess	No
Variables	Description	Default
<i>filename</i>	Specifies the name of the state file	<i>none</i>
<i>index</i>	integer index of the state file to use.	-1

## 13.2. Output Parameters

The data generated by Charon execution are written to output files of two different types. The primary output file is an exodus formatted record of all states generated during execution plus other user-requested output. Text files are generated for tabulated output of current as a function of time for transient simulations and as a function of parameter for parameter sweeps.

User control of how the output is configured is done in the output parameters block. The block sits at the root level and is formatted in the input file as:

```
start output parameters
    output specifications
end output parameters
```

The output specifications are individual lines contained in the block and are described in the remainder of this section.

**Table 13-2 Output state file syntax**

Output State File { <i>filename</i> }		
Option	Description	Required
	<i>None</i>	
Variables	Description	Default
<i>filename</i>	Specifies the name of the exodus formatted state file for output	<i>none</i>

By default, degree-of-freedom variables (potential, carrier concentration, temperature) are written to the exodus file at node locations in the underlying mesh. The global variables of contact current are also written to the exodus file by default. Other incidental variables are not written by default, but can be requested. The variables can be requested as output in two different ways. One is at nodal locations just as the degree of freedom variables are recorded. The other is as a cell average quantity. Some quantities, particularly those that are gradients of other variables are not well defined at nodes. These must be output as cell averaged quantities.

In the output variables lines, any number of variables may be specified. This requires a special form of input. When specifying the variables, the full section must be in §. And the variable

names must be comma separated. As in all interpreter variables, the output variable names are case sensitive.

**Table 13-3 Output nodal variables syntax**

Output nodal variables in { <i>regionName</i> } for { <i>variableNames</i> }		
Option	Description	Required
	<i>None</i>	
Variables	Description	Default
<i>regionName</i>	This is the geometry block where the variable is defined	<i>None</i>
<i>variableNames</i>	Names of the variable to be output to the exodus file	<i>None</i>

**Table 13-4 Output cell averaged variables syntax**

Output cell average variables in { <i>regionName</i> } for [ scalar { <i>variableNames</i> } [ vector { <i>variableNames</i> } ]]		
Option	Description	Required
scalar	The variables are all scalars	Yes
vector	The variables are all vectors	Yes
Variables	Description	Default
<i>regionName</i>	This is the geometry block where the variable is defined	<i>None</i>
<i>variableNames</i>	Names of the variable to be output to the exodus file	<i>None</i>

Any simulation that produces multiple states are either transient or they are sweeps of some parameter in the model. As stated earlier, the current at each contact can be printed as a function of time or parameter value to a text file. The name of the file to which these values are printed can be specified by the appropriate line as described in Tables 13-5 and 13-6.

**Table 13-5 Specify filename of tabulated currents for transient simulations**

Output tabulated transient currents to { <i>filename</i> }		
Option	Description	Required
	<i>None</i>	
Variables	Description	Default
<i>filename</i>	Name of the file where currents in a transient simulation are printed	<i>None</i>

Finally, because the scaling of the drift-diffusion equations is somewhat unwieldy, the solution of them can be numerically difficult. For this reason, the variables of the equations are scaled by characteristic quantities. They are also written to the exodus file as scaled quantities. If the user wishes unscaled quantities in the exodus file, they can request it in the output parameters block.

**Table 13-6 Specify filename of tabulated currents for parameter sweep simulations**

Output tabulated parameter currents to { <i>filename</i> }		
Option	Description	Required
	None	
Variables	Description	Default
<i>filename</i>	Name of the file where currents in a parameter sweep simulation are printed	<i>currents-loc.dat</i>

**Table 13-7 How to request unscaled quantities in the exodus file.**

Unscale Variables [ is on [ is off ]]		
Option	Description	Required
is on	Turn unscaling on	Yes
is off	Turn unscaling off	Yes-Default
Variables	Description	Default
	<i>None</i>	

### 13.3. Physics Block

This section describes input lines that appear at the first level of the physics block. Any description of physics be it in a semiconductor or insulating region of a device simulation must have a physics block associated with it. Any one physics block can be associated with multiple regions of a device. For instance, two semiconducting regions may be separated by an insulator. The physics block will contain a description of all physical mechanisms represented in the simulation for that region. Because there may be multiple physics blocks, each one must have a unique name—no spaces please—do differentiate it from the others. The syntax to create a physics block follows:

```
begin physics block {physicsBlockName}
    {physics descriptions}
end physics block {physicsBlockName}
```

#### 13.3.1. Geometry Block

One of the elements that must always be in a physics block is the geometry block specification. This line ties the physics block to at least one region of the device as it was created and named during the meshing stage of creating a simulation. Table 13-8 describes the line in the physics block that specifies the geometry block. In an instance where there are multiple regions the have identical physics descriptions, this line may be repeated for each named region,

Geometry Block is <i>geometryBlockName</i>		
Option	Description	Required
	<i>None</i>	
Variables	Description	Default
<i>geometryBlockName</i>	Name that corresponds to a geometry block specified in the meshing step.	<i>None</i>

**Table 13-8 Specify the geometry block to which these physics apply.**

### 13.3.2. **Material Model Specification**

Each physics block must be accompanied by a material model block located elsewhere in the input file. As in the case of the physics block, there can be a plurality of material blocks each with a unique name. The physics block and material block are linked by specifying the name of the material block in the appropriate physics block. Only one material block may be specified for each physics block and it is done so in a single line inside the physics block as described in Table 13-9.

Material Block is <i>materialBlockName</i>		
Option	Description	Required
	<i>None</i>	
Variables	Description	Default
<i>materialBlockName</i>	Name that corresponds to a named material block	<i>None</i>

**Table 13-9 Specify the material block that accompanies a physics block.**

### 13.3.3. **Discretization**

Charon solves the drift-diffusion, Poisson and Fickian heat transfer partial differential equations to predict the performance of semiconductor devices. The solution method—Galerkin, Scharfetter-Gummel, etc—method used to solve those equations must be specified in the physics block. The standard discretization type interpreter input line defines the method to be used.

## 13.4. **Material Block**

The material block is a complement to the physics block. Between the two, they give a complete description of the material properties and physical mechanisms of the device in the simulation. The material block contains all properties associated with the material contained in its associated physics block which in turn is associated with the geometry block specified in the physics block. Because there can be multiple materials in any one simulation, the material block must be uniquely named. The syntax to create a material block is

standard discretization type is drift diffusion gfem drift diffusion effpg nlp drift diffusion cvfem Laplace gfem Laplace cvfem ddlattice gfem with source term stabilization lattice gfem		
Option	Description	Required
drift diffusion gfem	Stabilized Galerkin method for drift-diffusion equations	Yes
drift diffusion effpg	Exponential flux stabilized petrov-Galerkin for drift-diffusion equations	Yes
nlp	Non-linear Poisson solve	Yes
drift diffusion cvfem	Scharfetter-Gummel solution for drift-diffusion	Yes
Laplace gfem	Galerkin method for insulators	Yes
Laplace cvfem	Scharfetter-Gummel solution for insulators	Yes
ddlattice gfem	Stabilized Galerkin method for drift-diffusion with lattice temperature	Yes
with source term stabilization	Include source term stabilization for stabilized Galerkin solution	No
lattice gfem	Lattice temperature only solve with Galerkin's method	Yes
Variables	Description	Default
	<i>None</i>	

**Table 13-10 Output cell averaged variables syntax**

```
begin material block {materialBlockName}
    {material descriptions}
end material block {materialBlockName}
```

where materialBlockName is the unique name of the material model.

#### **13.4.1. Material Name**

In some instances, common materials have properties pre-programmed into Charon, e.g. silicon and Gallium Arsenide. To associate those properties with the material block, the name of the material is specified in the material block. Note that the material name, specified in the material name line is case sensitive. The syntax is described in Table 13-11.

**Table 13-11 Specify the name of a material.**

Material name is <i>materialName</i>		
Option	Description	Required
	None	
Variables	Description	Default
<i>materialName</i>	Specify the name of the known material for default properties	<i>None</i>

### 13.4.2. Relative Permittivity

Relative permittivity is a material parameter that must be specified for all materials in a Charon simulation. For some materials that have properties already programmed into Charon, there will be an associated default value. In practice, it's a good idea to specify the value explicitly and it can always be specified as a value to supercede the default value. The relative permittivity is specified in the material block in a single line in the syntax described in Table 13-12.

**Table 13-12 Specify the relative permittivity of a material.**

Relative Permittivity = <i>relativePermittivity</i>		
Option	Description	Required
	None	
Variables	Description	Default
<i>relativePermittivity</i>	Numerical value of the relative permittivity of the material	<i>default for known material, 0 otherwise</i>

### 13.5. Carrier Recombination

Charon presently supports four types of carrier recombination models. They are Shockley-Reed-Hall (SRH) in both mid-gap and generic forms, direct and auger recombination. For details on how each is implemented, refer to section 7. To enable any type of recombination, entries are required in both the physics blocks associated with the region where recombination takes place and in the accompanying material model block. In the physics block, individual types of recombination are toggled on and off,

```
start physics block {\em physicsBlockName}
  <recombinationType> is on/off
end physics block
```

recombination toggle end physics block Parameters for each type of recombination are specified in the relevant material model block. The following sections tabulate the input lines required to toggle recombination on and off and set relevant parameters.

### 13.5.1. Shockley-Reed-Hall Recombination

SRH recombination is enabled for mid-gap traps or generic traps wherein the trap energy may be specified for any energy level in the band gap. The mid-gap recombination model is toggled on and off in the physics block via,

**Table 13-13 Mid-gap SRH recombination toggle**

srh recombination [ is on [ is off]]		
Option	Description	Required
is on	Toggle mid-gap recombination on	Yes
is off	Toggle mid-gap recombination off	Yes
Variables	Description	Default
	<i>None</i>	

Parameters for mid-gap SRH recombination are set in the carrier lifetime block inside the material model block,

```
start Material Block {\em materialBlockName}
  start Carrier Lifetime Block
    <set parameters>
  end Carrier Lifetime Block
end Material Block
```

For mid-gap SRH traps, the carrier lifetimes may be constant or concentration or temperature dependent. If the carrier lifetimes are concentration dependent.

**Table 13-14 Mid-gap SRH constant carrierlifetime**

<i>carrierType</i> lifetime is constant = <i>lifetime</i>		
Option	Description	Required
	<i>None</i>	
Variables	Description	Default
<i>carrierType</i>	Specified as either electron or hole	None
<i>lifetime</i>	Numerical value of the lifetime in seconds	Material Dependent

To specify that the mid-gap recombination model is temperature dependent,

The generic SRH trap model is toggled with



**Table 13-15 Concentration dependent SRH carrier lifetime**

<i>carrierType</i> lifetime is concentration dependent [with $N_{srh} = N_{srhParameter}$ ]		
Option	Description	Required
with $N_{srh}$	Use a specified the parameter value for the concentration dependent recombination	No
Variables	Description	Default
<i>CarrierType</i>	Specified as either electron or hole	None
<i>Nsrh</i>	Numerical value of the parameter for concentration dependent lifetime	Material Dependent

**Table 13-16 Concentration dependent SRH carrier lifetime  $\tau_{au0}$  value**

electron $\tau_{au0} = \tau_{au0}$		
Option	Description	Required
	<i>None</i>	
Variables	Description	Default
$\tau_{au0}$	Electron $\tau_{au0}$	Material dependent

**Table 13-17 Electron lifetime temperature dependence**

electron lifetime is temperature dependent		
Option	Description	Required
	<i>None</i>	
Variables	Description	Default
	<i>None</i>	

**Table 13-18 Generic SRH recombination toggle**

trap srh [ is on [ is off]]		
Option	Description	Required
is on	Toggle generic recombination on	Yes
is off	Toggle generic recombination off	Yes
Variables	Description	Default
	<i>None</i>	

### 13.5.2. Radiative (Direct) Recombination

Radiative, or direct, recombination for direct bandgap semiconductors is the simplest of the recombination models. It can be fully employed with the usual on/off toggle directive in the physics block and a specification of a single coefficient in the accompanying material block.

Parameters for mid-gap SRH recombination are set in the carrier lifetime block inside the

**Table 13-19 Direct recombination toggle**

radiative recombination [ is on [ is off]]		
Option	Description	Required
is on	Toggle radiative recombination on in physics block	Yes
is off	Toggle radiative recombination off in physics block	Yes
Variables	Description	Default
	<i>None</i>	

material model block,

```
start Material Block {\em materialBlockName}
  Radiative recombination coefficient = {coefficient}
end Material Block
```

**Table 13-20 Radiative recombination coefficient**

Radiative recombination coefficient = <i>coefficient</i>		
Option	Description	Required
	<i>None</i>	
Variables	Description	Default
<i>coefficient</i>	coefficient for radiative recombination	None

### 13.5.3. Auger Ionization/Recombination

The Auger model can account for both recombination and generation of charge carrier pairs. The details of the model are described in Section 7.3. In addition to toggling the model on as described above, coefficients for the Auger model may be defined in the material model block as follows.

```
start Material Block materialBlockName
  start Auger Recombination Parameters
    Auger Coefficient electron/hole = augerCoefficient
    Generation on/off
  end Auger Recombination Parameters
end Material Block materialBlockName
```

## 13.6. Variable Voltage at a Boundary

In order to perform current-voltage sweeps, or IV sweeps, the voltage at a contact must be varied over the desired range. In Charon this capability is implemented using the Library of Continuation Algorithms (LOCA) library. A specific example of how to use this capability was covered in section 3.5.1. More generally, to use this capability the first step is to modify the boundary condition associated with the contact over which voltage will be varied. The syntax for doing this is

```
bc is ohmic for {contact name} on {material name} swept from {start
voltage} to {stop voltage}
```

Next a section for controlling how the voltage will be swept needs to be added. The syntax for that is

```
start sweep options
  continuation method is arc length / natural
  predictor method is constant / secant / tangent
  (One parameter per line)
  (see table 13-21 for available parameters)
end sweep options
```

**Table 13-21 Parameters used to control voltage sweeping.**

Input file	Description	Default
initial step size	initial voltage increment	1.0
maximum number of steps	If the number of voltage steps taken reaches this value then the simulation is terminated.	<i>none</i>
minimum step size	If the voltage step size is reduced to this value due to step failures then the simulation is terminated.	$1.0 \times 10^{-12}$
maximum step size	The voltage step size will never exceed this value.	$1.0 \times 10^{12}$
step size aggressiveness	Floating point value between 0 and 1 that represents how aggressive the code should be about changing the step size.	1.0
successful step increase factor	If the code determines that a larger voltage step is possible it will increase the size by this factor.	1.26
failed step reduction factor	If the voltage step attempt fails then reduce the step size by this factor and try again.	0.5
min value	If the voltage value falls below this value then the simulation is terminated. See the text in section 13.6 for how this can be different than the starting value in the <i>bc</i> line.	<i>start voltage</i> or <i>stop voltage</i>
max value	If the voltage exceeds this value then the simulation is terminated. See the text in section 13.6 for how this can be different than the ending value in the <i>bc</i> line.	<i>start voltage</i> or <i>stop voltage</i>

It is important to note that because of the use of LOCA for voltage stepping within Charon there are a wide range of simulations possible. For example, while generally an IV sweep proceeds in a fairly straightforward way from the *start voltage* to the *stop voltage*, with LOCA that doesn't necessarily have to be the case.

Consider figure 13-1. The red line might represent the results of a typical IV sweep on, for example, a semiconductor resistor. The simulation starts at  $V_{\text{start}}$  and proceeds in a straightforward

manner to  $V_{\text{stop}}$ . In this case  $V_{\text{start}}$  is the minimum value that the voltage will ever attain and so there is no need to set *min value* in the sweep parameters to anything other than *start voltage*, and Charon will default to setting *min value* to *start voltage* if *min value* isn't set in the input file.

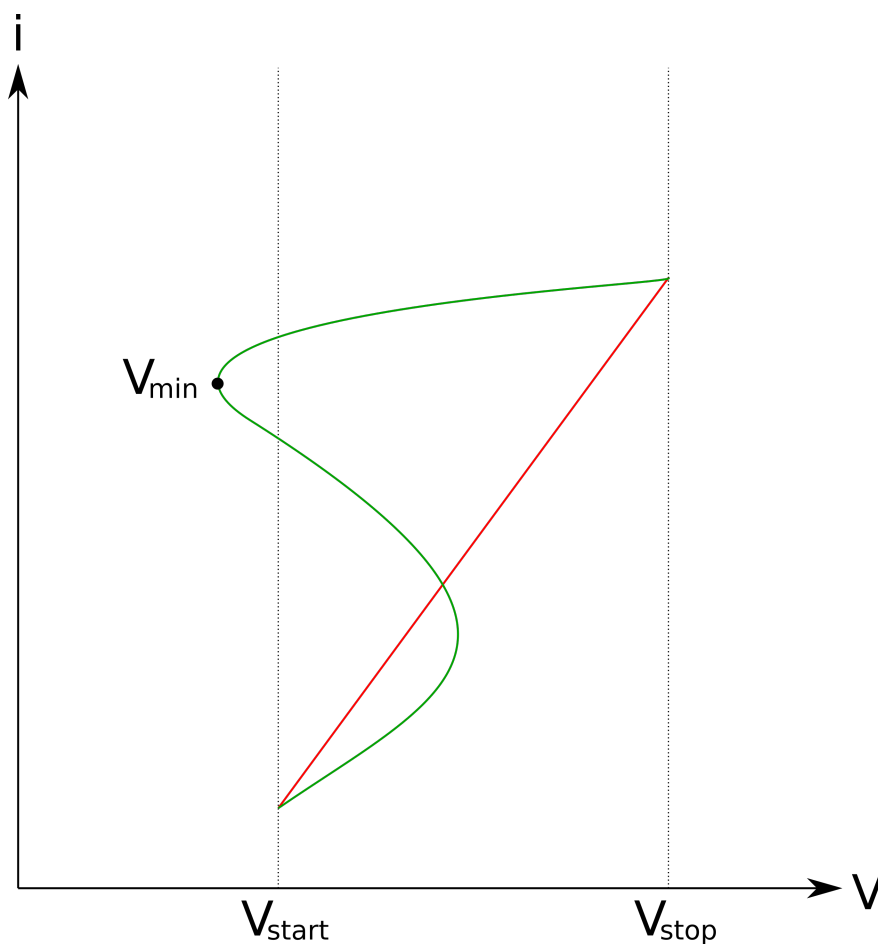


**Figure 13-1 Example of a non-typical IV sweep possible in Charon.**

Now consider a simulation in which the I-V characteristics are more complex, as represented by the green line in figure 13-1. In this case  $V_{\text{start}}$  will not be the minimum voltage. Charon is capable of performing such a simulation but you must set *min value* in the sweep parameters to something other than  $V_{\text{start}}$  since not doing so will cause the simulation to terminate once  $V$  curves back to  $V_{\text{start}}$ . In this situation the sweep option *max value* is redundant since the simulation will terminate if the voltage reaches either *stop voltage* or *max value*. For IV simulations in the reverse direction the situation is mirrored and the value of the sweep option *max value* becomes relevant in the same way *min value* is relevant in the forward case..

### 13.7. Doping

Doping is specified in the relevant `material` block section of the input file. In general doping is specified via a set of analytic functions within the area of the associated material block. Functions

are additive, unless otherwise noted, so each additional function that is specified adds to the previous ones that were specified for that material block.

Additionally a file may be specified which consists of a list of points and a value for doping at that point. Note that due to interpolations that are required for file doping specifications this can negatively impact the performance of the code.

Each of the following subsections gives information on the syntax for each specific doping function available.

### **13.7.1. Uniform Doping**

Uniform doping places a constant value of doping over the specified area. You can specify uniform doping via

```
start material block {materialBlockName}
...
start uniform doping named Function{i}
  spatial range is {minimum} to {maximum} in x / y / z
  type is donor / acceptor
  concentration = {value in  $\#/cm^2$  }
end
...
end
```

Where the  $\{i\}$  in `Function{i}` is replaced with an integer starting with 1 and going to the number of doping functions in the specific material block. You can use a `spatial range` specification for each coordinate direction when necessary. If a particular direction isn't specified then the doping will be applied for the entire block in that coordinate direction.

### **13.7.2. Step Junction**

You can use step doping for a doping profile that varies as a step function within the specified material with the specified parameters. In Charon the syntax for the step function is

```
start material block {materialBlockName}
...
start step junction doping
  acceptor concentration =  $\{N_A\}$ 
  donor concentration =  $\{N_D\}$ 
  junction location = {coordinate value}
  direction is x / y / z
  dopant order is pn / np
end
...
end
```

All of the statements shown above must be included for a valid step junction specification.

### 13.7.3. Gaussian Doping

You can use Gaussian doping for a doping profile that varies as a Gaussian function within the specified material with the specified parameters. In Charon the form of the Gaussian function, assuming a variation in the  $x$  direction, is:

$$N = \{N_{\max}\} \exp \left[ -\ln \left( \frac{\{N_{\max}\}}{\{N_{\min}\}} \right) \left( \frac{x - \{peak\}}{\{width\}} \right)^2 \right] \quad (121)$$

The syntax for Gaussian doping is

```
start material block {materialBlockName}
...
start gauss doping named Function{i}
  concentration range is {N_min} to {N_max} in x / y / z
  spatial range is {minimum} to {maximum} in x / y / z
  gradient width = {width} in x / y / z
  peak location = {peak} in x / y / z
  direction is Positive / Negative / Both in x / y / z
  type is donor / acceptor
end
...
end
```

Where the  $\{i\}$  in `Function{i}` is replaced with an integer starting with 1 and going to the number of doping functions in the specific material block. If a `spatial range` specification isn't made for a particular direction then the doping will be applied over the entire material block in which it is specified.

### 13.7.4. Modified Gaussian Doping

You can use *MGauss* (modified Gaussian) doping for a doping profile that varies as a Gaussian function within the specified material with the specified parameters. In Charon the form of the MGauss function, assuming a variation in the  $x$  direction, is:

$$N = \begin{cases} \exp \left[ -\frac{\{N_{\max}\}}{\{N_{\min}\}} \left( \frac{x - \{min\}}{\{width\}} \right)^2 \right] & x < \{min\}, N_{\min} > 0 \text{ and } erfc \text{ is not set} \\ \exp \left[ -\left( \frac{x - \{min\}}{\{width\}} \right)^2 \right] & x < \{min\}, N_{\min} \leq 0 \text{ and } erfc \text{ is not set} \\ \exp \left[ -\frac{\{N_{\max}\}}{\{N_{\min}\}} \left( \frac{x - \{max\}}{\{width\}} \right)^2 \right] & x > \{max\}, N_{\min} > 0 \text{ and } erfc \text{ is not set} \\ \exp \left[ -\left( \frac{x - \{max\}}{\{width\}} \right)^2 \right] & x > \{max\}, N_{\min} \leq 0 \text{ and } erfc \text{ is not set} \\ \frac{1}{2} \left[ erfc \left( \frac{x - \{max\}}{\{width\}} \right) - erfc \left( \frac{x - \{min\}}{\{width\}} \right) \right] & \text{if } erfc \text{ is set} \end{cases} \quad (122)$$

The syntax for MGauss doping is

```

start material block {materialBlockName}
...
start mgauss doping named Function{i}
  concentration range is { $N_{min}$ } to { $N_{max}$ } in x / y / z
  spatial range is {min} to {max} in x / y / z
  gradient width = {width} in x / y / z
  direction is Positive / Negative / Both in x / y / z
  erfc in x / y / z
  type is donor / acceptor
end
...
end

```

Where the  $\{i\}$  in `Function{i}` is replaced with an integer starting with 1 and going to the number of doping functions in the specific material block. If a `spatial range` specification isn't made for a particular direction then the doping will be applied over the entire material block in which it is specified.

## REFERENCES

- [1] The Cubit tool suite. Internet URL <http://cubit.sandia.gov>.
- [2] *Reaction Design* chemkin website. Internet URL <http://www.reactiondesign.com/products/open/chemkin.html>.
- [3] The Exodus II file format. Internet URL [http://analyst.ran.sandia.gov/index.php?option=com\\_content&task=view&id=122&Itemid=72](http://analyst.ran.sandia.gov/index.php?option=com_content&task=view&id=122&Itemid=72).
- [4] SNL chemkin website. Internet URL <http://www.ca.sandia.gov/chemkin>.
- [5] SNL ensight website. Internet URL <http://nestor.ran.sandia.gov/ensight>.
- [6] SNL paraview website. Internet URL <http://www.ran.sandia.gov/paraview>.
- [7] The Trilinos Project website. Internet URL <http://www.trilinos.org/>.
- [8] J.D. Albrecht et al. Electron transport characteristics of GaN for high temperature device modeling. *Journal of Applied Physics*, 83(9):4777–4781, May 1998.
- [9] O. Ambacher et al. Two-dimensional electron gasses induced by spontaneous and piezoelectric polarization in undoped and doped algan/gan heterostructures. *Journal of Applied Physics*, 87(1):334–344, January 2000.
- [10] N.D. Arora, J.R. Hauser, and D.J. Roulston. Electron and hole mobilities in silicon as a function of concentration and temperature. *IEEE Trans. Electron Devices*, 29:292–295, 1982.
- [11] G. A. Baraff. Distribution functions and ionization rates for hot electrons in semiconductors. *Phys. Rev.*, 128:2507–2517, Dec 1962.
- [12] D. Bednarczyk and J. Bednarczyk. The approximation of the fermi-dirac integral  $f(1/2)(\eta)$ . *Physics Letters*, 64A(4):409–410, January 1978.
- [13] H.A. Bethe and Massachusetts Institute of Technology. Radiation Laboratory. *Theory of the Boundary Layer of Crystal Rectifiers*. Report (Massachusetts Institute of Technology. Radiation Laboratory). Radiation Laboratory, Massachusetts Institute of Technology, 1942.
- [14] P. Bochev, K. Peterson, and X. Gao. A new control volume finite element method for the stable and accurate solution of the drift-diffusion equations on general unstructured grids. *Computer Methods in Applied Mechanics and Engineering*, 254:126–145, 2013.
- [15] A. N. Brooks and T. J.R. Hughes. Streamline upwind petrov-galerkin formulations for convection dominated flows with particular emphasis on the incompressible navier-stokes equations. *Computer Methods in Applied Mechanics and Engineering*, 32(13):199–259, 1982.
- [16] D.M. Caughey and R.E. Thomas. Carrier mobilities in silicon empirically related to doping and field. *Proceedings of the IEEE*, 55(12):2192–2193, December 1967.



- [17] C. R. Crowell and S. M. Sze. Temperature dependence of avalanche multiplication in semiconductors. *Applied Physics Letters*, 9(6):242–244, 1966.
- [18] M. Farahmand et al. Monte Carlo Simulation of Electron Transport in the III-Nitride Wurtzite Phase Materials System: Binaries and Ternaries. *IEEE Transactions on Electron Devices*, 48(3):535–542, March 2001.
- [19] X. Gao, A. Huang, and B. Kerr. Efficient band-to-trap tunneling model including heterojunction band offset. *ECS Transactions*, 80:1005–1015, 2017.
- [20] X. Gao, B. Kerr, and A. Huang. Analytic band-to-trap tunneling model including band offset for heterojunction devices. *Journal of Applied Physics*, 125, 054503, 2018.
- [21] X. Gao, B. Kerr, A. Huang, G. Hennigan, L. Musson, and M. Negoita. Analytic band-to-trap tunneling model including electric field and band offset enhancement. *Proceedings of International Conference on Simulation of Semiconductor Processes and Devices 2018*, 2018.
- [22] E.S. Harmon, M.R. Melloch, and M.S. Lundstrom. Effective bandgap shrinkage in gaas. *Applied Physics Letters*, 64(4):502–504, January 1994.
- [23] D. Hente and R.H. Jansen. Frequency domain continuation method for the analysis and stability investigation of nonlinear microwave circuits. *IEEE Proceedings*, part H, vol. 133, no.5, Oct. 1986.
- [24] M. Heroux, R. Bartlett, V. Howle, R. Hoekstra, J. Hu, T. Kolda, R. Lehoucq, K. Long, R. Pawlowski, E. Phipps, A. Salinger, H. Thornquist, R. Tuminaro, J. Willenbring, and A. Williams. An Overview of Trilinos. Technical Report SAND2003-2927, Sandia National Laboratories, 2003.
- [25] K. Horio and H. Yanai. Numerical modeling of heterojunctions including the thermionic emission mechanism at the heterojunction interface. *IEEE Transactions on Electron Devices*, 37(4):1093–1098, 1990.
- [26] R.J. Lomax J.J. Barnes and G.I. Haddad. Finite-element simulation of gaas mesfets with lateral doping profiles and submicron gates. *IEEE Transactions on Electron Devices*, ED-23(9):1042–1048, September 1976.
- [27] J.B. Joyce and R.W. Dixon. Analytic approximations for the fermi energy of an ideal fermi gas. *Applied Physics Letters*, 31:354–356, September 1977.
- [28] D. B. M. Klaassen. A unified mobility model for device simulation i. *Solid-State Electronics*, pages 953–959, 1992.
- [29] D. B. M. Klaassen. A unified mobility model for device simulation ii. *Solid-State Electronics*, pages 961–967, 1992.
- [30] D.B.M. Klaassen, J.W. Slotboom, and H.C. [de Graaff]. Unified apparent bandgap narrowing in n- and p-type silicon. *Solid-State Electronics*, 35(2):125–129, 1992.
- [31] Kevin M. Kramer and W. Nicholas G. Hitchon. *Semiconductor Devices A Simulation Approach*. Prentice Hall PTR, Upper Saddle River, NJ, 1997.

- [32] A. Kurganov and J. Rauch. The order of accuracy of quadrature formulae for periodic functions. *Advances in Phase Space Analysis of Partial Differential Equations: In Honor of Ferruccio Colombini's 60th Birthday*, 2009.
- [33] J.M. Lopez-Gonzalez and L. Prat. The importance of bandgap narrowing distribution between the conduction and valence bands in abrupt hbt's. *IEEE Transactions on Electron Devices*, 44(7):1046–1051, July 1997.
- [34] Mark Lundstrom. Notes on heterostructure fundamentals. EE-650Y, 1995. Course notes.
- [35] Sam M. Myers and William R. Wampler. Dual-track physics modeling of III-V HBTs under transient neutron irradiation. Technical Report SAND2010-6026P, Sandia National Laboratories, 2010.
- [36] N.G. Nilsson. An accurate approximation of the generalized einstein relation for degenerate semiconductors. *Physica Status Solidi (a)*, pages K75–K78, 1973.
- [37] J. C. Pedro and N. B. Carvalho. Efficient harmonic balance computation of microwave circuits's response to multi-tone spectra. *29th European Microwave Conference Proc.*, vol. I, Oct. 1999.
- [38] C. Persson, U. Lindefelt, and B. E. Sernelius. Band gap narrowing in n-type and p-type 3c-, 2h-, 4h-, 6h-sic, and si. *Journal of Applied Physics*, 86(8):4419–4427, 1999.
- [39] F. M. Rotella, Z. Yu G. Ma, and R. W. Dutton. Modeling and simulation of an rf ldmos device using harmonic balance pisces. *TECHCON*, 1998.
- [40] A. Schenk. A model for the field and temperature dependence of shockley-read-hall lifetimes in silicon. *Solid-State Electronics*, 35:1585–1596, 1992.
- [41] Thomas I. Seidman. Time-dependent solutions of a nonlinear system arising in semiconductor theorem, ii: Boundedness and periodicity. *IMA Preprint Series 80*, July 1984.
- [42] J. W. Slotboom. The  $pn$ -product in silicon. *Solid-State Electronics*, 20:279–283, 1977.
- [43] S.M. Sze and Kwok K. Ng. *Physics of Semiconductor Devices*. John Wiley and Sons, Inc., Hoboken, New Jersey, 2007.
- [44] B. Troyanovsky. Frequency domain algorithms for simulating large signal distortion in semiconductor devices. *Ph.D. Thesis*, Nov. 1997.
- [45] B. Troyanovsky, Rotella, Yu, Dutton, and Sato-Iwanaga. Large signal analysis of rf/microwave devices with parasitics using harmonic balance device simulation. *SASIMI*, 1996.
- [46] B. Troyanovsky, Z. Yu, and R.W. Dutton. Large signal frequency domain device analysis via the harmonic balance technique. *Simulation of Semiconductor Devices and Processes*, Sep. 1995.
- [47] R. Tsu and L. Esaki. Tunneling in a finite superlattice. *Applied Physics Letters*, 22(11):562–564, 1973.

- [48] William R. Wampler and Samuel M. Myers. Model for transport and reaction of defects and carriers within displacement cascades in gallium arsenide. *Journal of Applied Physics*, 117(045707), 2015.
- [49] C. M. Wu and E. S. Yang. Carrier transport across heterojunction interfaces. *Solid-State Electronics*, 22:241–248, 1979.
- [50] K. Yang, J. R. East, and G. I. Haddad. Numerical modeling of abrupt heterojunctions using a thermionic-field emission boundary condition. *Solid-State Electronics*, 36(3):321–330, 1993.

## APPENDIX A. HISTORICAL PERSPECTIVE

## APPENDIX B. BAND-TO-TRAP TUNNELING MODELS

In this appendix, the supported band-to-trap tunneling models are described in some level of details. Charon supports four variation forms of the Schenk band-to-trap tunneling model [40] and also a new model designed for heterojunction devices [20].

The first form is the Schenk model in the high temperature limit, where the electron field enhancement factor is given by

$$g_n(T, F) = \left(1 + \frac{2E_R k_B T}{(\hbar\Theta)^{3/2} \sqrt{E_t - E_0}}\right)^{-1/2} \frac{E_{act}^0 + E_t}{k_B T} \left(\frac{\hbar\Theta}{E_t + E_R}\right)^{3/2} \times \exp\left[\frac{E_{act}^0 - E_{act}(F)}{k_B T}\right] \exp\left(\frac{E_t - E_0}{k_B T}\right) \exp\left[-\frac{4}{3} \left(\frac{E_t - E_0}{\hbar\Theta}\right)^{3/2}\right]. \quad (123)$$

$E_R = S\hbar\omega_0$ , the lattice relaxation energy, with  $S$  being the Huang-Rhys factor and  $\hbar\omega_0$  being the effective optical phonon energy.  $E_0$  is the optimum transition energy and given by

$$E_0 = 2\sqrt{E_F} \left[\sqrt{E_F + E_t + E_R} - \sqrt{E_F}\right] - E_R, \quad E_F = \frac{(2E_R k_B T)^2}{(\hbar\Theta)^3}, \quad \hbar\Theta = \left(\frac{\hbar^2 q^2 F^2}{2m_n^*}\right)^{1/3}. \quad (124)$$

Here  $q$  is the elemental charge,  $F$  is the local electric field,  $m_n^*$  is the electron effective mass.  $\hbar\Theta$  is known as the electrooptical energy.  $E_{act}^0 = (E_t - E_R)^2 / (4E_R)$ , the activation energy for capturing an electron from the conduction band edge.  $E_{act} = (E_0 - E_R)^2 / (4E_R)$ , the field-dependent activation energy. The first model is enabled by specifying `model is hightemp approx` in the trap `srh` block.

The second form is the Schenk model in the low temperature limit, where the electron field enhancement factor is given by

$$g_n(T, F) = \left[1 + \frac{(\hbar\Theta)^{3/2} \sqrt{(E_t - E_0)}}{E_0 \hbar\omega_0}\right]^{-1/2} \frac{(\hbar\Theta)^{3/4} (E_t - E_0)^{1/4}}{2\sqrt{E_t E_0}} \left(\frac{\hbar\Theta}{k_B T}\right)^{3/2} \times \exp\left[-\frac{E_t - E_0}{\hbar\omega_0} + \frac{\hbar\omega_0 - k_B T}{2\hbar\omega_0} + \frac{E_t + 0.5k_B T}{\hbar\omega_0} \ln\left(\frac{E_t}{E_R}\right) - \frac{E_0}{\hbar\omega_0} \ln\left(\frac{E_0}{E_R}\right)\right] \times \exp\left(\frac{E_t - E_0}{k_B T}\right) \exp\left[-\frac{4}{3} \left(\frac{E_t - E_0}{\hbar\Theta}\right)^{3/2}\right]. \quad (125)$$

The  $E_R$ ,  $E_0$ , and  $\hbar\Theta$  parameters have the same definitions as in Eq. (123). The second model is enabled by specifying `model is lowtemp approx` in the trap `srh` block.

The above two  $g_n$  expressions were obtained from the Schenk model in the high and low temperature limits, respectively. Without any temperature approximation, it can be shown [20] that the general  $g_n$  formula from the Schenk model takes the form of

$$g_n(T, F) = \frac{\int_0^{E_t} \rho_n(E) I_{E/\hbar\omega_0}(z) \exp\left(\frac{-E}{2k_B T}\right) dE}{\int_{E_t}^{\infty} \rho_n^{F=0}(E) I_{E/\hbar\omega_0}(z) \exp\left(\frac{-E}{2k_B T}\right) dE}. \quad (126)$$

The modified Bessel function for large orders (i.e.,  $l = E/\hbar\omega_0 \gg 1$ , which generally holds for deep-level traps that are relevant for band-to-trap tunneling) is equal to

$$I_l(z) = \frac{1}{\sqrt{2\pi}} \frac{1}{(l^2 + z^2)^{1/4}} \exp\left(\sqrt{l^2 + z^2}\right) \exp\left[-l \ln\left(\frac{l}{z} + \sqrt{1 + \frac{l^2}{z^2}}\right)\right], \quad (127)$$

with

$$z = 2S\sqrt{f_B(f_B + 1)}, \quad f_B = \left[\exp\left(\frac{\hbar\omega_0}{k_B T}\right) - 1\right]^{-1}. \quad (128)$$

$f_B$  is the Bose distribution function. The zero-field density of states (DOS),  $\rho_n^{F=0}(E)$ , is given by

$$\rho_n^{F=0}(E) = \frac{1}{2\pi^2} \left(\frac{2m_n^*}{\hbar^2}\right)^{3/2} \sqrt{E - E_t}. \quad (129)$$

The field dependent density of states,  $\rho_n(E)$ , in the Schenk model was derived based on the constant field assumption. It is given by

$$\rho_n(E) = \frac{1}{2\pi} \left(\frac{2m_n^*}{\hbar^2}\right)^{3/2} \sqrt{\hbar\Theta} \mathcal{F}\left(\frac{E_t - E}{\hbar\Theta}\right), \quad \mathcal{F}(y) = A_i'^2(y) - yA_i^2(y). \quad (130)$$

$\mathcal{F}(y)$  is known as the electrooptical function.  $A_i(\cdot)$  is the Airy function of the first kind.  $A_i'(\cdot)$  is the first derivative of the Airy function. For large positive arguments, the electrooptical function  $\mathcal{F}$  takes the asymptotic form of

$$\mathcal{F}\left(\frac{E_t - E}{\hbar\Theta}\right) = \frac{1}{8\pi} \frac{\hbar\Theta}{E_t - E} \exp\left[-\frac{4}{3} \left(\frac{E_t - E}{\hbar\Theta}\right)^{3/2}\right]. \quad (131)$$

To use the general Schenk model in Eq. (126) with the constant field DOS in Eq. (130), it is required to specify `model is constant field` in the trap `srh` block. To use the Schenk model with the asymptotic DOS in Eq. (131), we need to replace `constant field` with `asymptotic field` in the input file.

The four Schenk models described above can be used for modeling band-to-trap tunneling in homojunction devices under different conditions. They provide different accuracies and require different computation time. That is, the `hightemp approx` and `lowtemp approx` models are faster than `asymptotic field`, which is faster than `constant field`, in terms of calculation time. However,

the constant field model has the least number of assumptions, so it is the most accurate among the four.

Figure 1(a) shows the electron field enhancement factor for the gold traps in silicon at 300 K. The legend texts in the following figures have the following correspondence: *Schenk HighTemp* corresponds to `hightemp approx`, *Schenk LowTemp* corresponds to `lowtemp approx`, *Schenk AsymConstFDOS* corresponds to `asymptotic field`, *Schenk ConstFDOS* corresponds to `constant field`, and *Schenk NewDOS* corresponds to `new`. The parameters used for the calculation are  $\hbar\omega_0 = 0.068$  eV,  $S = 3.5$ ,  $E_t = 0.55$  eV,  $m_n^* = \sqrt{0.92 \times 0.19} = 0.42$ , and  $T = 300$  K. For the gold traps in silicon, we can make three observations: (i) the *Schenk LowTemp* and *Schenk AsymConstFDOS* models produce the same electron enhancement factors for the whole range of electric fields; (ii) the results from the two models are very close to the more accurate *Schenk ConstFDOS* model, except at the low field regime where the field factors are small anyway; (iii) the results from *Schenk HighTemp* model show somewhat larger errors when compared to other three models. Figure 1(b) shows the electron field enhancement factor for the E5 traps in GaAs at 300 K. The parameters used for this calculation are  $\hbar\omega_0 = 0.02$  eV,  $S = 12.2$ ,  $E_t = 0.66$  eV,  $m_n^* = 0.067$ , and  $T = 300$  K. For the E5 traps in GaAs at 300 K, we can see that the *Schenk LowTemp* model is broken down, while other three Schenk models produce good results.

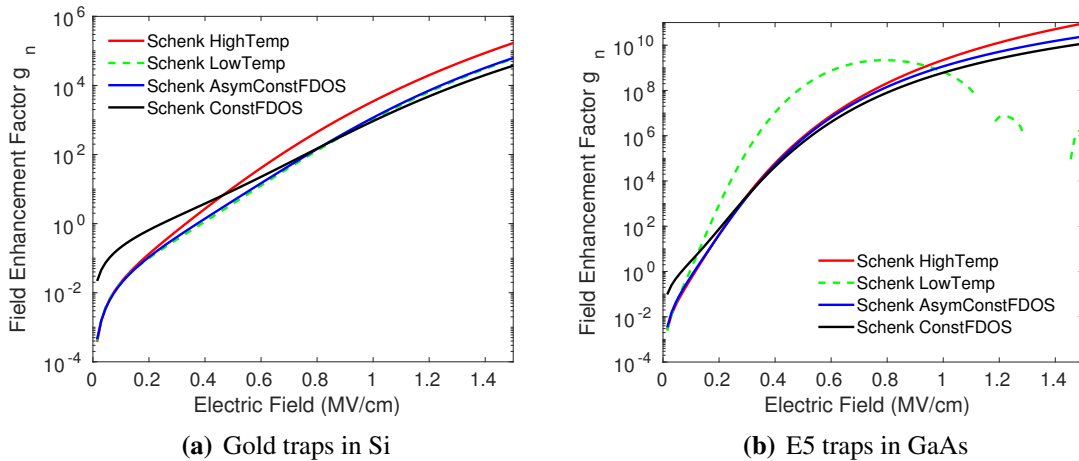


**Figure B-1 Electron field enhancement factor for traps at 300 K as a function of electric field computed using the four Schenk models.**

The Schenk model with the constant field DOS and its approximated versions were derived for silicon devices. Therefore, the models may be adequate for modeling band-to-trap tunneling in homojunction devices. However, they are unsuitable for modeling heterojunction structures, since they do not capture the effect of heterojunction band offset. This effect can be very strong near the heterojunction. As seen from the typical band profile of an  $\text{In}_{0.5}\text{Ga}_{0.5}\text{P}/\text{GaAs}$   $\text{NP}^+\text{N}$  heterojunction bipolar transistor (HBT) in figure B-2, the tunneling of holes in the base to traps in the emitter is determined by the valence band profile. And it is evident that the valence band deviates significantly from the constant field assumption due to the large band offset.

To address the limitation of the constant field assumption, we have developed an analytic DOS model [19, 21, 20] that includes both the electric field and band offset effects. The new model

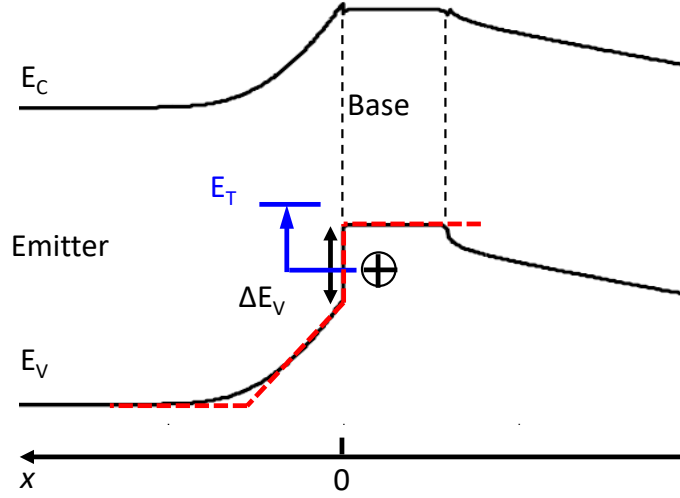


**Figure B-2** Typical band profile in the emitter and base regions of an  $\text{In}_{0.5}\text{Ga}_{0.5}\text{P}/\text{GaAs}$   $\text{NP}^+\text{N}$  HBT. Here  $E_C$  is the conduction band,  $E_V$  is the valence band,  $\Delta E_V$  is the valence band offset, and  $E_T$  indicates the trap location. The circle with a plus represents a hole, and the blue arrow denotes the hole-to-trap tunneling path. The red dashed curve is a linearized potential to approximate the actual valence band.

allows us to accurately simulate the band-to-trap tunneling near a heterojunction. For the typical valence band in figure B-2, the actual potential profile is first linearized with the band offset included, as shown by the red dashed curve. Then the DOS for the linearized potential is given by

$$\rho_n(x, E) = \frac{1}{2\pi^2} \left( \frac{2m_n^*}{\hbar^2} \right)^{\frac{3}{2}} \int_0^{E^*} \frac{|A_i(\alpha x + \beta)|^2}{|A_i(\beta)|^2 + \frac{\hbar\Theta}{E_x} |A'_i(\beta)|^2} \frac{dE_x}{\sqrt{E_x}}. \quad (132)$$

$E^* = qFx + V_0 - E_t + E$ , where  $q$  is the elemental charge,  $F$  is the local electric field in the emitter side,  $x$  is the positive distance (in the emitter side) from the heterojunction,  $V_0$  is the band offset (e.g.,  $\Delta E_V$  in figure B-2), and  $0 \leq E \leq E_t$ .  $A_i(\cdot)$  is the Airy function of the first kind, and  $A'_i(\cdot)$  is the first derivative of the Airy function.  $\alpha$ ,  $\beta$ , and  $\hbar\Theta$ , are given by

$$\alpha = \left( \frac{2m_n^*qF}{\hbar^2} \right)^{\frac{1}{3}}, \quad \beta = \frac{V_0 - E_x}{\hbar\Theta}, \quad \hbar\Theta = \left( \frac{\hbar^2 q^2 F^2}{2m_n^*} \right)^{\frac{1}{3}}. \quad (133)$$

For the approximated valence potential in figure B-2 (red dashed curve), the *Schenk NewDOS* model was used to compute the electron enhancement factor at different locations (in the emitter side) from the heterojunction. The results are plotted in figure B-3 and also compared to those computed using the *Schenk ConstFDOS* model. The parameters used for the calculation are the same as those for the E5 traps in GaAs. At 15 and 20 nm locations, the *Schenk NewDOS* model produces nearly the same results as the *Schenk ConstFDOS* model. However, at 5 and 10 nm locations, the *Schenk NewDOS* model predicts much larger field factors than the *Schenk ConstFDOS* model because of the strong band offset enhancement.

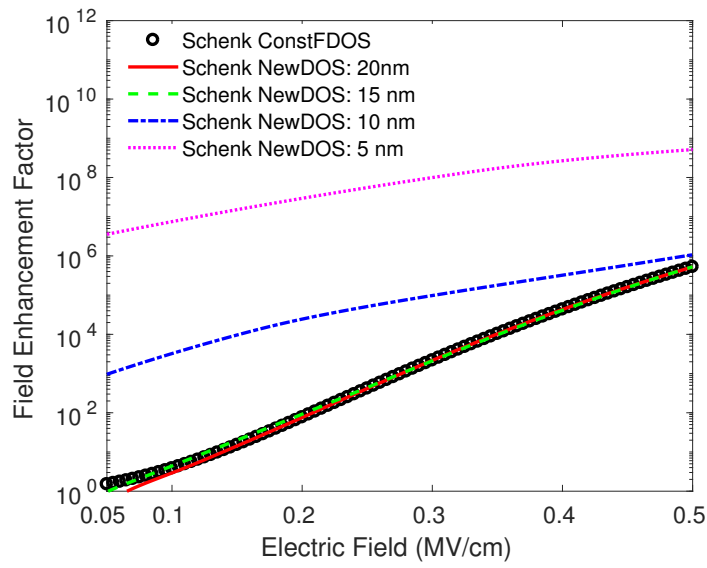


Figure B-3 Electron field enhancement factor for the approximated potential in figure B-2 at 300 K as a function of electric field computed using the *Schenk ConstFDOS* and *Schenk NewDOS* models. The calculations were done for four different locations that are 5, 10, 15, and 20 nm in the emitter away from the heterojunction. The trap parameters are the same as those for the E5 traps in GaAs.



## APPENDIX C. DERIVATION OF HETEROJUNCTION MODELS

In this appendix the thermionic emission (TE) and local tunneling (LT) models given in Sec. 9 are derived in detail for electrons. The same derivation is valid for holes.

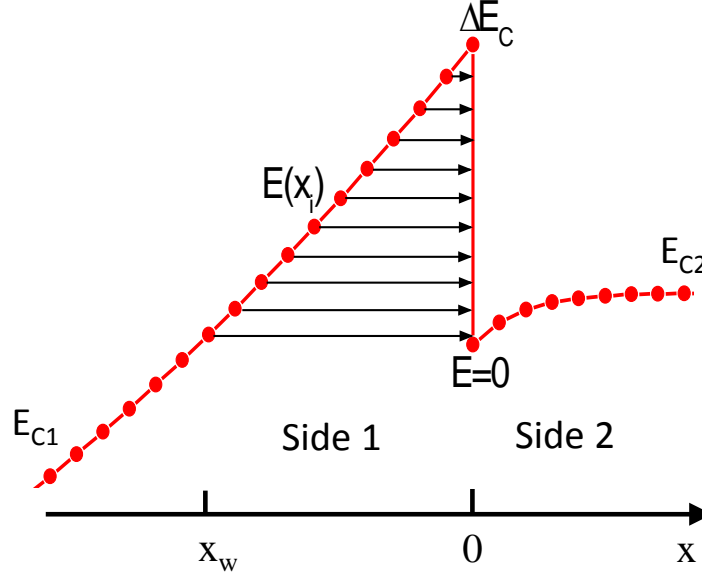


Figure C-1 Example of conduction band diagram illustrating the carrier transport across a heterojunction.

The transport of carriers from one side of a heterojunction to the other is characterized by the quantum mechanical transmission coefficient. According to [49], the electron current per unit area from side 1 to side 2 of the heterojunction in the x-direction illustrated in Fig. C-1 is given by

$$J_{1 \rightarrow 2} = \frac{-2q}{V} \sum_{\mathbf{k}} v_x T(E, k_y, k_z) f_1(E) [1 - f_2(E)],$$

where 2 is due to spin degeneracy,  $q$  is the elemental charge,  $V$  is a normalization volume,  $v_x$  is the carrier velocity in the x-direction, and  $\mathbf{k}$  is the three-dimensional wave vector which contains three components of  $k_x$ ,  $k_y$ , and  $k_z$ .  $E$  is the kinetic energy of the carrier and given by (assuming isotropic electron effective mass and parabolic conduction band dispersion)

$$E = \frac{\hbar^2}{2m_n^*} |\mathbf{k}|^2 = \frac{\hbar^2}{2m_n^*} (k_x^2 + k_y^2 + k_z^2).$$

In addition,  $T(E, k_y, k_z)$  is the quantum mechanical transmission coefficient of the carrier across the junction,  $f_1(E)$  and  $f_2(E)$  are the probability of the carrier occupancy at the energy  $E$  in side 1 and side 2, respectively.

The net electron current across the heterojunction is the difference of the two current components flowing in opposite directions, i.e.,

$$\begin{aligned}
J_n &= J_{1 \rightarrow 2} - J_{2 \rightarrow 1} \\
&= \frac{-2q}{V} \sum_{\mathbf{k}} v_x T(E, k_y, k_z) f_1(E) [1 - f_2(E)] + \frac{2q}{V} \sum_{\mathbf{k}} v_x T(E, k_y, k_z) f_2(E) [1 - f_1(E)] \\
&= \frac{-2q}{V} \sum_{\mathbf{k}} v_x T(E, k_y, k_z) [f_1(E) - f_2(E)] \\
&= \frac{-2q}{V} \frac{V}{(2\pi)^3} \int d^3 \mathbf{k} v_x T(E, k_y, k_z) [f_1(E) - f_2(E)] \quad \text{use the sum-to-integral rule} \\
&= \frac{-2q}{V} \frac{V}{(2\pi)^3} \int \int \int dk_x dk_y dk_z \left( \frac{\hbar k_x}{m_n^*} \right) T(E, k_y, k_z) [f_1(E) - f_2(E)]
\end{aligned}$$

The last equality uses the relation that  $v_x = p_x/m_n^* = \hbar k_x/m_n^*$ . To perform the integration over the wave vector components we rewrite the integration over the carrier kinetic energy by noting that

$$E = E_{||} + E_x, \quad \text{where } E_{||} = \frac{\hbar^2}{2m_n^*} k_{||}^2 = \frac{\hbar^2}{2m_n^*} (k_y^2 + k_z^2), \quad E_x = \frac{\hbar^2}{2m_n^*} k_x^2.$$

From the above, the derivatives of the wave vector components can be expressed as

$$dk_x = \frac{m_n^*}{\hbar^2 k_x} dE_x, \quad dk_y dk_z = d^2 k_{||} = 2\pi k_{||} dk_{||} = \frac{2\pi m_n^*}{\hbar^2} dE_{||}.$$

Then  $J_n$  becomes

$$\begin{aligned}
J_n &= \frac{-2q}{(2\pi)^3} \frac{1}{\hbar} \frac{2\pi m_n^*}{\hbar^2} \int dE_{||} \int dE_x T(E_{||}, E_x) [f_1(E) - f_2(E)] \\
&= \frac{-qm_n^*}{2\pi^2 \hbar^3} \int dE_{||} \int dE_x T(E_{||}, E_x) [f_1(E) - f_2(E)].
\end{aligned}$$

To further simplify the expression of  $J_n$  we need to assume Boltzmann statistics for the carrier occupation, i.e.,

$$\begin{aligned}
f_1(E) &= \exp\left(\frac{E_{Fn1} - E_{||} - E_x}{k_B T}\right), \\
f_2(E) &= \exp\left(\frac{E_{Fn2} - E_{||} - E_x}{k_B T}\right).
\end{aligned}$$

Moreover, we note that there is no barrier in the y and z directions at the junction, hence the transmission coefficient is 1 in the two directions, i.e.,  $T(E_{||}, E_x) = 1 \times T(E_x) = T(E_x)$ . Then  $J_n$  becomes

$$\begin{aligned}
J_n &= \frac{-qm_n^*}{2\pi^2 \hbar^3} \int_0^{+\infty} dE_{||} \exp\left(\frac{-E_{||}}{k_B T}\right) \int_{E_{min}}^{+\infty} dE_x T(E_x) \left[ \exp\left(\frac{E_{Fn1} - E_x}{k_B T}\right) - \exp\left(\frac{E_{Fn2} - E_x}{k_B T}\right) \right] \\
&= \frac{-qm_n^* k_B T}{2\pi^2 \hbar^3} \int_{E_{min}}^{+\infty} dE_x T(E_x) \left[ \exp\left(\frac{E_{Fn1} - E_x}{k_B T}\right) - \exp\left(\frac{E_{Fn2} - E_x}{k_B T}\right) \right] \\
&= \frac{-A_n^* T}{k_B} \int_{E_{min}}^{+\infty} dE_x T(E_x) \left[ \exp\left(\frac{E_{Fn1} - E_x}{k_B T}\right) - \exp\left(\frac{E_{Fn2} - E_x}{k_B T}\right) \right],
\end{aligned}$$

where  $A_n^*$  is the electron Richardson constant and defined as

$$A_n^* = \frac{qm_n^*k_B^2}{2\pi^2\hbar^3} = \frac{4\pi qm_n^*k_B^2}{h^3}.$$

To perform the integration over the energy  $E_x$  in computing  $J_n$ , the energy lower bound  $E_{min}$  must be determined. In general,  $E_{min}$  can be any value between 0 and  $\Delta E_C$ . Figure C-2 provides an example of conduction band diagram where  $E_{min} > 0$ , while the band diagram in Fig. C-1 has  $E_{min} = 0$ . It is noted that  $T(E_x) = 1$  for  $E_x > \Delta E_C$ . Next, let us write  $J_n = J_{n1} - J_{n2}$ . Then we

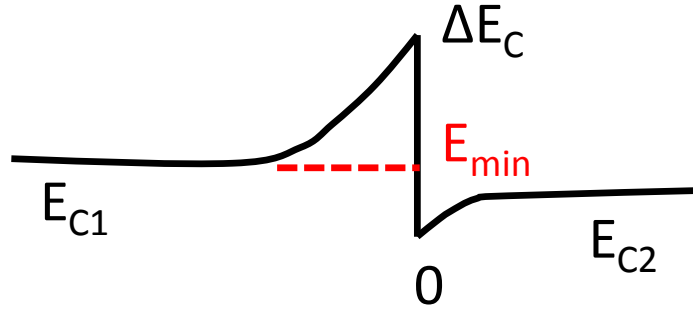


Figure C-2 Example of conduction band diagram illustrating the case of  $E_{min} > 0$ .

have

$$\begin{aligned} J_{n1} &= \frac{-A_n^*T}{k_B} \int_{E_{min}}^{\Delta E_C} dE_x T(E_x) \exp\left(\frac{E_{Fn1} - E_x}{k_B T}\right) - \frac{A_n^*T}{k_B} \int_{\Delta E_C}^{+\infty} dE_x \exp\left(\frac{E_{Fn1} - E_x}{k_B T}\right) \\ &= \frac{-A_n^*T}{k_B} \int_{E_{min}}^{\Delta E_C} dE_x T(E_x) \exp\left(\frac{E_{Fn1} - E_x}{k_B T}\right) - A_n^*T^2 \exp\left(\frac{E_{Fn1} - \Delta E_C}{k_B T}\right) \\ &= -A_n^*T^2 \exp\left(\frac{E_{Fn1} - \Delta E_C}{k_B T}\right) \left[ 1 + \frac{\exp\left(\frac{\Delta E_C}{k_B T}\right)}{k_B T} \int_{E_{min}}^{\Delta E_C} dE_x T(E_x) \exp\left(\frac{-E_x}{k_B T}\right) \right] \\ &= -A_n^*T^2 \exp\left(\frac{E_{Fn1} - \Delta E_C}{k_B T}\right) (1 + \delta_n), \end{aligned}$$

with  $\delta_n$  equal to

$$\delta_n = \frac{\exp\left(\frac{\Delta E_C}{k_B T}\right)}{k_B T} \int_{E_{min}}^{\Delta E_C} dE_x T(E_x) \exp\left(\frac{-E_x}{k_B T}\right).$$

Similarly,  $J_{n2}$  is given by

$$J_{n2} = -A_n^*T^2 \exp\left(\frac{E_{Fn2} - \Delta E_C}{k_B T}\right) (1 + \delta_n).$$

Therefore,  $J_n$  is simplified to

$$J_n = J_{n1} - J_{n2} = -A_n^*T^2 \left[ \exp\left(\frac{E_{Fn1} - \Delta E_C}{k_B T}\right) - \exp\left(\frac{E_{Fn2} - \Delta E_C}{k_B T}\right) \right] (1 + \delta_n).$$

From the conduction band diagrams in Figs. C-1 and C-2, it is seen that  $\Delta E_C = E_{C1} - E_{C2} = E_{C1} - 0 = E_{C1} > 0$  at the junction without loss of generality. Finally,  $J_n$  across the heterojunction can be written as

$$\begin{aligned} J_n &= -A_n^* T^2 \left[ \exp\left(\frac{E_{Fn1} - E_{C1}}{k_B T}\right) - \exp\left(\frac{E_{Fn2} - E_{C2}}{k_B T}\right) \exp\left(\frac{-\Delta E_C}{k_B T}\right) \right] (1 + \delta_n) \\ &= J_{TE,n} (1 + \delta_n), \end{aligned}$$

where  $J_{TE,n}$  is the net electron thermionic emission current density and equal to

$$J_{TE,n} = -A_n^* T^2 \left[ \exp\left(\frac{E_{Fn1} - E_{C1}}{k_B T}\right) - \exp\left(\frac{E_{Fn2} - E_{C2}}{k_B T}\right) \exp\left(\frac{-\Delta E_C}{k_B T}\right) \right]. \quad (134)$$

Next, in order to compute the tunneling contribution, i.e.,  $\delta_n$ , we focus on the conduction band diagram in Fig. C-1 where  $E_{min} = 0$ , since the NPN HBT device of interest has a similar conduction band profile. Applying the Wentzel-Kramers-Brillouin (WKB) approximation to the tunneling, the transmission coefficient  $T(E_x)$  for  $0 \leq E_x \leq \Delta E_C$  is equal to

$$T(E_x) = \exp \left[ -2 \int_{x_w}^0 dx \sqrt{\frac{2m_{nt}^*}{\hbar^2} [E_C(x) - E_x]} \right]^{1/2}.$$

By approximating the conduction band in Fig. C-1 to a triangular shape, the conduction band  $E_C(x)$  for tunneling is given by

$$E_C(x) = \frac{E_x - \Delta E_C}{x_w} x + \Delta E_C = q\xi x + \Delta E_C \quad \text{with} \quad \xi = \frac{\nabla E_C}{q} = \frac{E_x - \Delta E_C}{qx_w},$$

where  $\xi$  is the electric field in the tunneling source side (e.g., side 1 in Fig. C-1). Substituting  $E_C(x)$  into the expression of  $T(E_x)$ , we obtain

$$\begin{aligned} T(E_x) &= \exp \left[ -2 \int_{x_w}^0 dx \sqrt{\frac{2m_{nt}^*}{\hbar^2} (q\xi x + \Delta E_C - E_x)} \right]^{1/2} \\ &= \exp \left[ -2 \sqrt{\frac{2m_{nt}^*}{\hbar^2}} \frac{2}{3q\xi} (\Delta E_C - E_x)^{3/2} \right] \\ &= \exp \left[ \frac{-8\pi}{3hq\xi} \sqrt{2m_{nt}^*} (\Delta E_C - E_x)^{3/2} \right]. \end{aligned}$$

Given the above  $T(E_x)$ ,  $\delta_n$  can be rewritten as

$$\begin{aligned} \delta_n &= \frac{1}{k_B T} \int_0^{\Delta E_C} dE_x T(E_x) \exp\left(\frac{-E_x}{k_B T}\right) \exp\left(\frac{\Delta E_C}{k_B T}\right) \\ &= \frac{1}{k_B T} \int_0^{\Delta E_C} dE_x \exp \left[ \frac{-8\pi}{3hq\xi} \sqrt{2m_{nt}^*} (\Delta E_C - E_x)^{3/2} \right] \exp\left(\frac{\Delta E_C - E_x}{k_B T}\right). \end{aligned}$$

Let  $u = \frac{\Delta E_C - E_x}{k_B T}$ , then  $du = \frac{-1}{k_B T} dE_x$ .  $\delta_n$  is further simplified to

$$\begin{aligned}\delta_n &= \frac{1}{k_B T} \int_{\frac{\Delta E_C}{k_B T}}^0 (-k_B T) \exp \left[ \frac{-8\pi}{3hq\xi} \sqrt{2m_{nt}^*} (k_B T)^{3/2} u^{3/2} \right] \exp(u) du \\ &= \int_0^{\frac{\Delta E_C}{k_B T}} \exp \left[ u - \left( \frac{u}{u_0} \right)^{3/2} \right] du,\end{aligned}\tag{135}$$

where  $u_0$  is given by

$$u_0 = \frac{1}{k_B T} \left( \frac{3hq\xi}{8\pi\sqrt{2m_{nt}^*}} \right)^{2/3}.$$

If the band diagram in Fig. C-1 is flipped in the  $x$  direction,  $\Delta E_C$  will become negative, but Eq. (135) is still valid except using the absolute value of  $\Delta E_C$ . It is noted that tunneling process is non-local by nature. However, by using the WKB approximation and the triangular barrier assumption, the quantum mechanical transmission coefficient  $T(E_x)$  for tunneling depends only on the local electric field, hence the tunneling model given by Eq. (135) is called the local tunneling model.

## APPENDIX D. CHARON INPUT FILE FOR A PN STEP JUNCTION DIODE EXAMPLE

This appendix contains input file listings for examples given in the document.

### D.1. NLP input file for PN step junction diode in Section 3.4

Listing 1 Input file for NLP simulation of the PN step junction diode.

```
1 # Name of the input exodus file, geometry only
2 import state file pndiode.exo
3
4 # Output exodus file for results of this simulation
5 start output parameters
6   output state file pndiode.nlp.exo
7 end output parameters
8
9 start physics block semiconductor
10
11   # geometry block name IS case sensitive, note however that Cubit
12   # often downcases names prior to output so it is recommended
13   # that in Cubit you use all lower case for naming entities to
14   # avoid confusion.
15   geometry block is si
16
17   # The type of physics to be solved, in this case a nonlinear
18   # Poisson, or nlp, simulation will be performed
19   standard discretization type is nlp
20
21   # The name of the material model IS case sensitive. The name is
22   # used as a key for the associated material block, also contained
23   # in this input file.
24   material model is siliconParameter
25
26 end physics block semiconductor
27
28 # The material block where most material parameters for this
29 # simulation are set. It is specified in the physics block by it's
30 # name, siliconParameter.
31 start material block siliconParameter
32
33   # Material name IS case sensitive
34   material name is Silicon
35
36   # Simple, scalar, material property
37   relative permittivity = 11.9
38
39   # The doping for the diode
40   start step junction doping
41     acceptor concentration = 1e16
```

```

42     donor concentration = 1e16
43     junction location = 0.5
44     dopant order is PN
45     direction is x
46 end step junction doping
47
48 end material block siliconParameter
49
50 # Boundary condition specifications. Required, but must be set to zero
51 # for the NLP simulation
52 bc is ohmic for anode on si fixed at 0
53 bc is ohmic for cathode on si fixed at 0
54
55 # Initial conditions for the ELECTRIC_POTENTIAL will come from an
56 # equilibrium approximation
57 initial conditions for ELECTRIC_POTENTIAL in si is equilibrium potential
58
59 # Section to specify the solvers, nonlinear and linear, for the
60 # problem. Most of the settings are encapsulated in "solver packs" for
61 # convenience.
62 start solver block
63     use solver pack 1
64 end solver block

```

## D.2. I-V sweep input file for PN step junction diode in Section 3.5

**Listing 2 Input file for I-V sweep of the PN step junction diode.**

```

1 # Name of the input exodus file, which includes the results for
2 # ELECTRIC_POTENTIAL as obtained from a previous NLP simulation
3 import state file pndiode.nlp.exo at index 1
4
5 # Output exodus file for results of this simulation
6 start output parameters
7     output state file pndiode.dd.iv.exo
8 end output parameters
9
10 start physics block Semiconductor
11
12     # geometry block name IS case sensitive, note however that Cubit
13     # often downcases names prior to output so it is recommended that
14     # in Cubit you use all lower case for naming entities to avoid
15     # confusion.
16     geometry block is si
17
18     # The type of physics to be solved, in this case a nonlinear
19     # Poisson, or nlp, simulation will be performed
20     standard discretization type is drift diffusion gfem
21
22     # The name of the material model IS case sensitive. The name is
23     # used as a key for the associated material block, also contained
24     # in this input file.
25     material model is siliconParameter

```

```

26
27     # Turn on Schokley-Reed-Hall recombination
28     srh recombination is on
29
30 end physics block
31
32 # The material block where most material parameters for this
33 # simulation are set. It is specified in the physics block by it's
34 # name, siliconParameter.
35 start material block siliconParameter
36
37     # Material name IS case sensitive
38     material name is Silicon
39     relative permittivity = 11.9
40
41     start step junction doping
42         acceptor concentration =1.0e16
43         donor concentration =1.0e16
44         junction location = 0.5
45         dopant order is PN
46         direction is x
47     end step junction doping
48
49 end material block siliconParameter
50
51 # This is taken from the NLP file. Note that it is read from "index 1"
52 # as specified in the input file specification. In this case there is
53 # only a single result in that file.
54 initial conditions for ELECTRIC_POTENTIAL in si is exodus file
55
56 # The NLP simulation does not include a solution for the carrier
57 # densities, therefore some other type of estimate, in this case an
58 # equilibrium calculation, is used to obtain an initial guess for
59 # the carrier densities.
60 initial conditions for ELECTRON_DENSITY in si is equilibrium density
61 initial conditions for HOLE_DENSITY in si is equilibrium density
62
63 # Boundary condtions at the contacts.
64 bc is ohmic for cathode on si fixed at 0.0
65 bc is ohmic for anode on si swept from 0.0 to 1.0
66
67 # Sweep parameter controls
68 start sweep options
69     initial step size = 0.02
70     minimum step size = 0.02
71     maximum step size = 0.02
72 end sweep options
73
74 # Use a straightforward solver pack for this simulation.
75 start solver block
76     use solver pack 1
77 end solver block

```



## INDEX

### B

box method . *see* discretizations, box method

### C

C++11 ..... 13

carrier lifetimes

    concentration dependent ..... 57

Cubit ..... 16

### D

discretizations

    box method ..... 12

    finite element ..... 12

doping

    acceptor ..... 11

    analytic function

        Gaussian ..... 118

        MGauss ..... 118

        Step ..... 117

    donor ..... 11

    net ..... 11

### E

equations

    drift-diffusion ..... 11

    nonlinear Poisson ..... 12

Exodus ..... 16, 20

### G

generation-recombination

    avalanche ..... 64

    impact ionization ..... 64

    SRH

        standard ..... 57

### I

Input file keywords

    Boundary Conditions ..... 23

    Initial Conditions ..... 23

    Mesh ..... 21

    material block ..... 22

    physics block ..... 22

### N

NLP ..... *see* equations, nonlinear Poisson

### T

Trilinos ..... 13, 14







Sandia  
National  
Laboratories

Sandia National Laboratories is a  
multimission laboratory managed  
and operated by National  
Technology & Engineering  
Solutions of Sandia LLC, a wholly  
owned subsidiary of Honeywell  
International Inc., for the U.S.  
Department of Energy's National  
Nuclear Security Administration  
under contract DE-NA0003525.